Binary Neutron Stars I:
bulk dynamics and gravitational waves

Luciano Rezzolla

Institute for Theoretical Physics, Frankfurt

Timisoara, May 27 2026

Blended Intensive Programme (BIP):

Relativistic Fluid Dynamics

Plan of the talk I

- The richness of merging binary neutron stars
- EOS from GW spectroscopy
- Signatures of quark-hadron phase transitions
- Listening to the long ringdown

The two-body problem in GR

- For black holes the process is very **simple**:

BH + BH → BH + GWs

- For NSs the question is more **subtle:** t
hyper-massive neutron star (HMNS), ie a

NS + NS → HMNS+... ? → BH+to

- **HMNS** phase can provide clear information on **EOS**

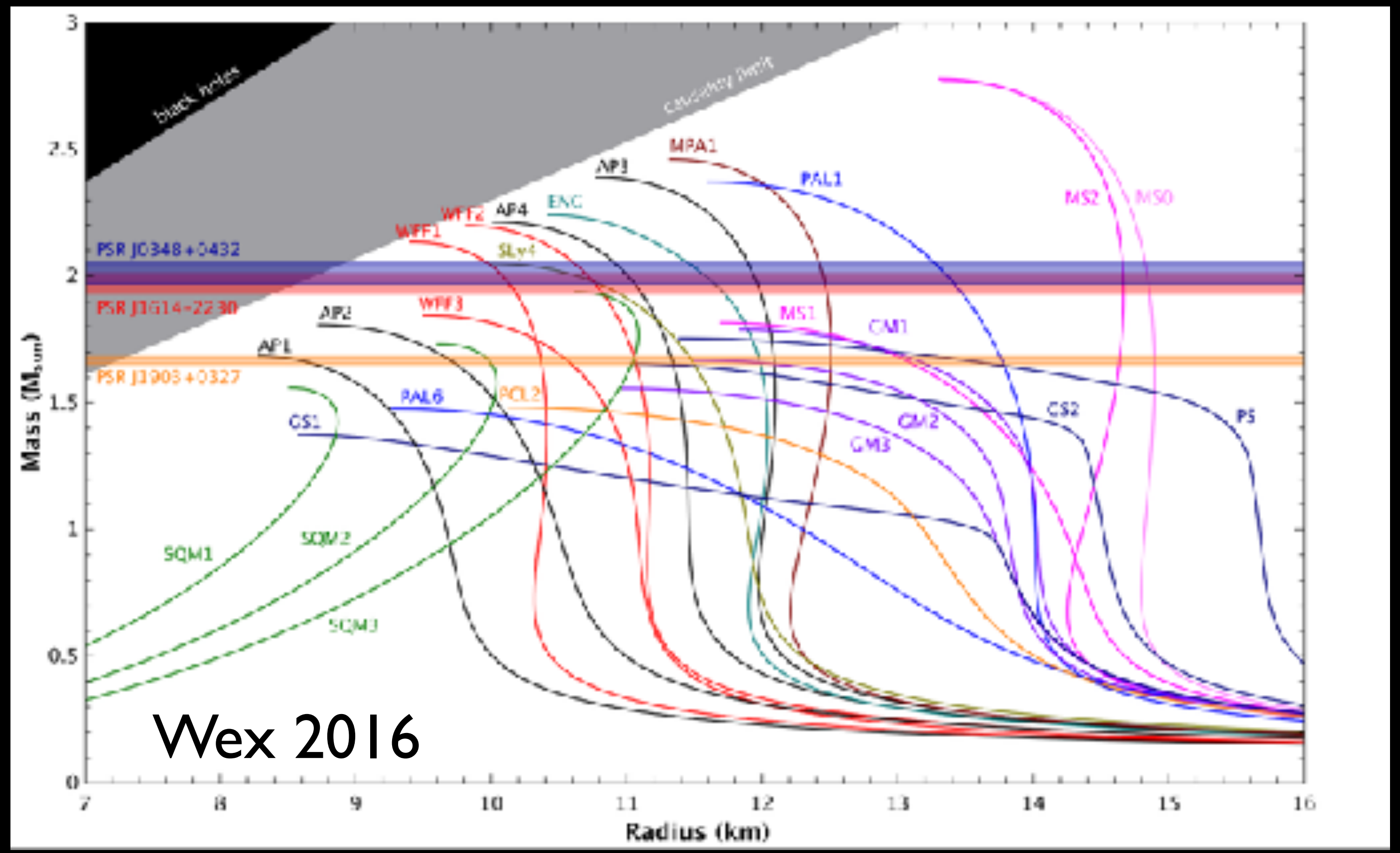

Wex 2016

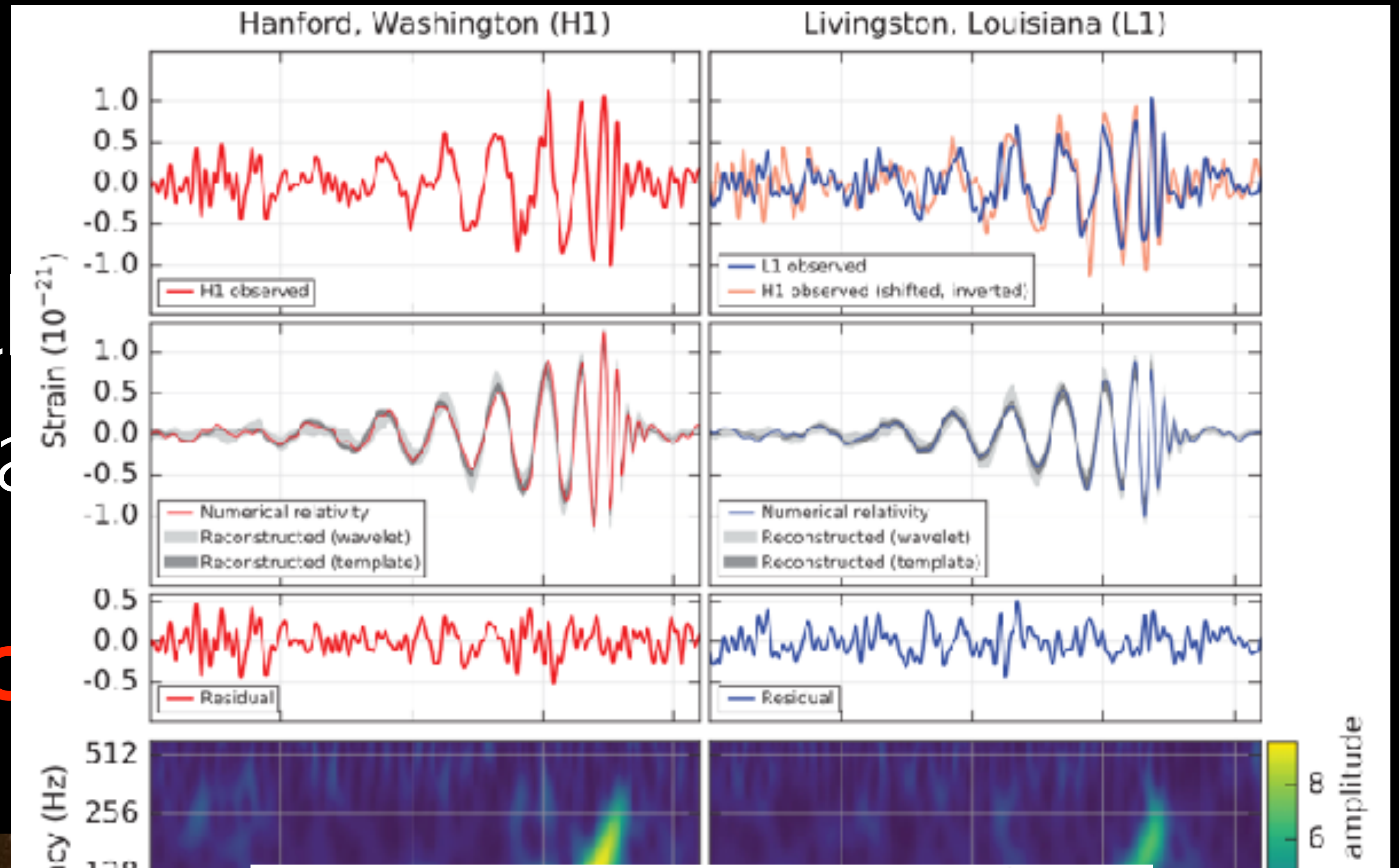

GW150914

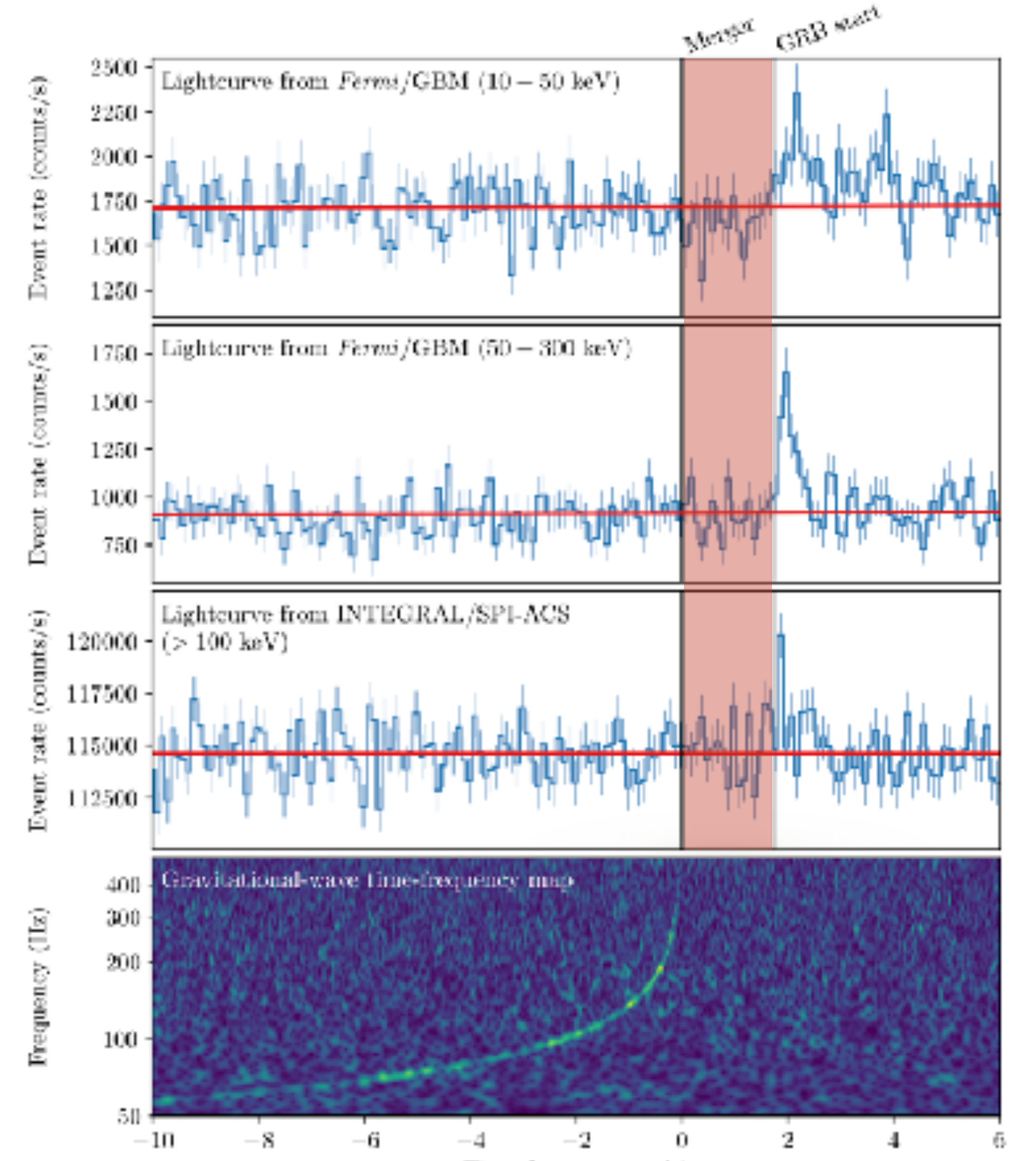

- **BH+toru** s
on the ce Bs

GW170817

The two-body problem in GR

- For black holes the process is very **simple**:

BH + BH → BH + GWs

- For NSs the question is more **subtle:** the merger leads to an hyper-massive neutron star (HMNS), ie a metastable equilibrium:

NS + NS → HMNS+… ? → BH+torus+… ? → BH + GWs

- **ejected matter** undergoes nucleosynthesis of heavy elements

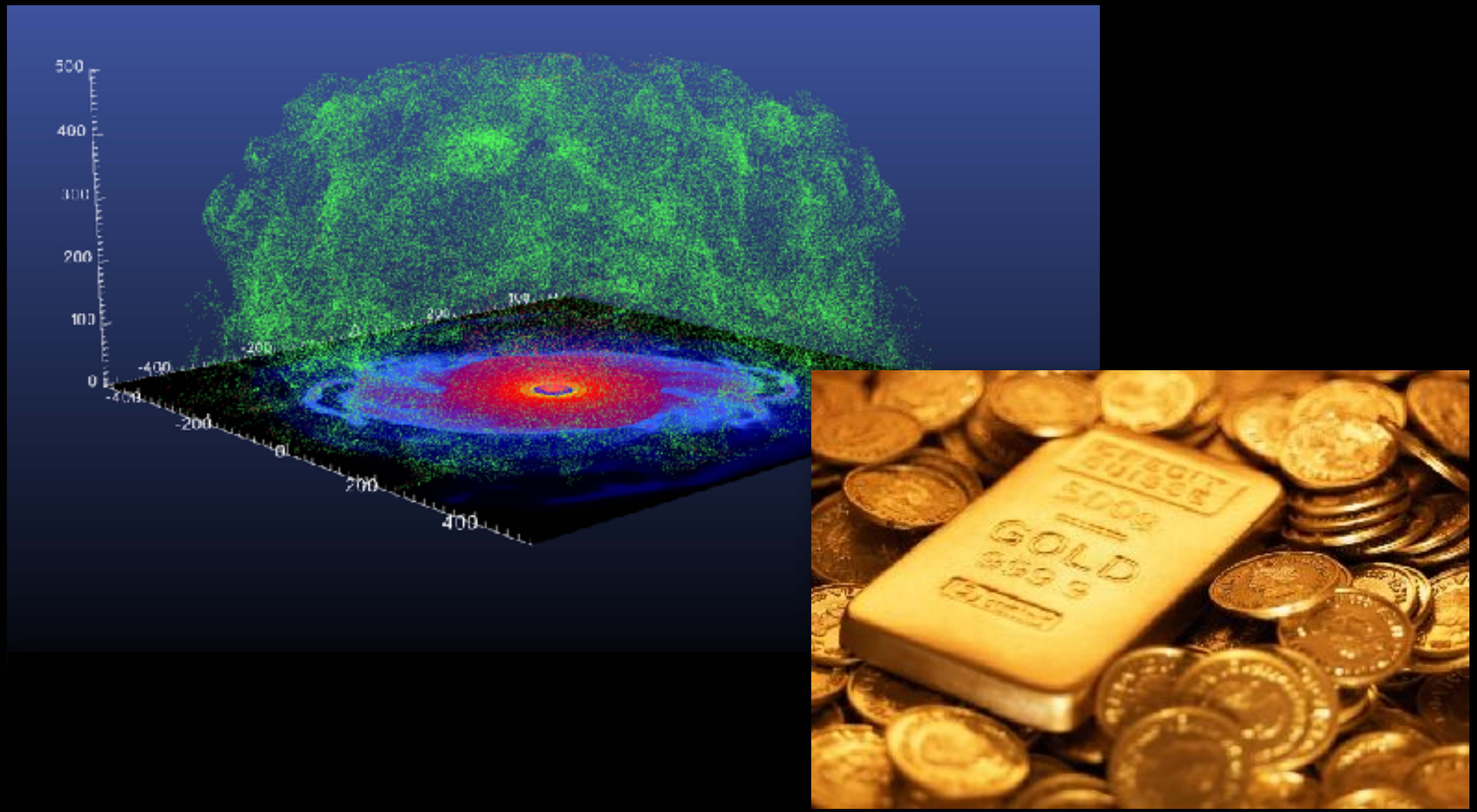

Animations: Breu, Radice, LR

A prototypical simulation with possibly the best code looks like this…

merger → HMNS → BH + torus

$M = 2 \times 1.35\, M_\odot$

timescale for all this is 0.01-1 sec

LS220 EOS

merger ⟶ HMNS ⟶ BH + torus

Quantitative differences are produced by:

- **total mass (prompt vs delayed collapse)**

Threshold mass

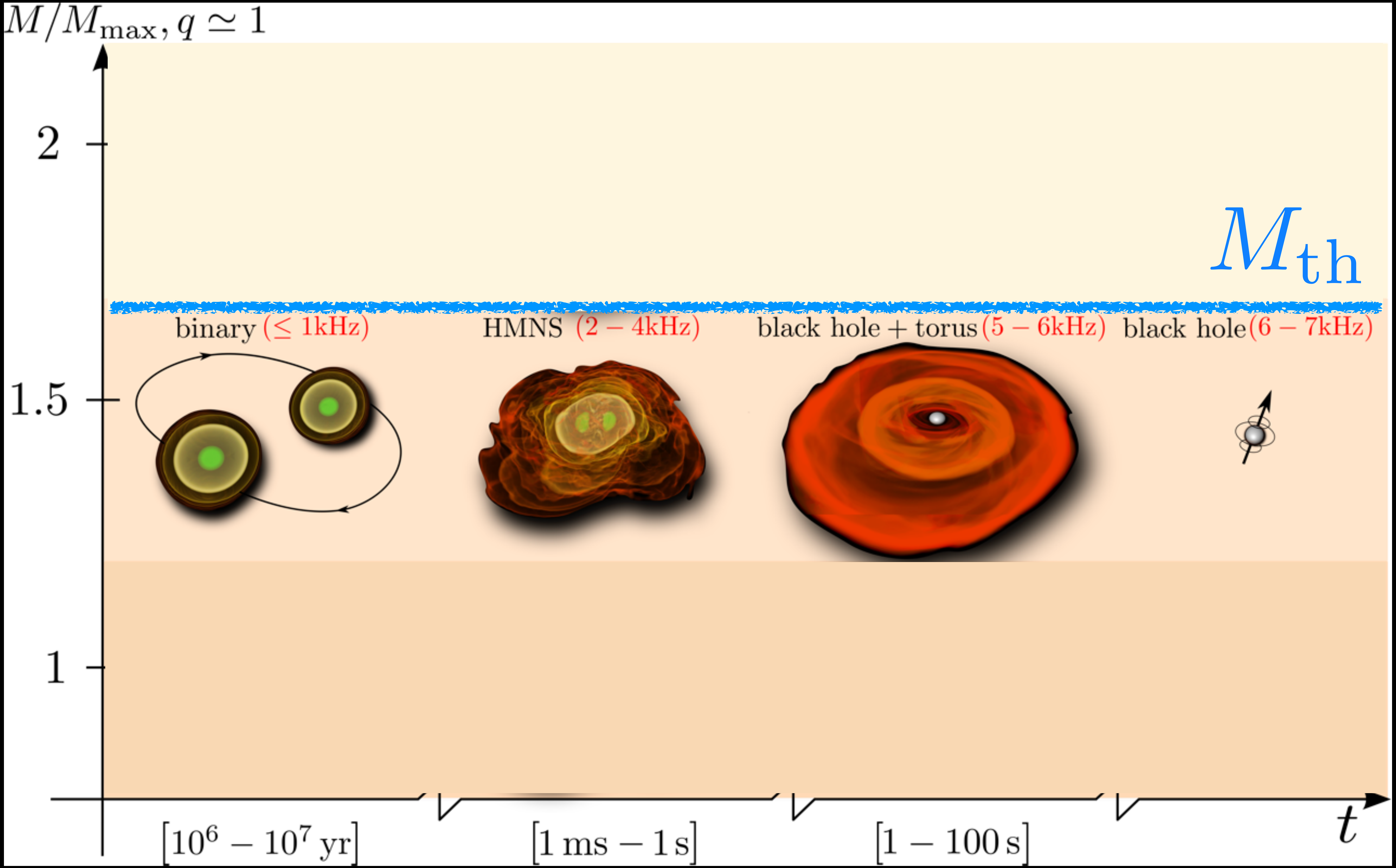

merger → HMNS → BH + torus

Quantitative differences are produced by:

- total **mass** (prompt vs delayed collapse)
- mass **asymmetries** (HMNS and torus)

Animations: Giacomazzo, Koppitz, LR

Total mass : $3.37\,M_\odot$; mass ratio :0.80;

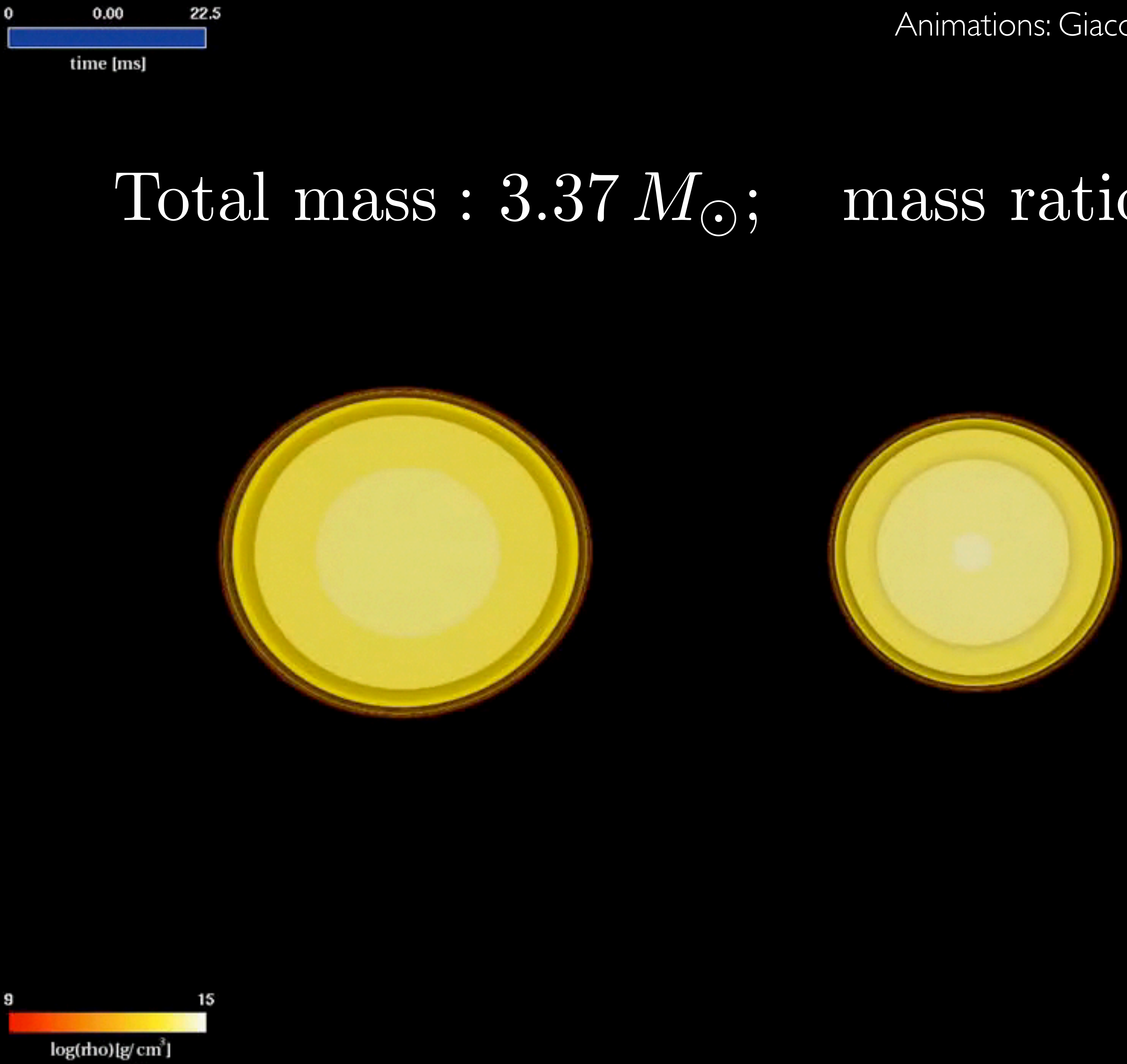

Qualitatively, this is what normally happens:

merger $\longrightarrow$ HMNS $\longrightarrow$ BH + torus

Quantitatively, differences are produced by:

- total mass (collapse and maximum mass)
- mass asymmetries (HMNS and torus)
- soft/stiff EOS (inspiral and post-merger, PT)
- magnetic fields (equil. and EM emission)
- radiative losses (equil. and nucleosynthesis)

GW spectroscopy: EOS from frequencies

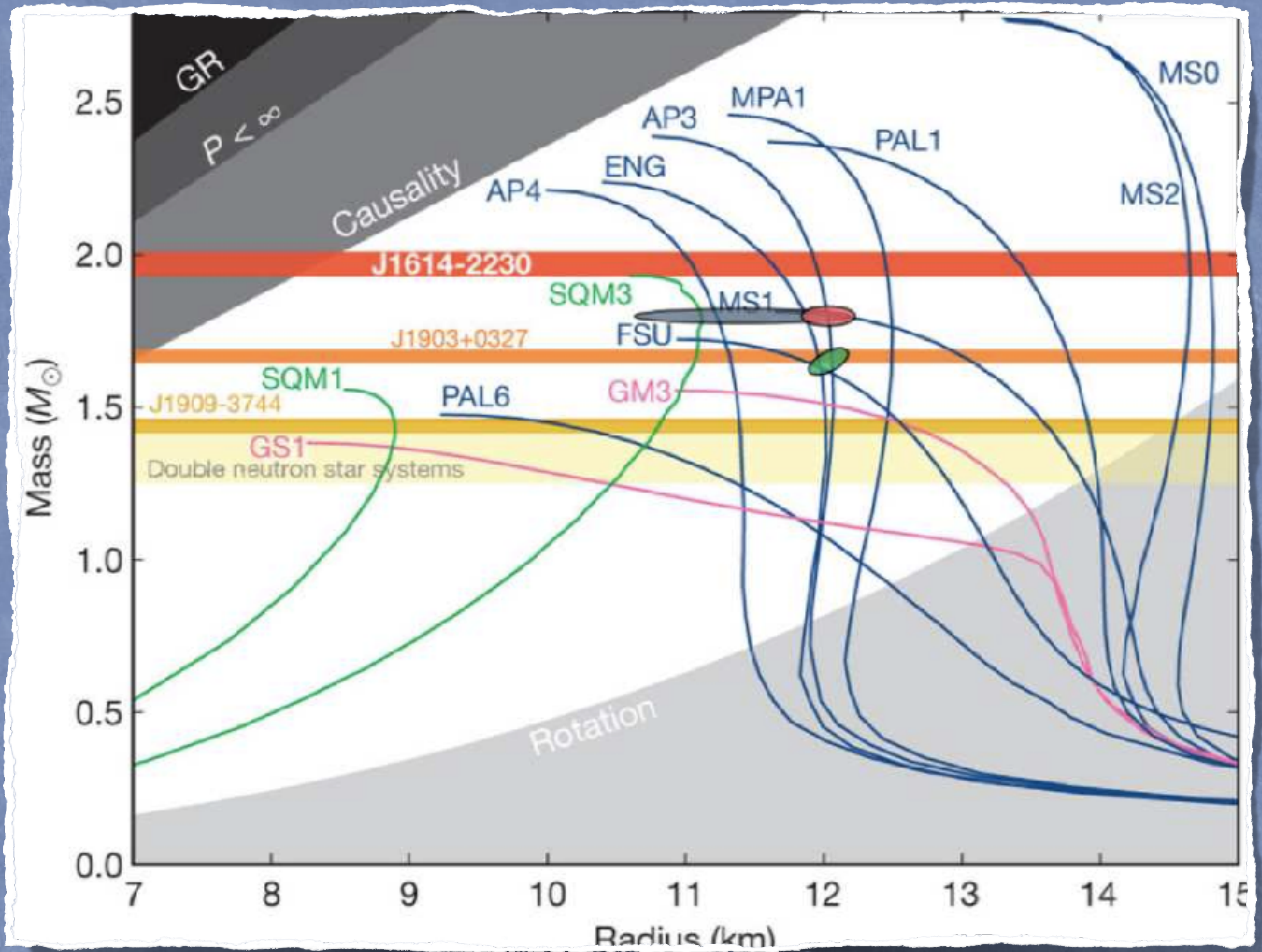

Reviews:

Baiotti & LR (2017)
Paschalidis (2018)
Radice, Bernuzzi, Perego (2022)

Anatomy of the GW signal

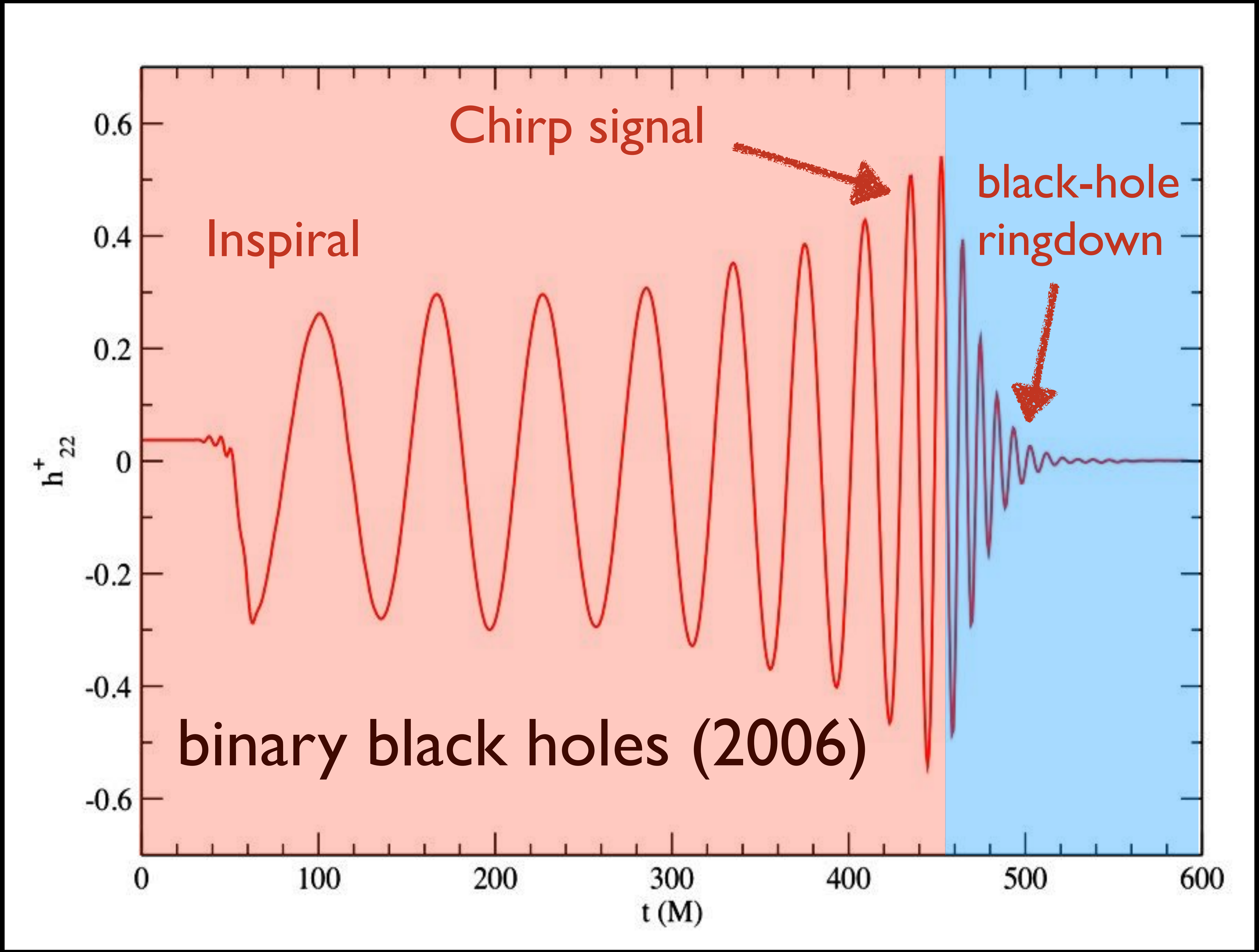

Anatomy of the GW signal

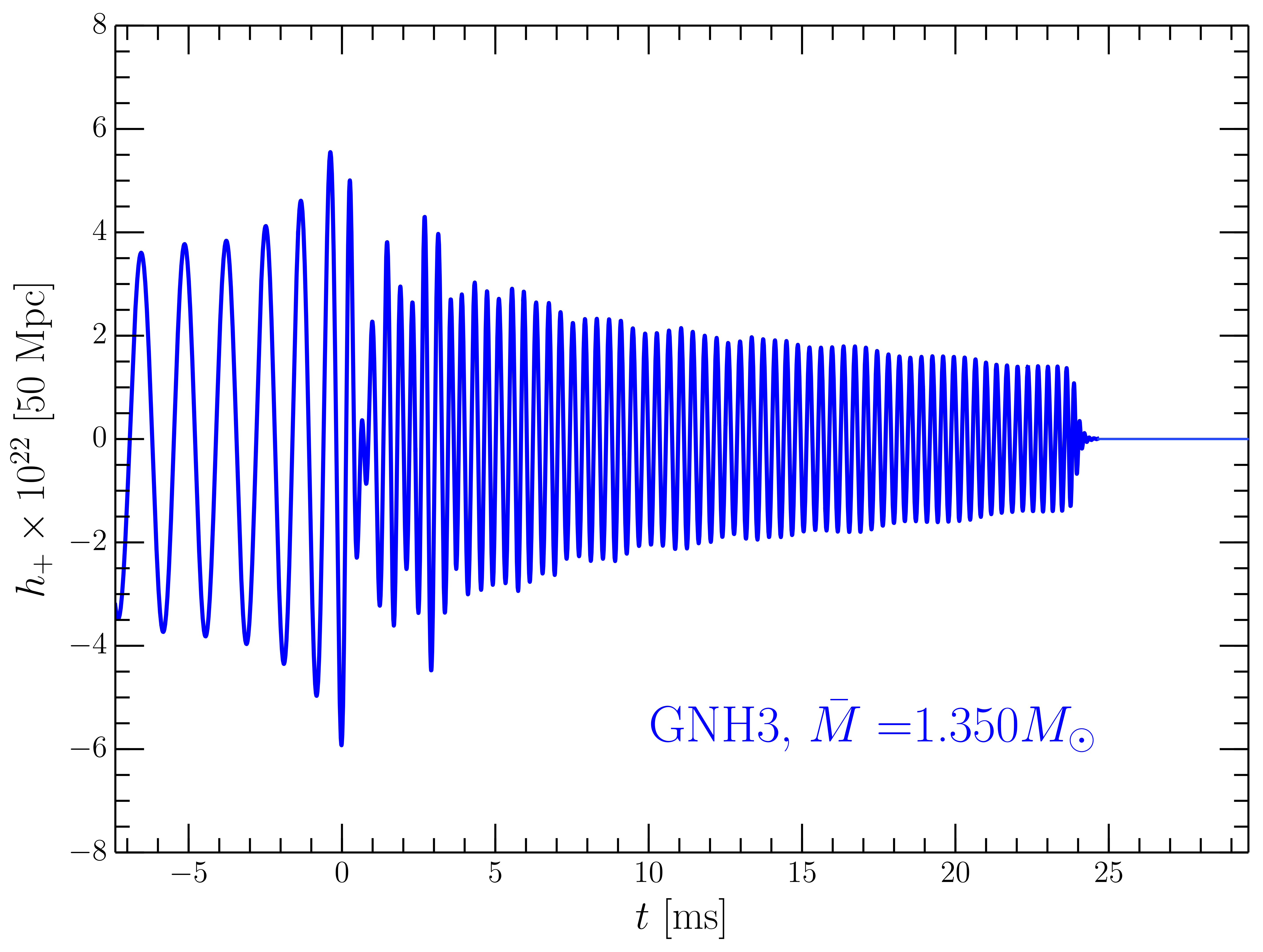

Anatomy of the GW signal

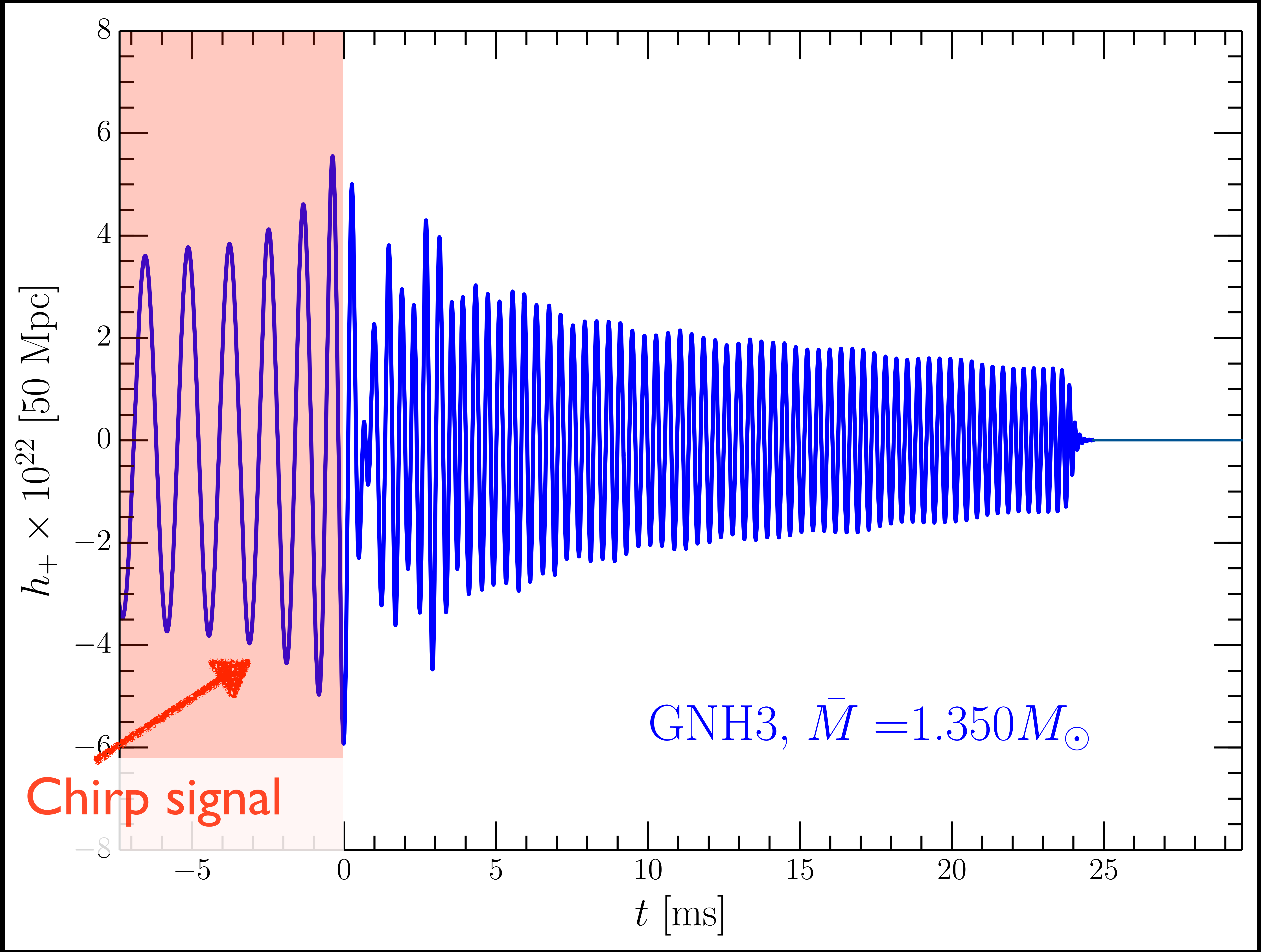

Inspiral: well approximated by PN/EOB; tidal effects important

Anatomy of the GW signal

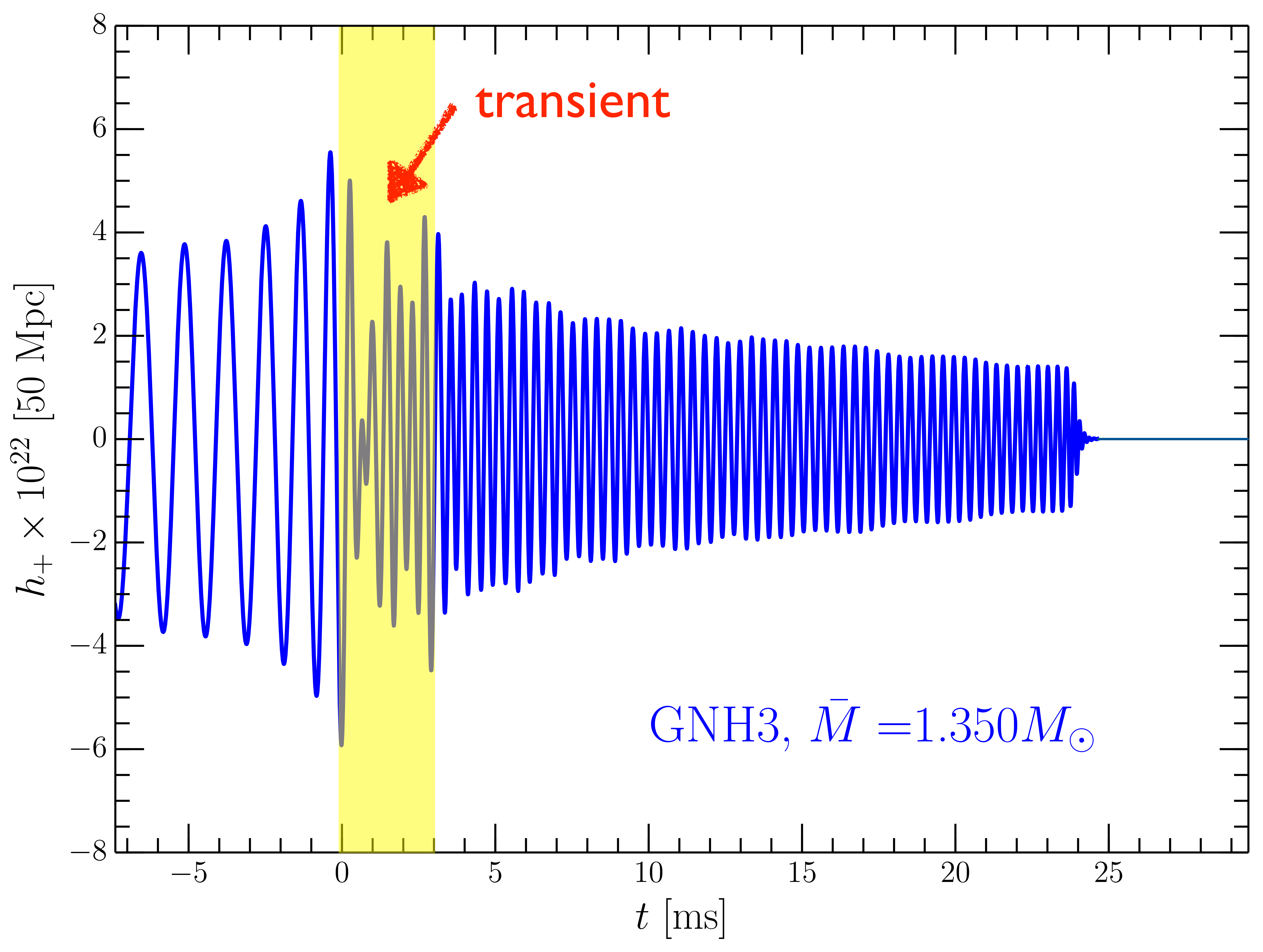

Merger: highly nonlinear but analytic description possible

Anatomy of the GW signal

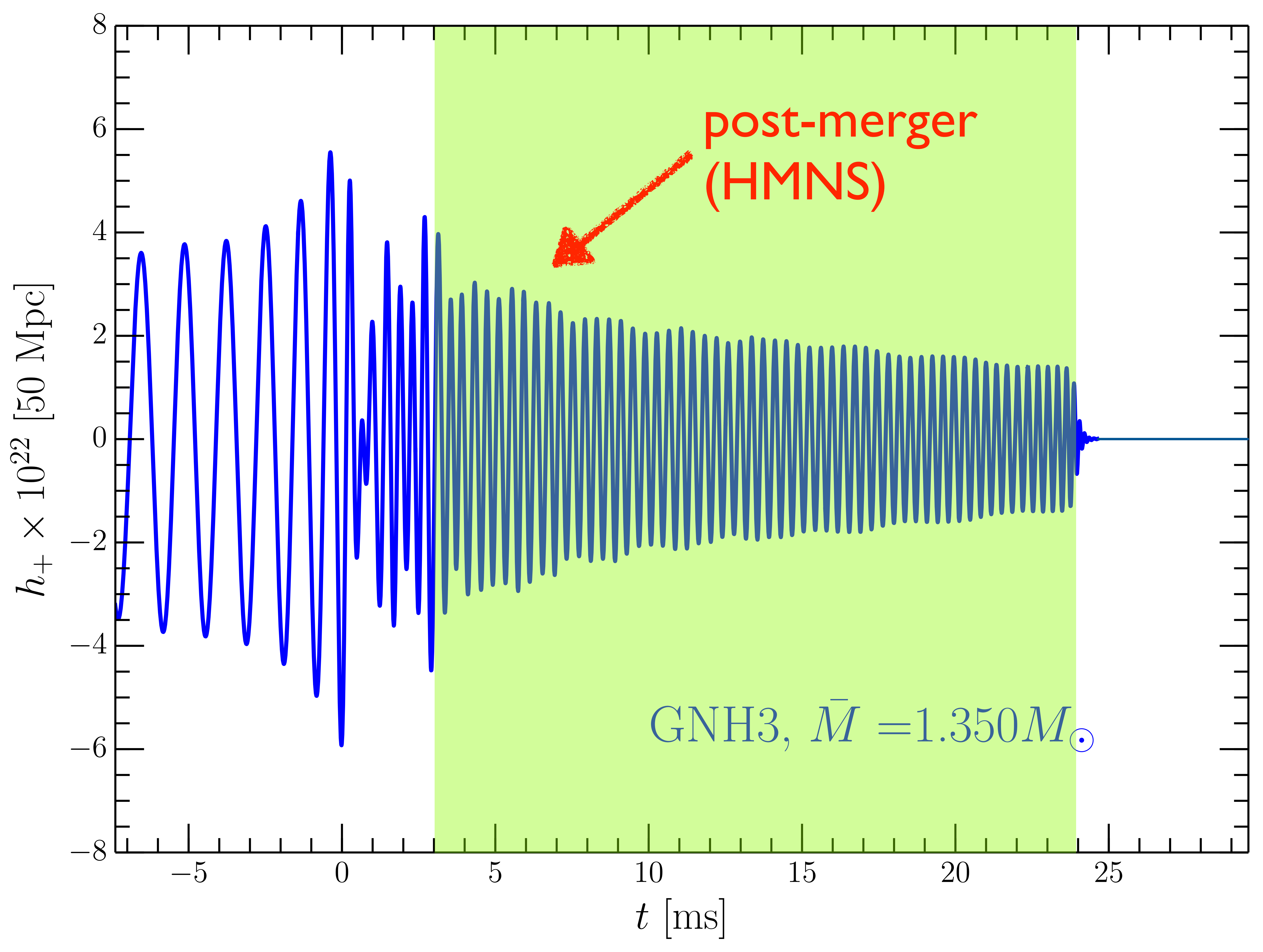

post-merger: quasi-periodic emission of bar-deformed HMNS

Anatomy of the GW signal

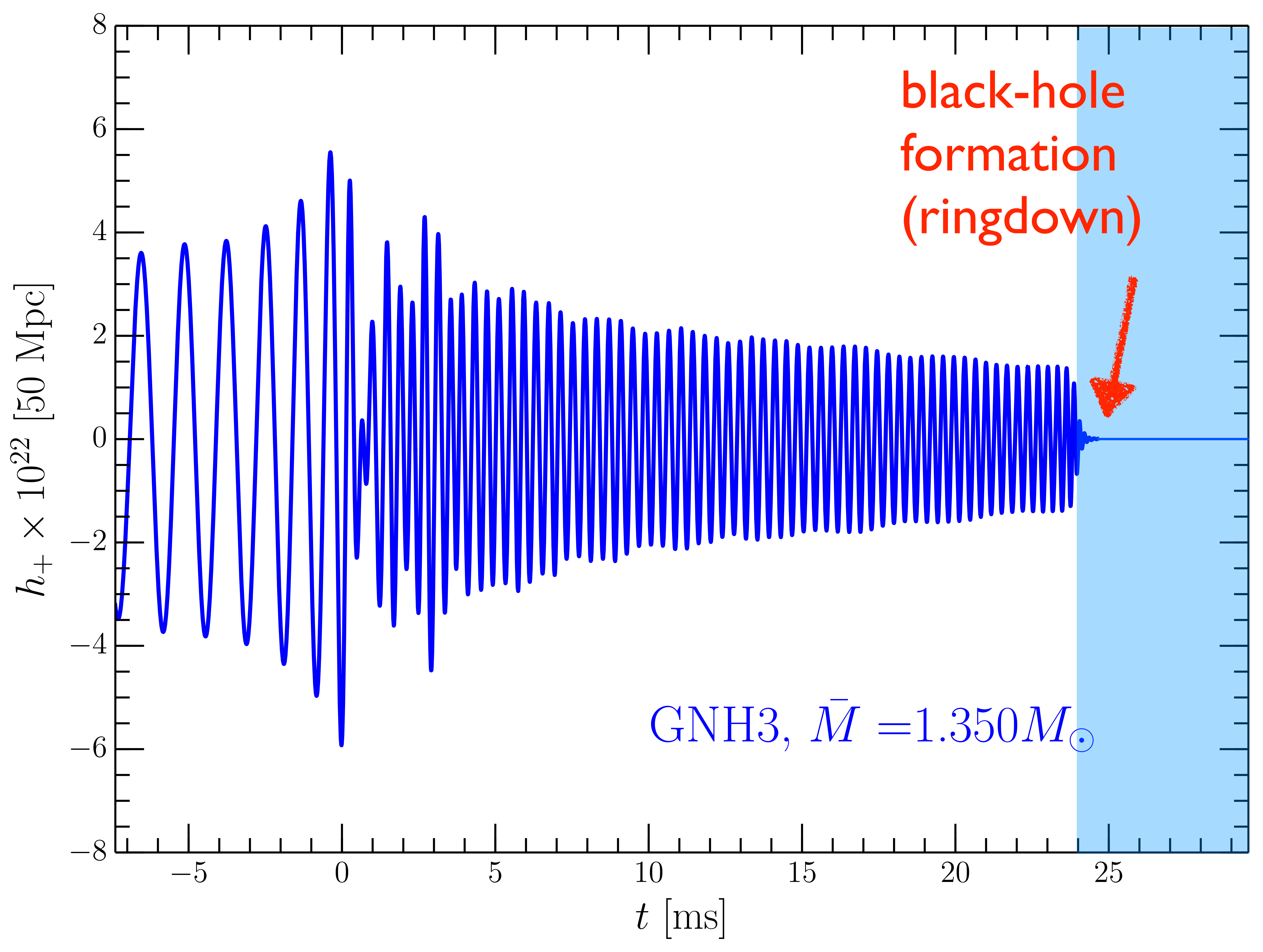

black-hole formation (ringdown)

Collapse-ringdown: signal essentially shuts off

Anatomy of the GW signal

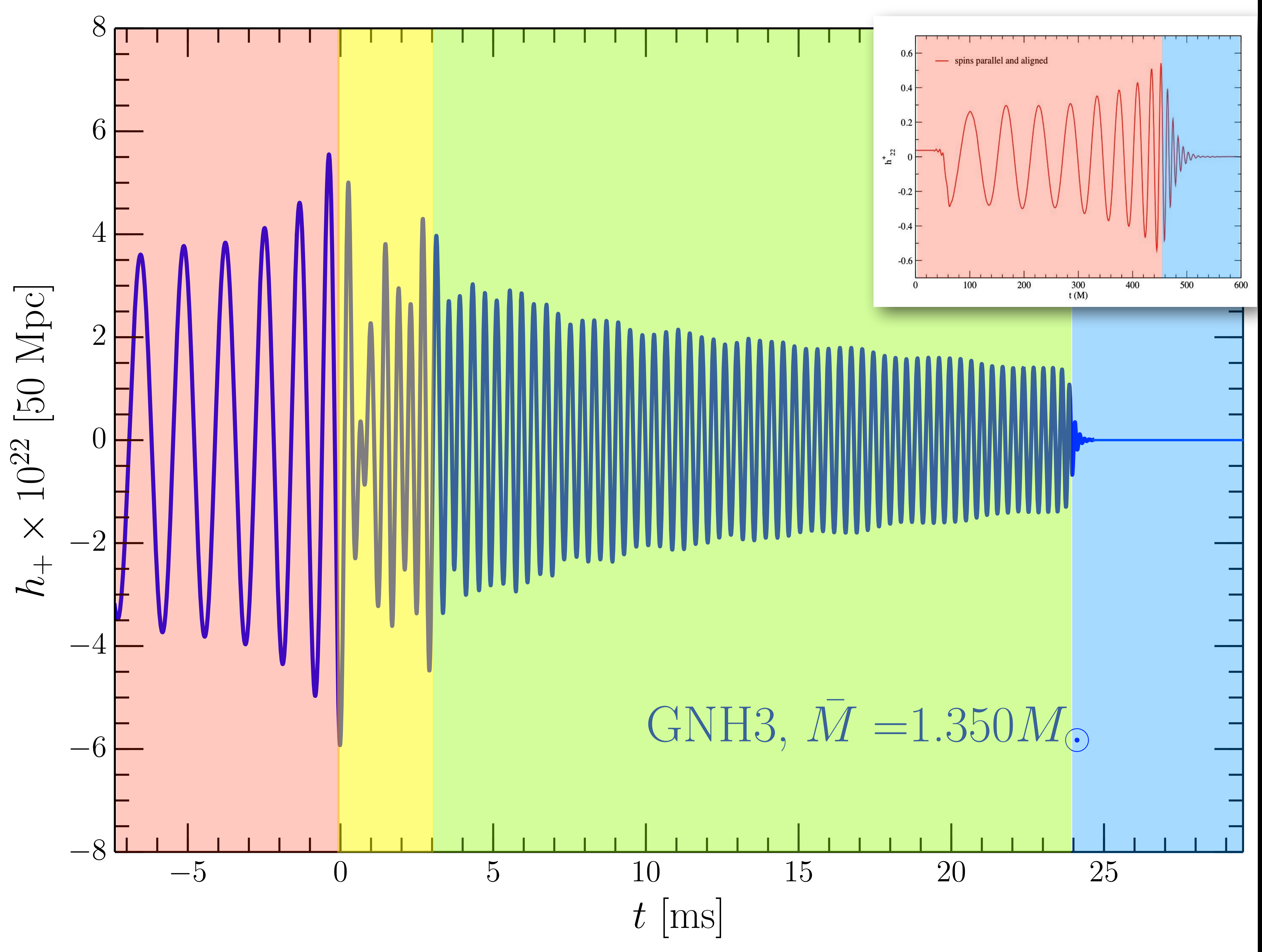

Postmerger signal: peculiar of binary NSs

What we can do nowadays

Takami, LR, Baiotti (2014, 2015), LR+ (2016)

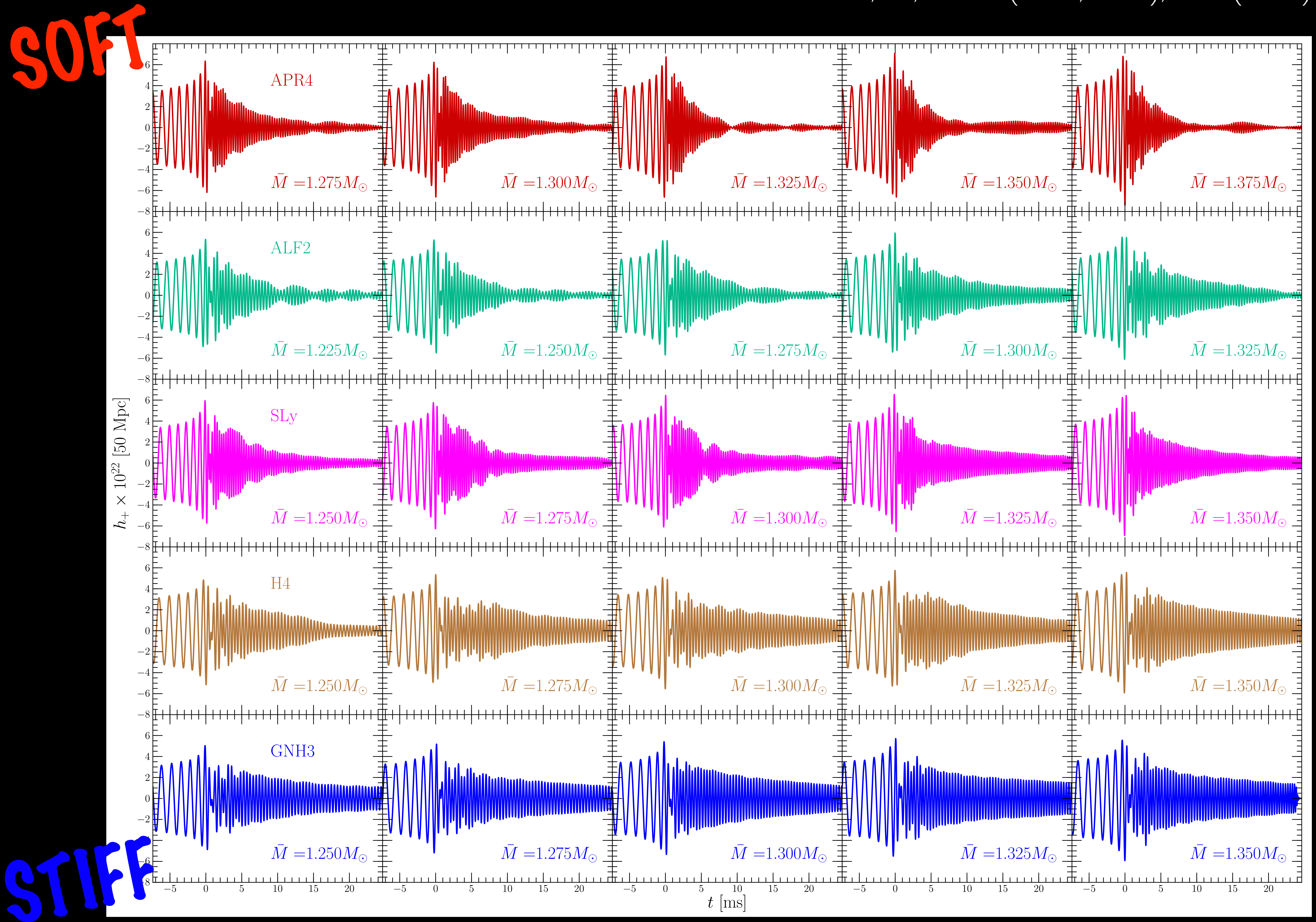

Extracting information from the EOS

Takami, LR, Baiotti (2014, 2015), LR+ (2016)

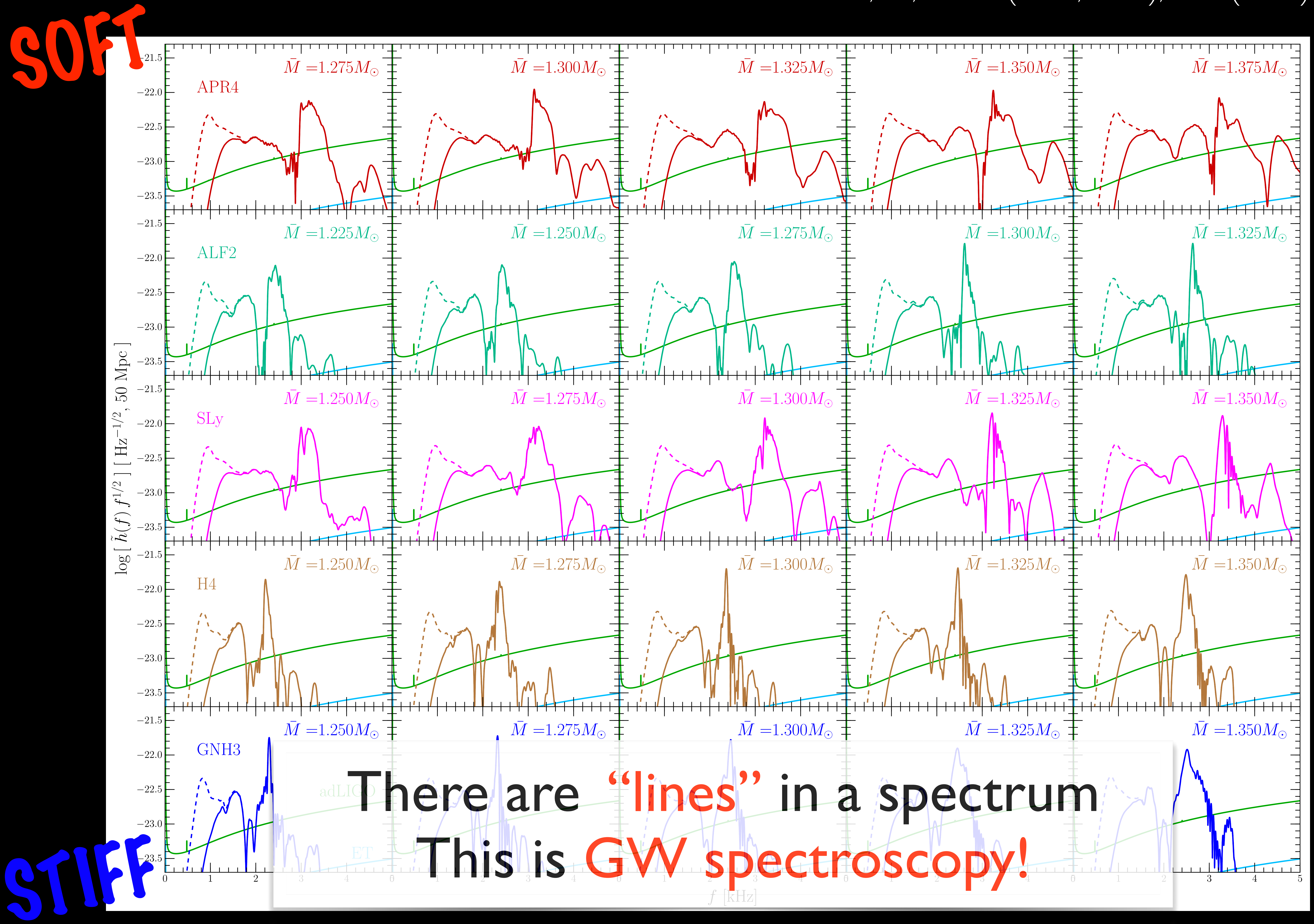

There are "lines" in a spectrum

This is GW spectroscopy!

A spectroscopic approach to the EOS

Oechslin+2007, Baiotti+2008, Bauswein+ 2011, 2012, Stergioulas+ 2011, Hotokezaka+ 2013, Takami 2014, 2015, Bernuzzi 2014, 2015, Bauswein+ 2015, Clark+ 2016, LR+2016, de Pietri+ 2016, Feo+ 2017, Bose+ 2017 …

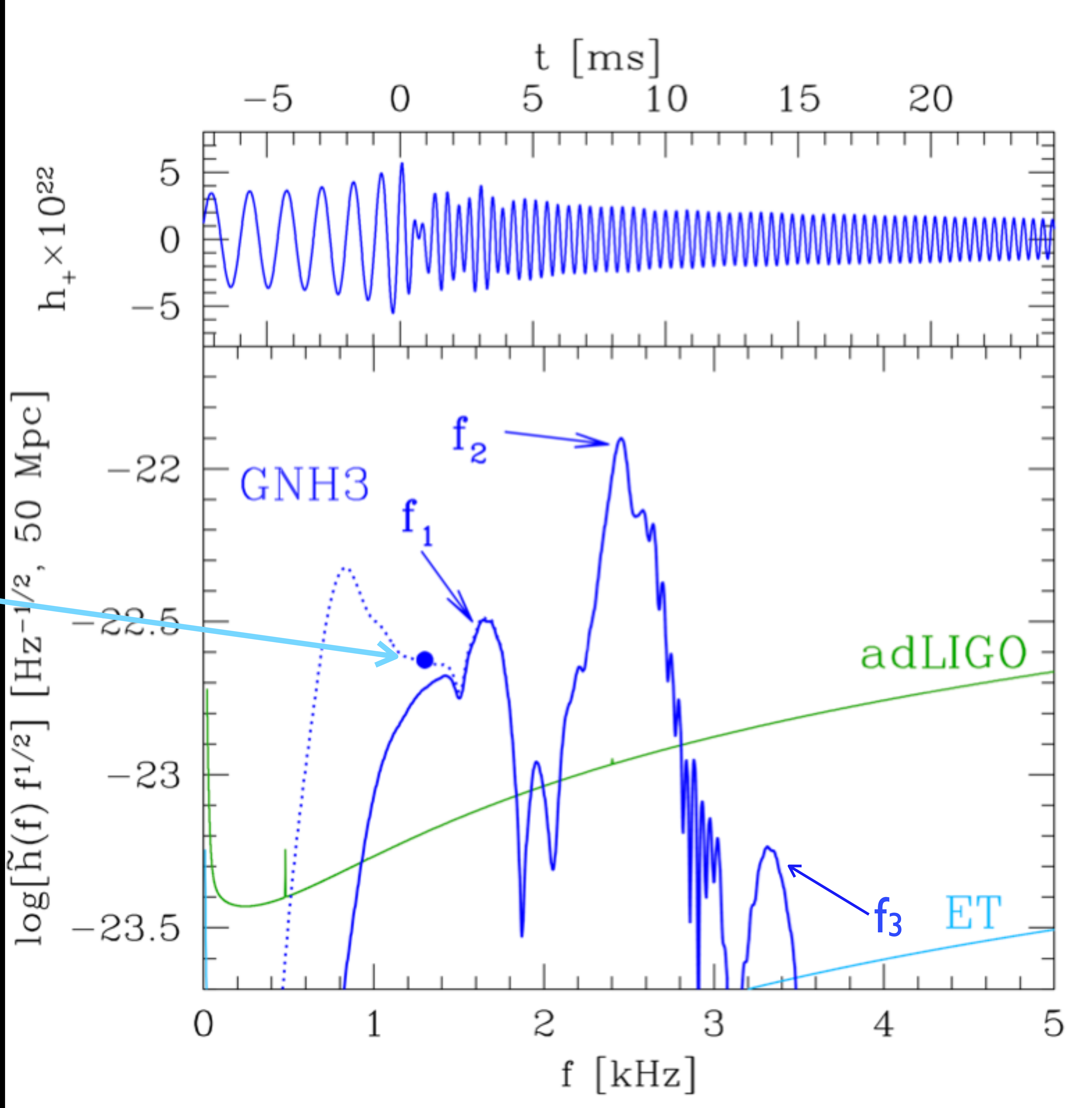

merger frequency

A spectroscopic approach to the EOS

Oechslin+2007, Baiotti+2008, Bauswein+ 2011, 2012, Stergioulas+ 2011, Hotokezaka+ 2013, Takami 2014, 2015, Bernuzzi 2014, 2015, Bauswein+ 2015, Clark+ 2016, LR+2016, de Pietri+ 2016, Feo+ 2017, Bose+ 2017 …

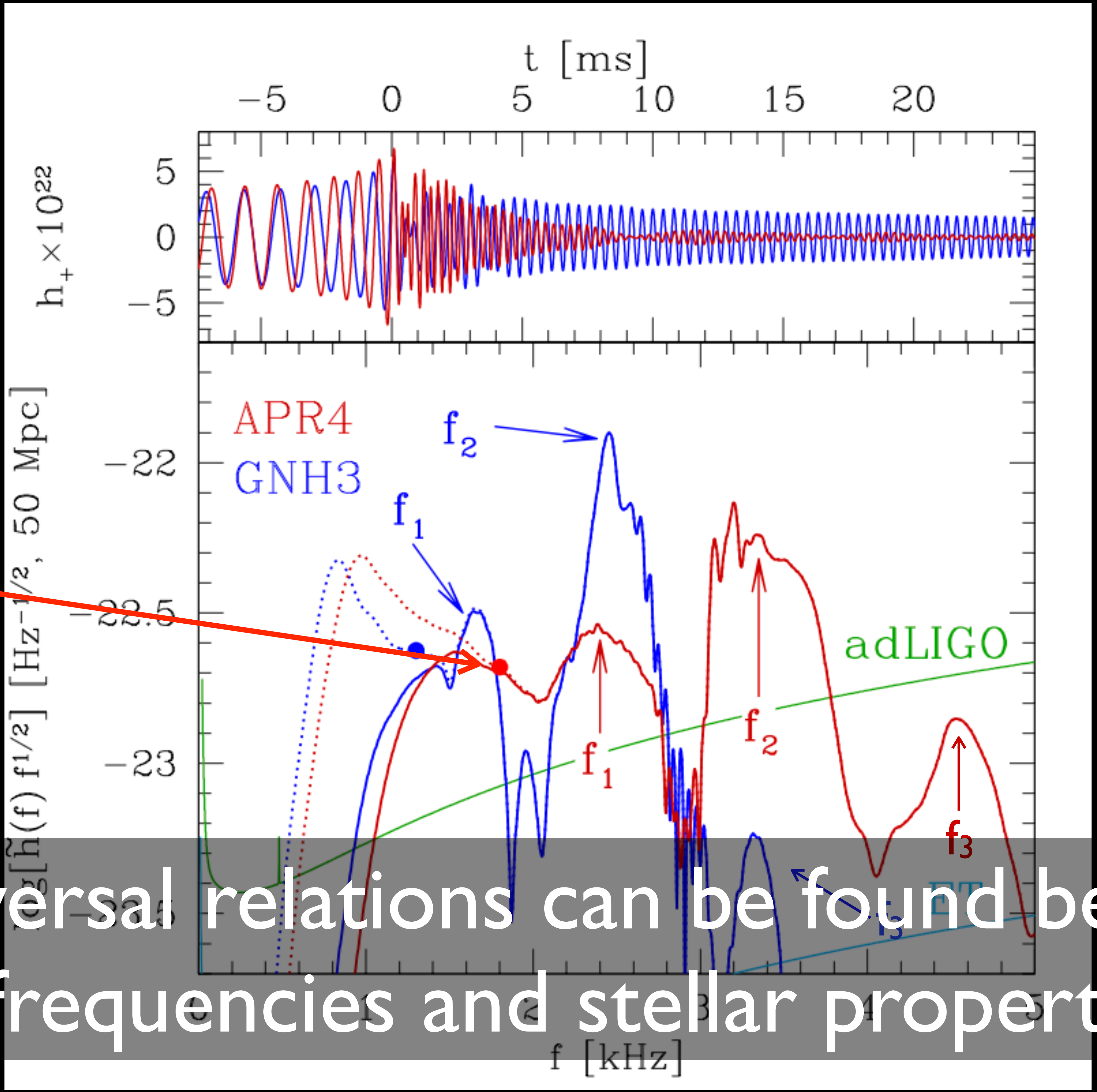

Universal relations can be found between frequencies and stellar properties

Example of quasi-universal behaviour: f_{max}

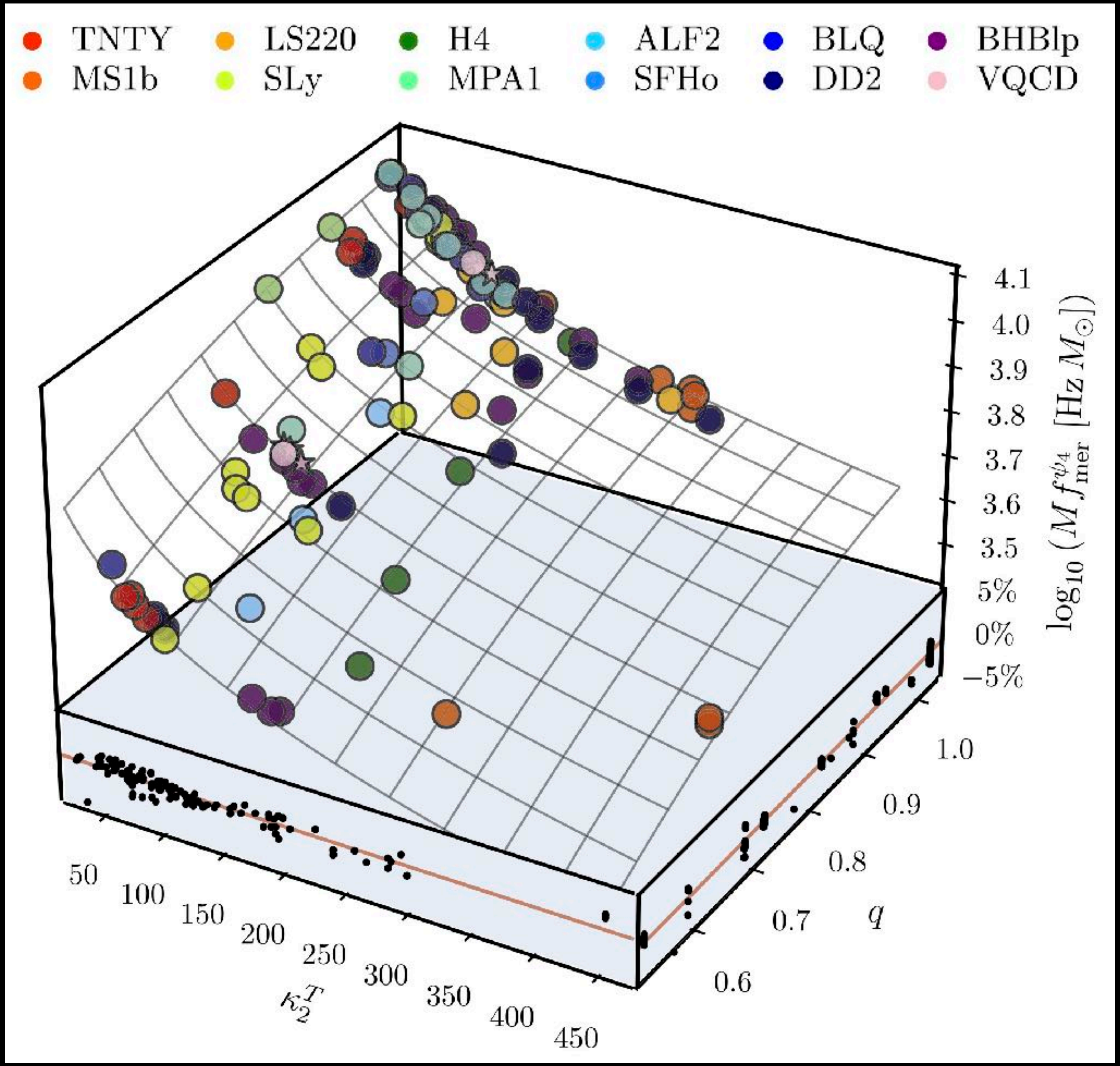

Quasi-universal behaviour of GW frequency at amplitude peak (Baiotti, LR 2016, Radice+2022 for reviews)

In other words, once $f_{\rm mer}$ is measured, so is the tidal deformability but also $I, Q, M/R\ldots$

Signatures of HQ phase transitions

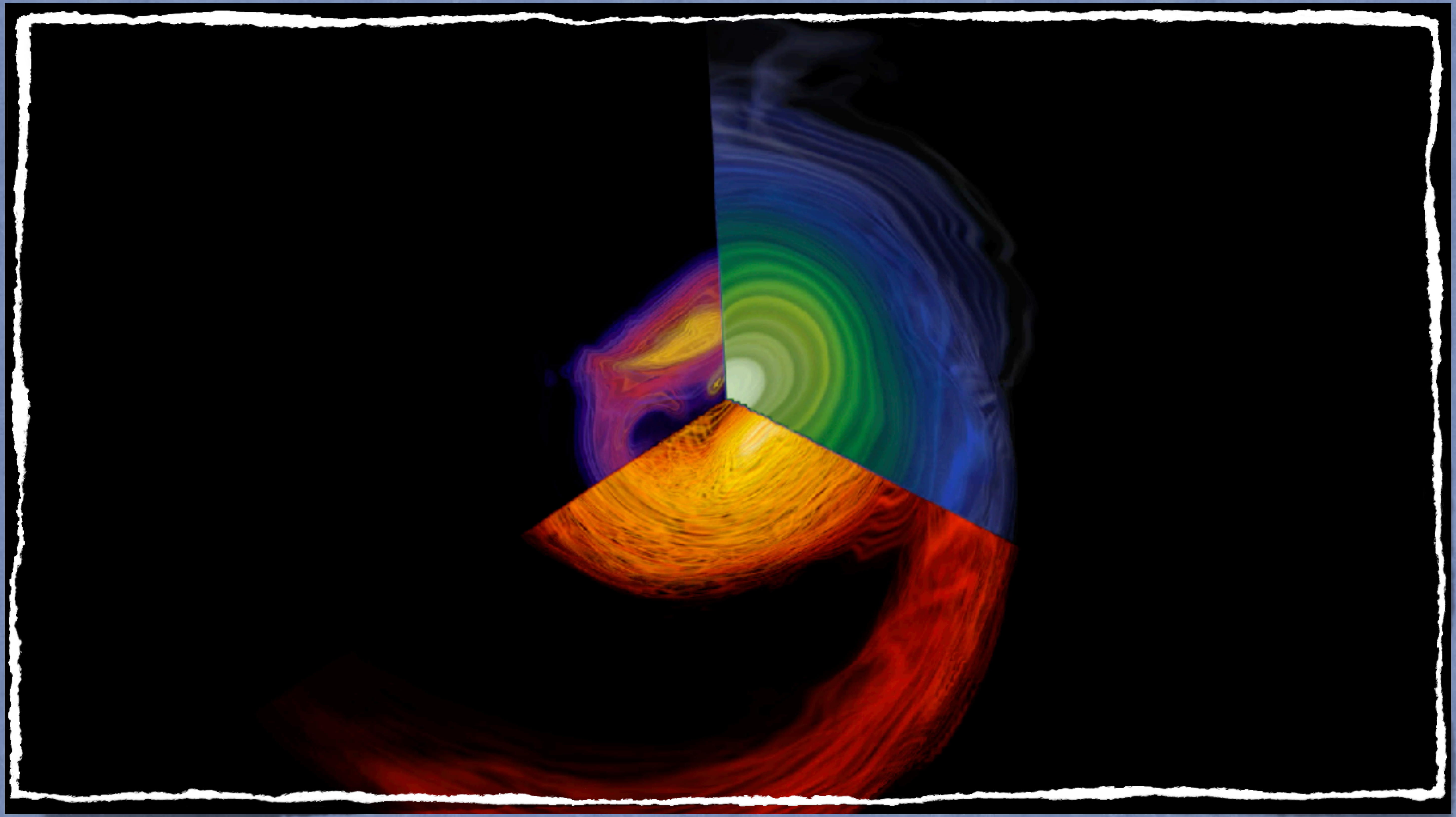

Most, Papenfort, Dexheimer, Hanauske, Schramm, Stoecker, LR (2019)
Weih, Hanauske, LR (2020)
Tootle, Ecker, Topolski, Demircik, Järvinen, LR (2022)

- Neutron-star **binary** mergers reach temperatures up to 80 MeV and probe regions complementary to accelerator experiments

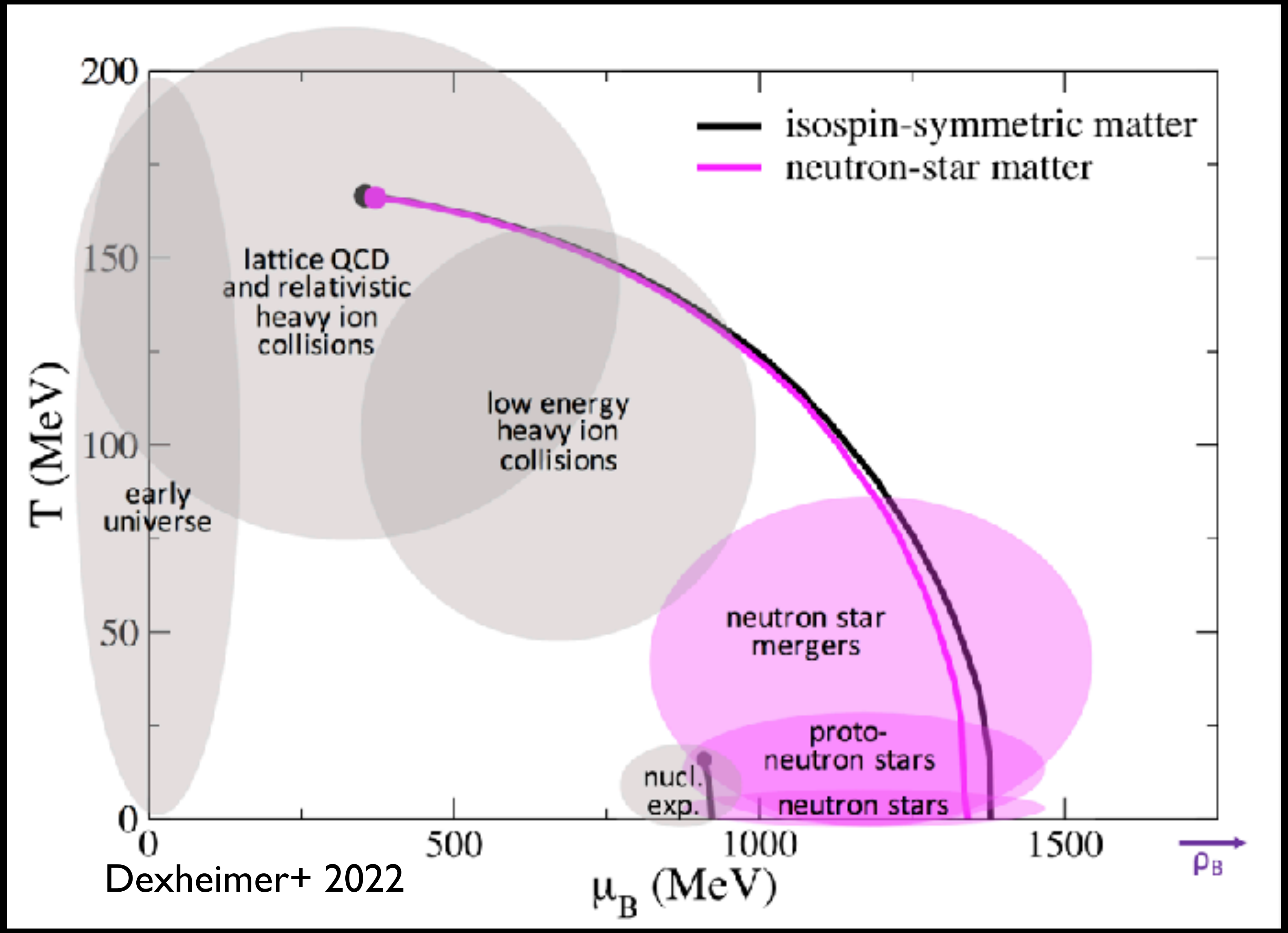

Dexheimer+ 2022

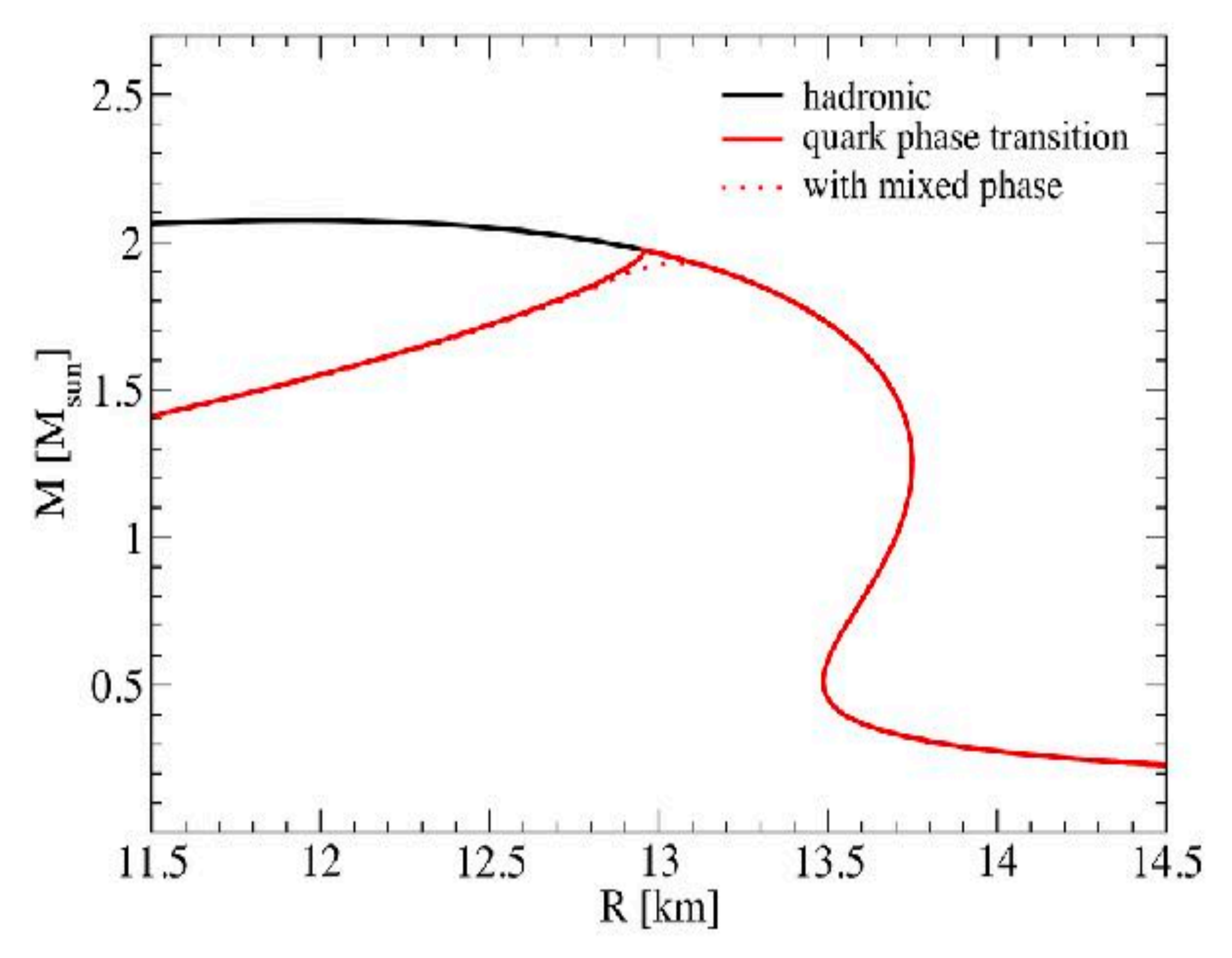

- Considered EOS based on Chiral Mean Field (CMF) model, based on a nonlinear SU(3) sigma model.

Temperature

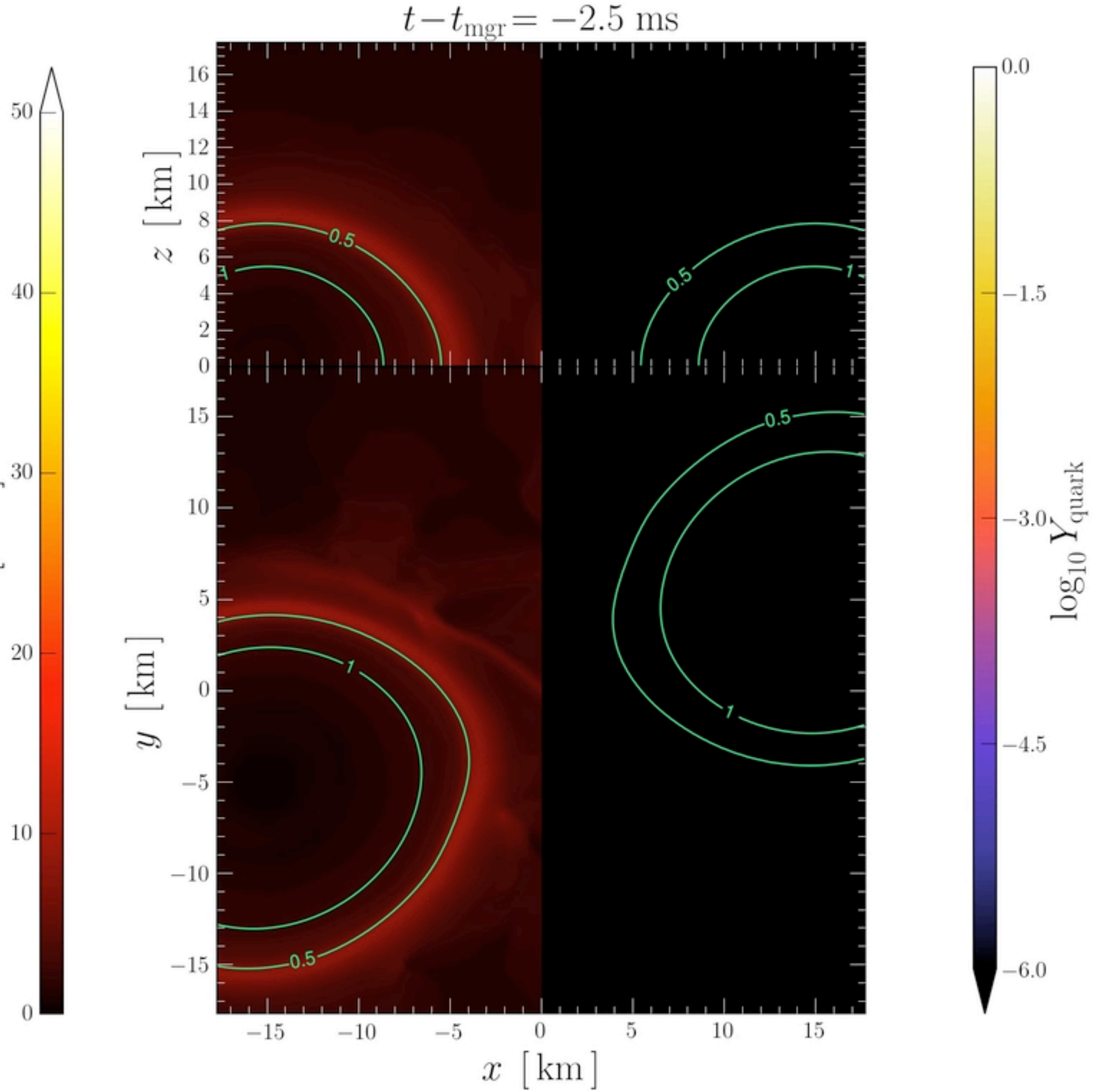

Quark fraction

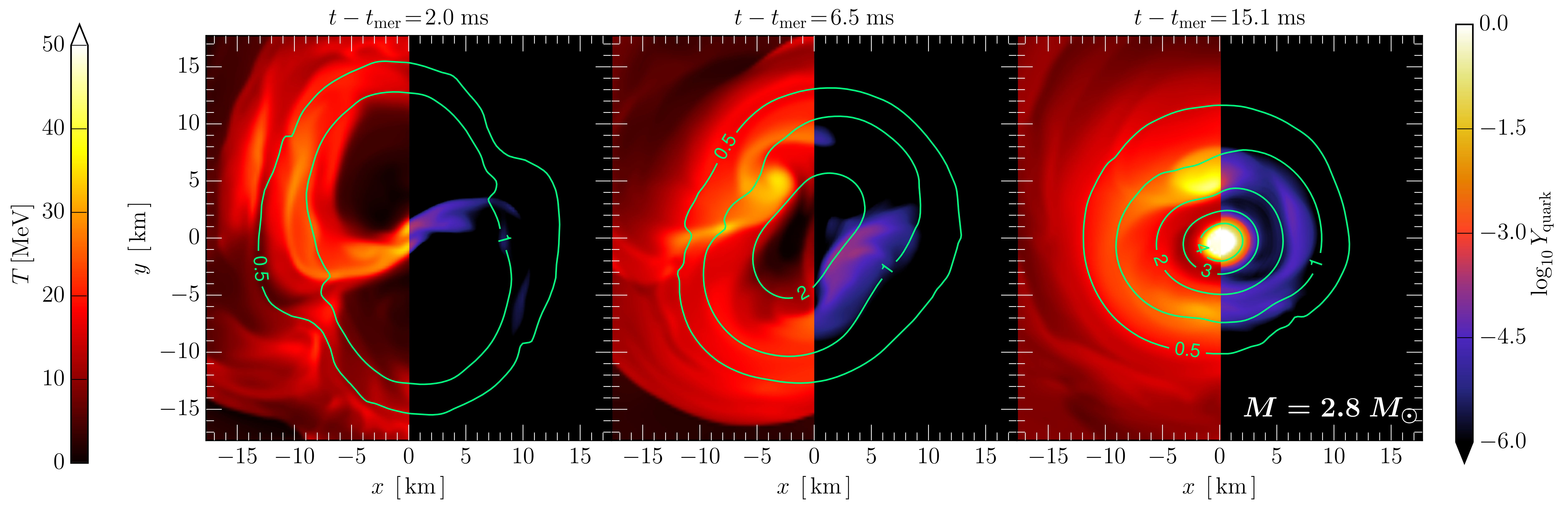

Quarks appear at sufficiently large temperatures and densities.

When this happens the EOS is considerably softened and a BH produced.

Comparing with the phase diagram

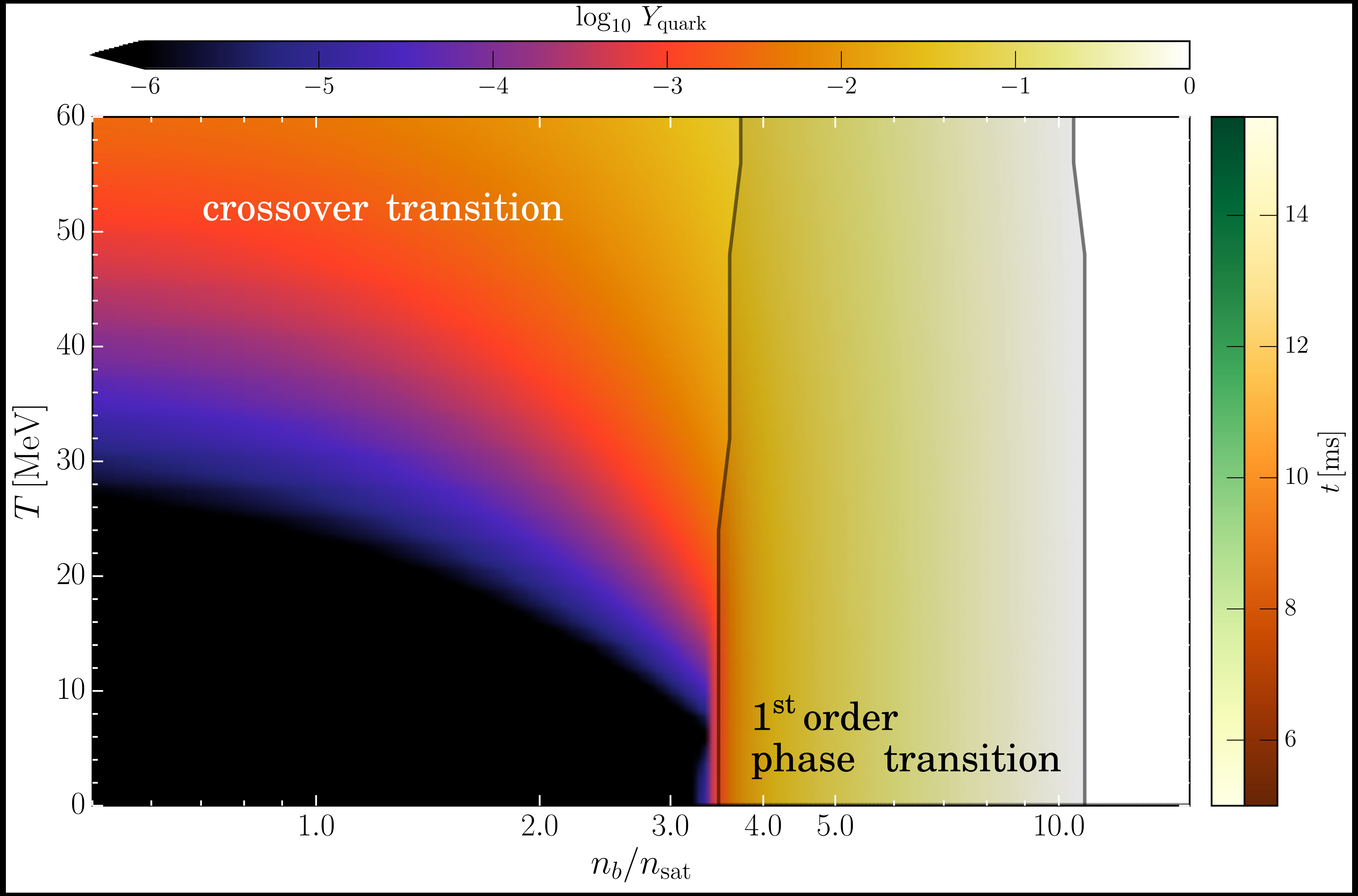

- Phase diagram with quark fraction

Comparing with the phase diagram

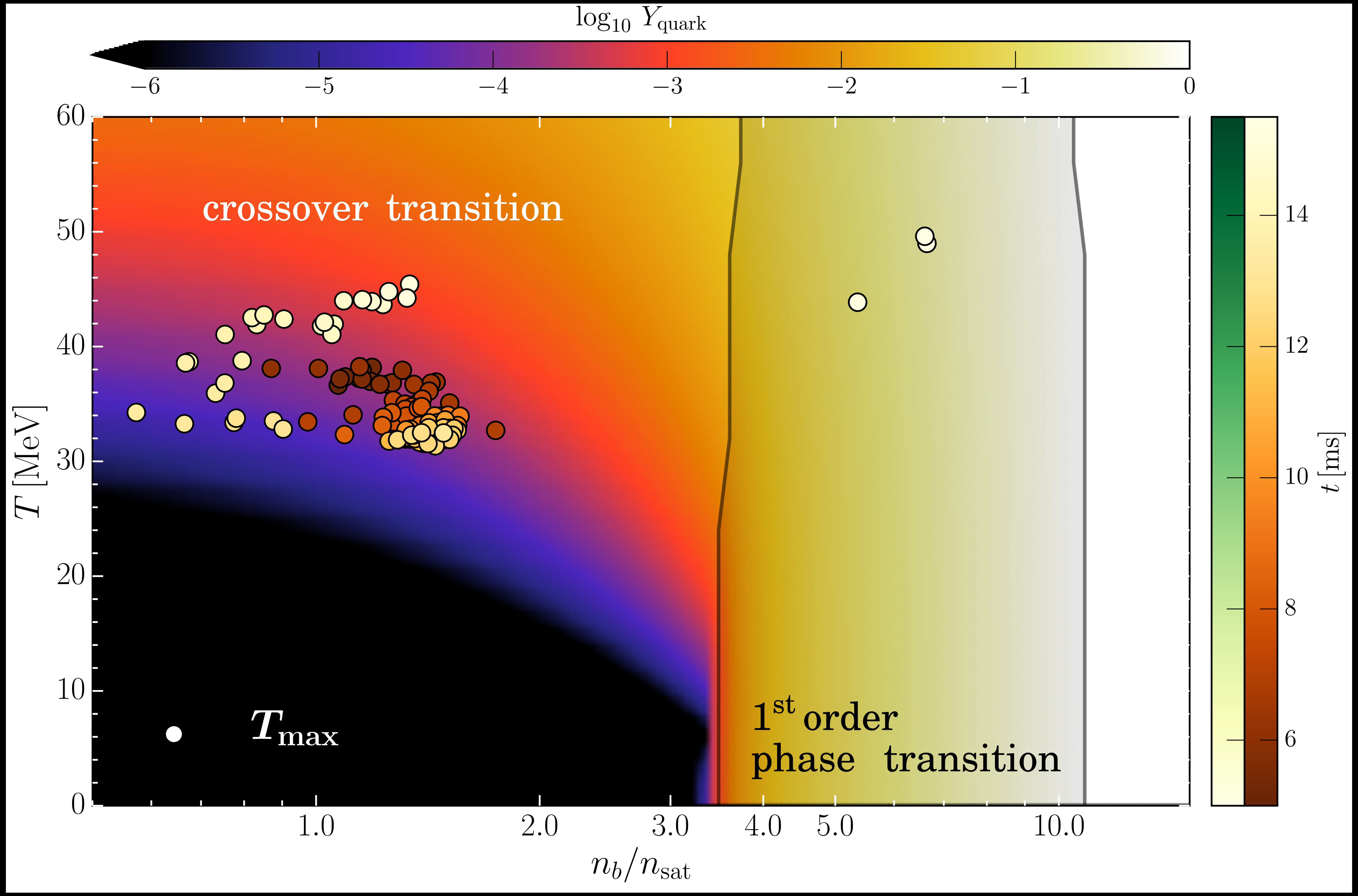

- Phase diagram with quark fraction
- Circles show the position in the diagram of the maximum temperature as a function of time

Comparing with the phase diagram

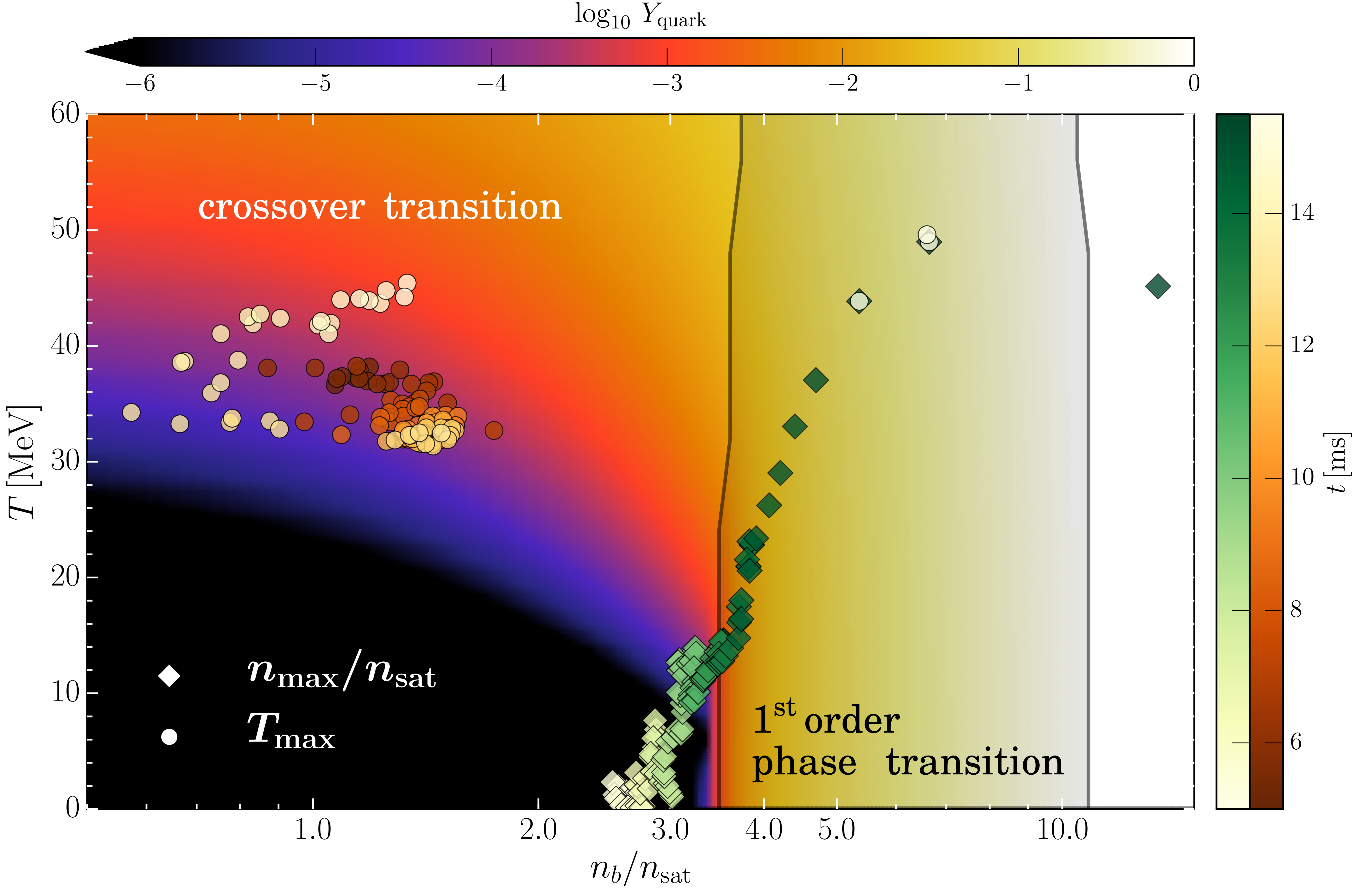

- Reported are the evolution of the max. temperature and density.
- Quarks appear already early on, but only in small fractions.
- Once sufficient density is reached, a full phase transition takes place.

Gravitational-wave emission

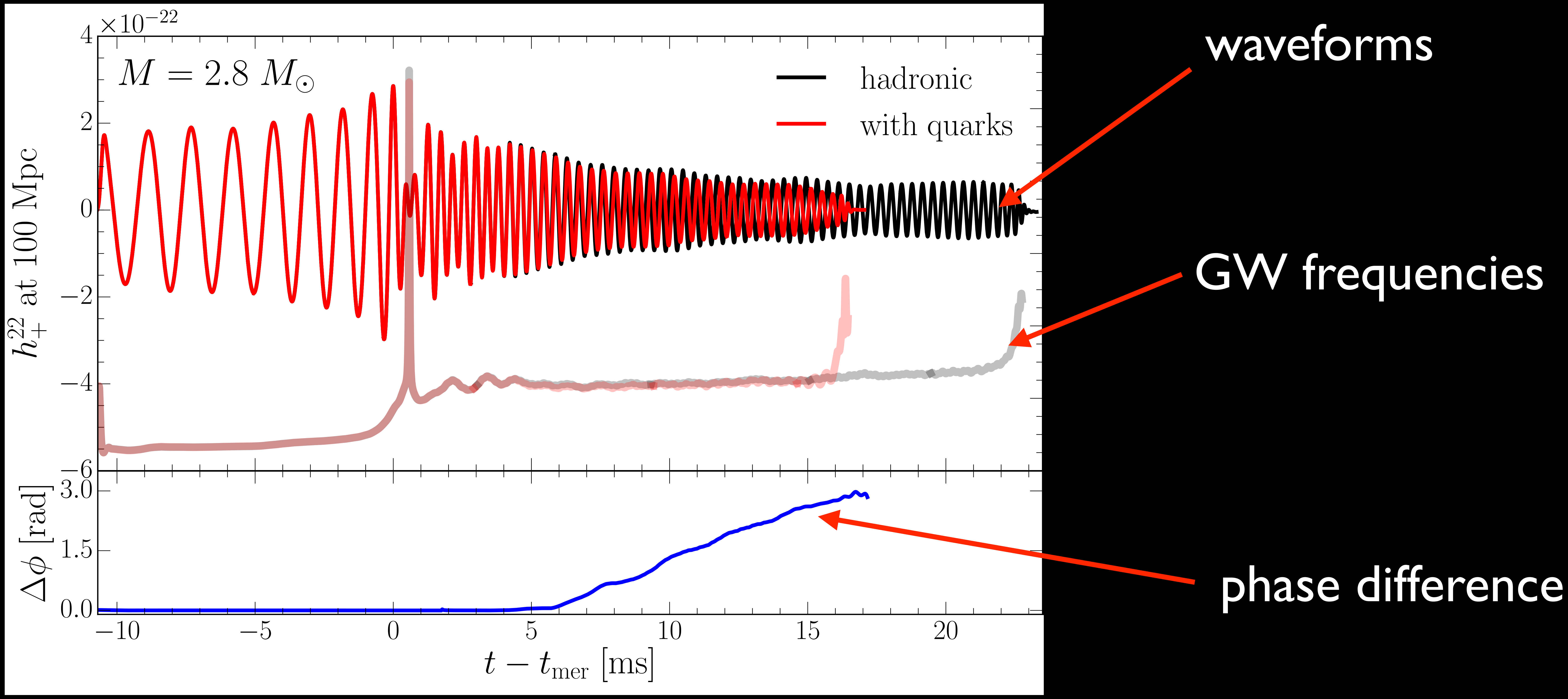

waveforms

GW frequencies

phase difference

- After ~5 ms, quark fraction large enough to yield differences in GWs
- Softening of PT leads to collapse and **different** phase evolution.

Observing mismatch between **inspiral** (fully hadronic) and **post-merger** (phase transition): clear **signature** of a **PT**

More consistent microphysics: V-QCD

Tootle, Ecker, Topolski, Demircik, Järvinen, LR (2022)

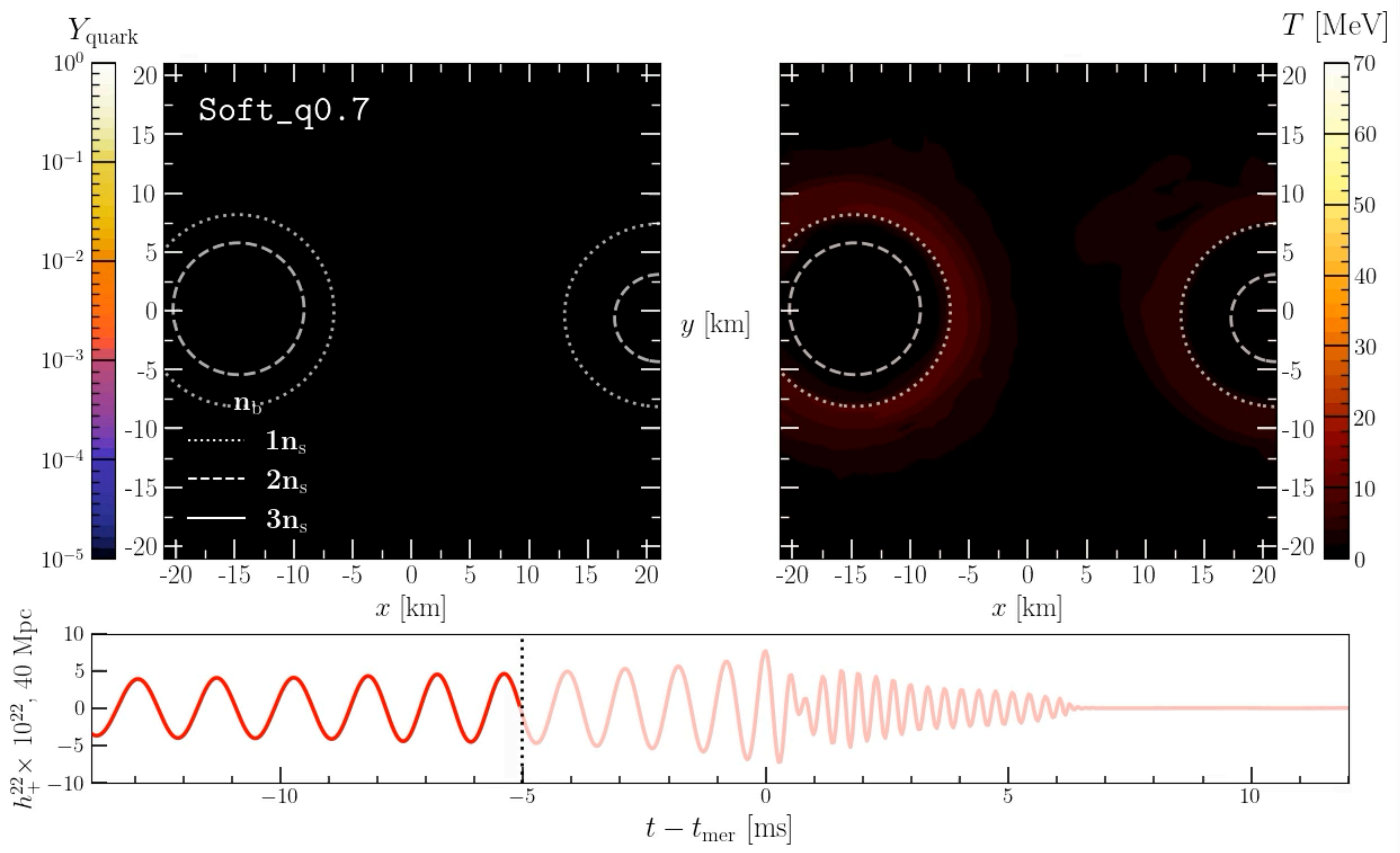

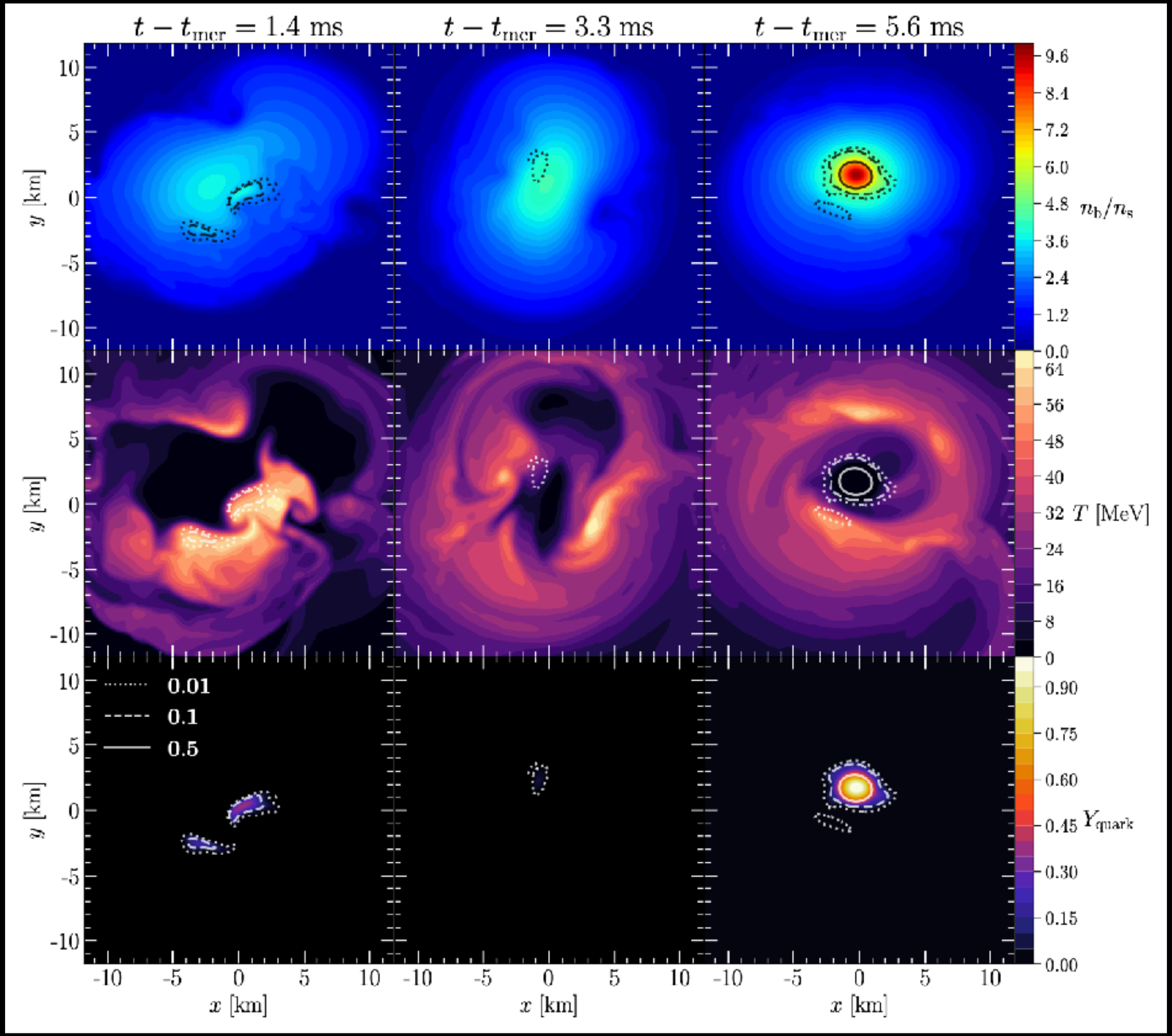

The dynamics is very similar to previous simplified thermal treatment: as soon as the PT takes place, softening induces a rapid collapse.

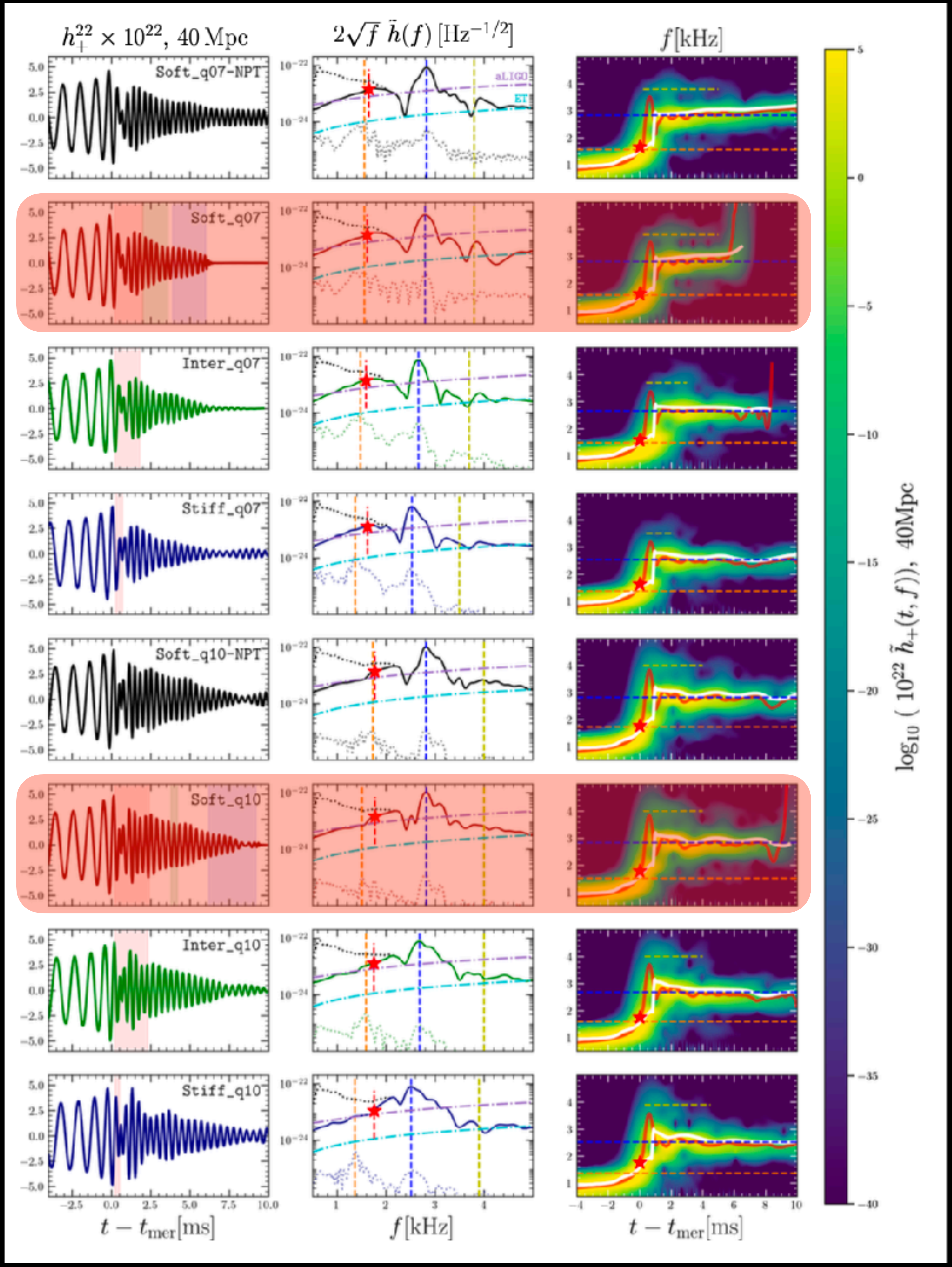

From GWs to the phase diagram

Soft version of V-QCD ruled out by **GW170817:** collapse too early.

Expectation is the collapse has been after 0.9 s.

Example that GW events can constrain appearance of QCD PT.

A zoology of possible behaviours

The occurrence of a PT can take place in a number of different ways. What shown is only one. Here are the other possibilities:

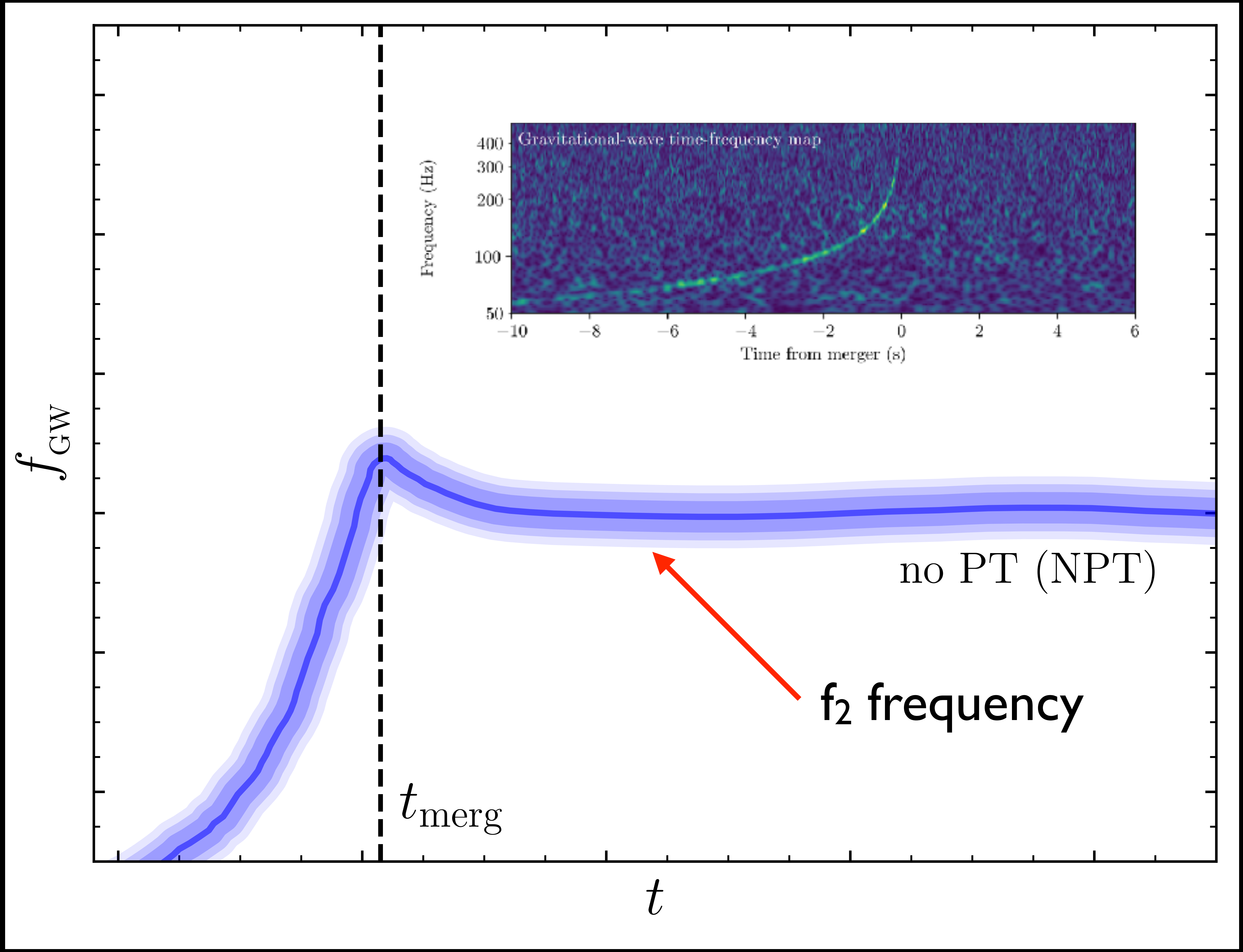

f_2 frequency

A zoology of possible behaviours

The occurrence of a PT can take place in a number of different ways. What shown is only one. Here are the other possibilities:

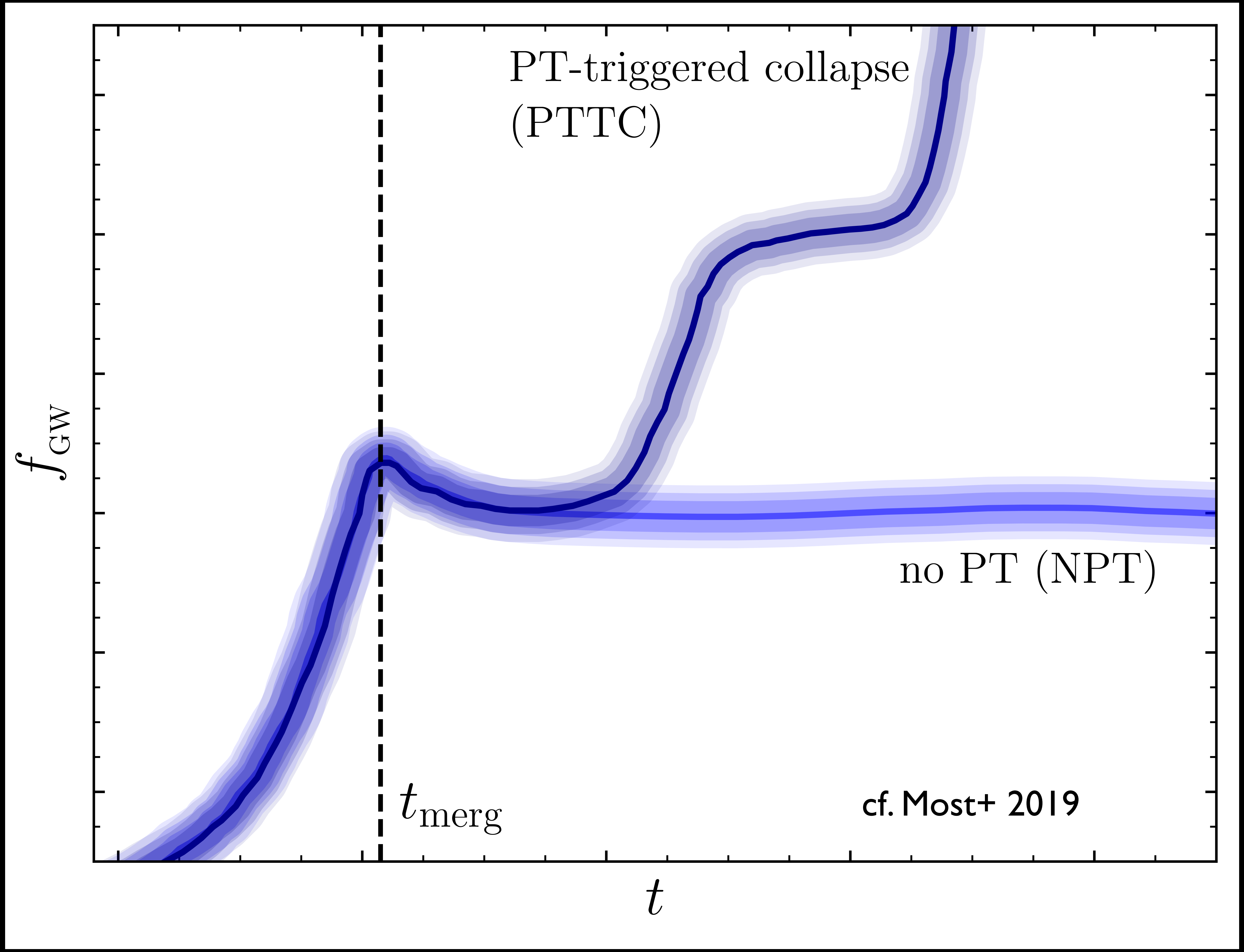

A zoology of possible behaviours

The occurrence of a PT can take place in a number of different ways.
What shown is only one. Here are the other possibilities:

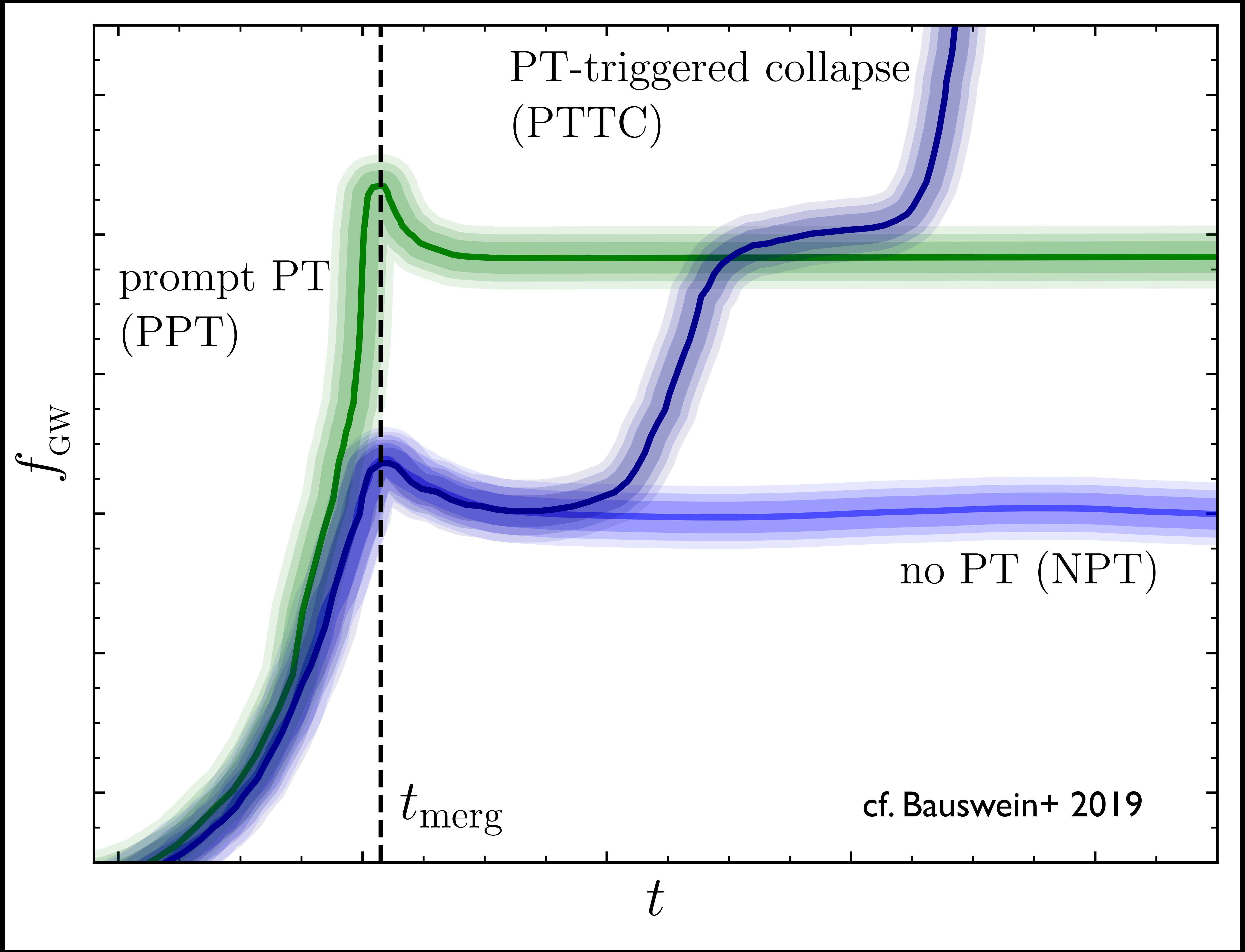

A zoology of possible behaviours

The occurrence of a PT can take place in a number of different ways. What shown is only one. Here are the other possibilities:

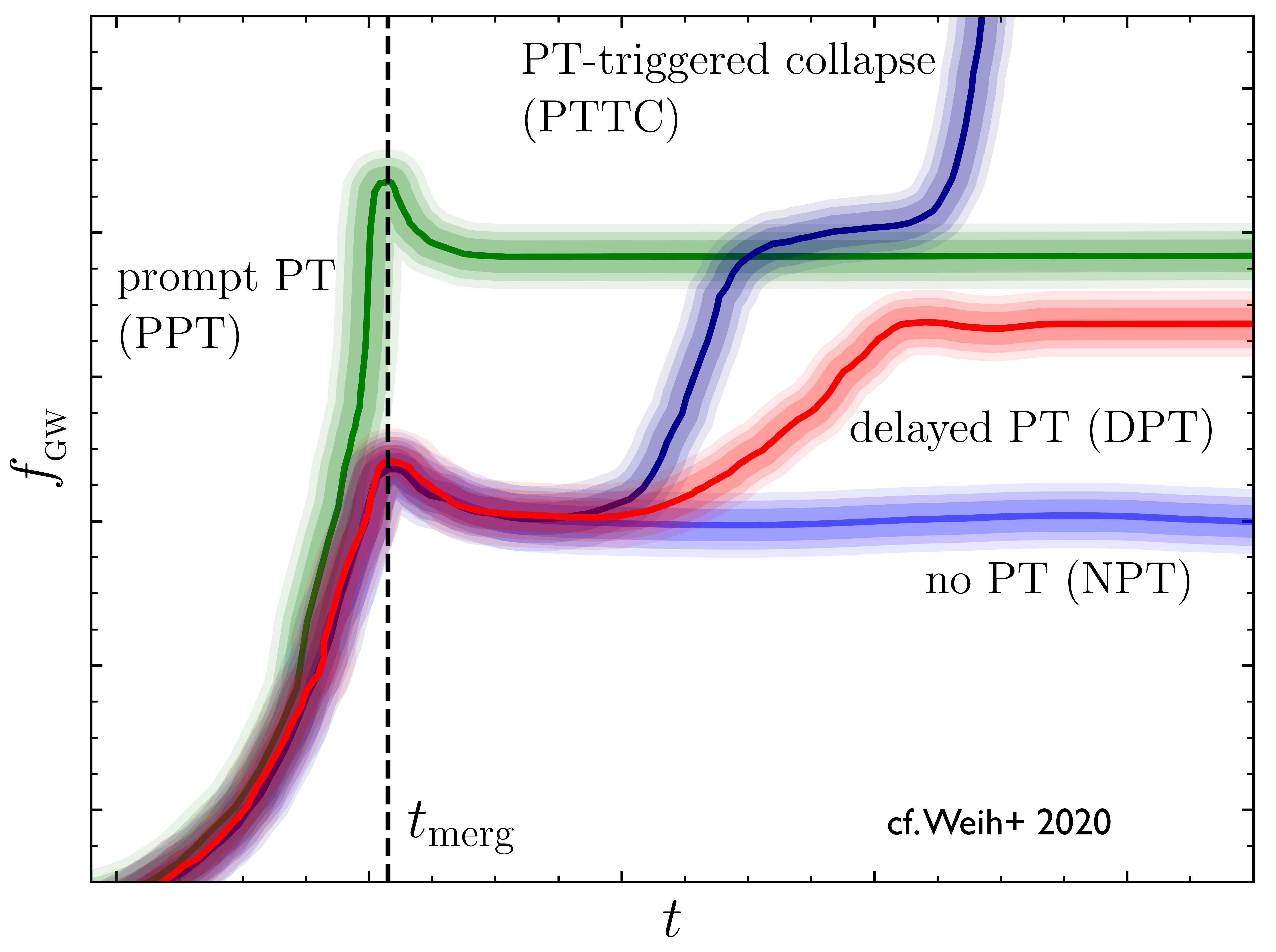

cf. Weih+ 2020

A more comprehensive picture

Zoology discussed above can be recognised when shown in terms of the gravitational waves and their spectrograms.

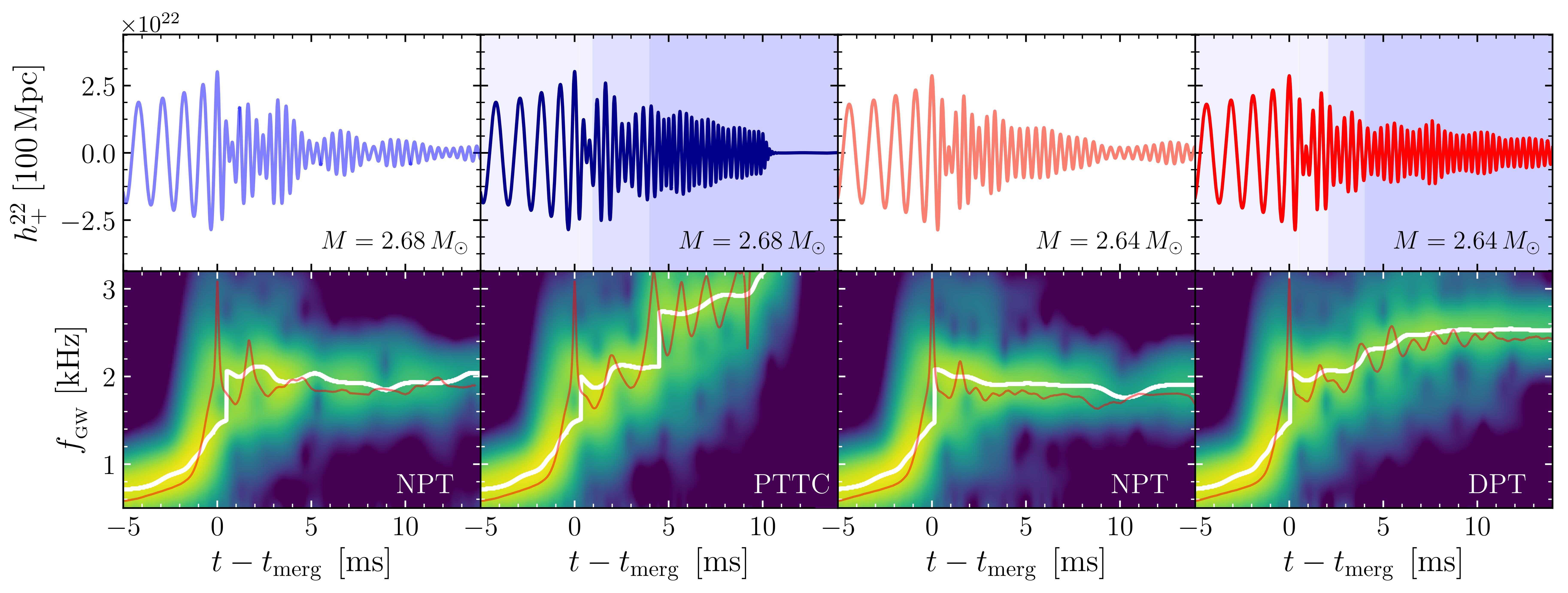

A more comprehensive picture

Zoology discussed above can be recognised when shown in terms of the gravitational waves and their spectrograms.

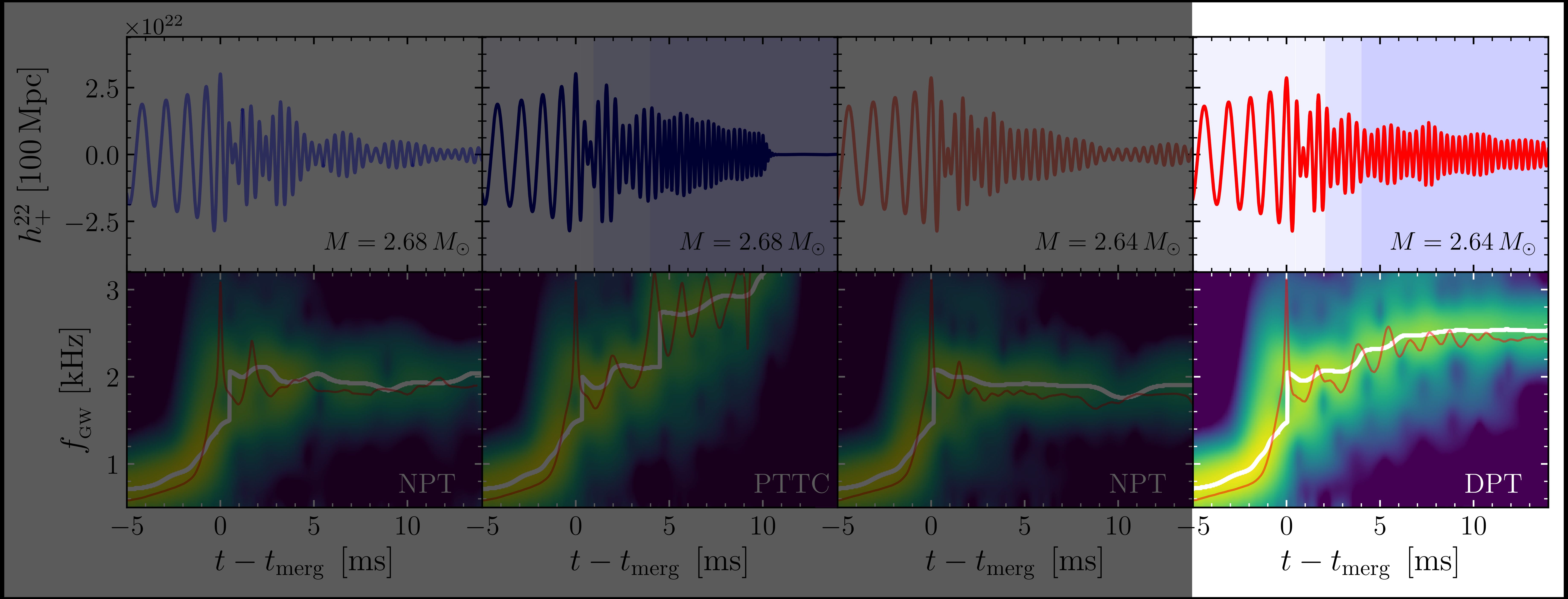

Importance of **DPT** is that it leads to **two** different "stable" f_2 **frequencies** that are easily distinguishable in the PSD

Why DPT is the most interesting case

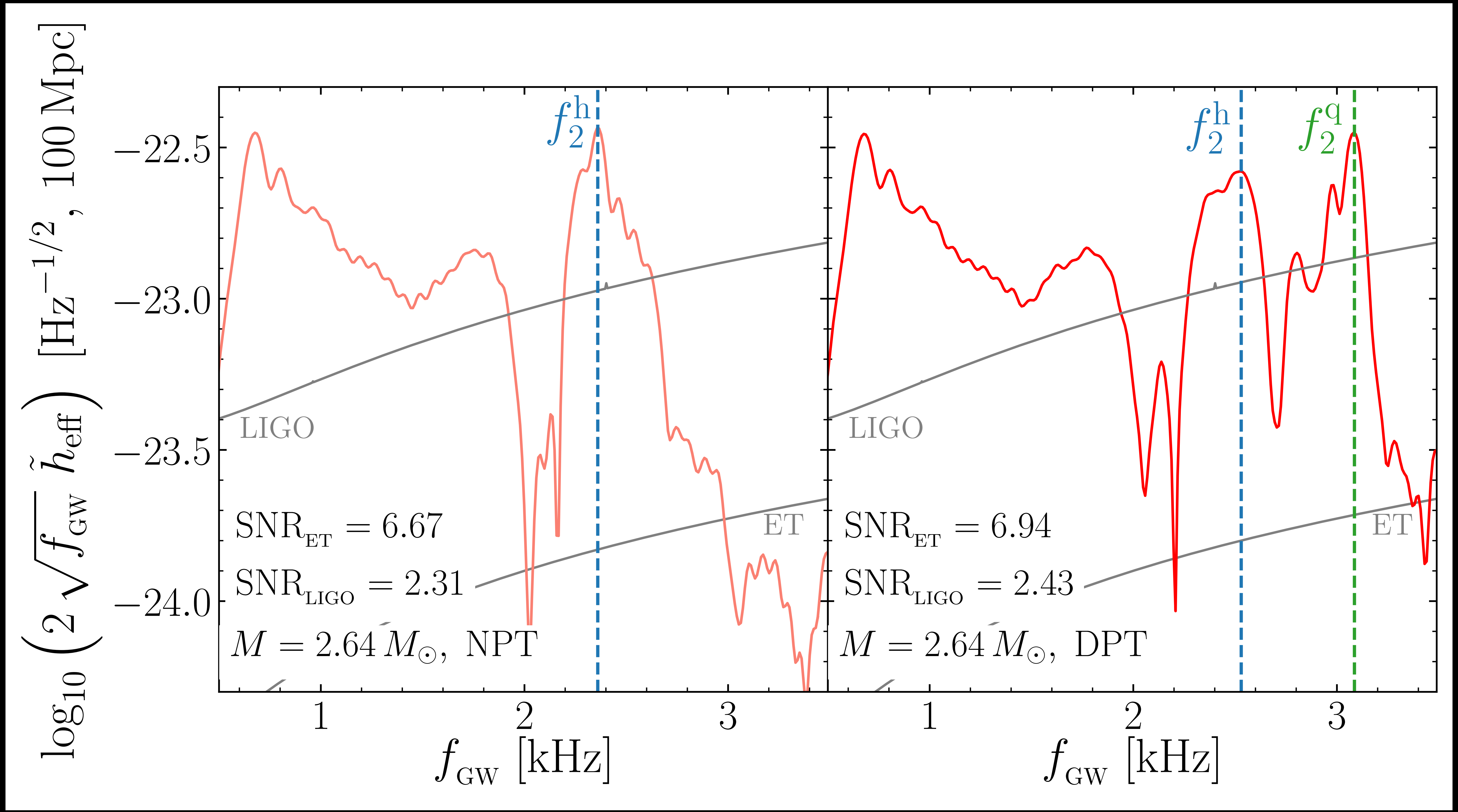

Importance of **DPT** is that it leads to **two** different "stable" f_2 **frequencies** that are easily distinguishable in the PSD

Conclusions

- Spectra of post-merger shows peaks, some "quasi-universal".
- When used together with tens of observations, they will set tight constraints on EOS: radius known with **~1 km** precision.
- A **phase transition** after a BNS merger leaves GW **signatures** and opens a gate to access quark matter beyond accelerators.

EXTRAS

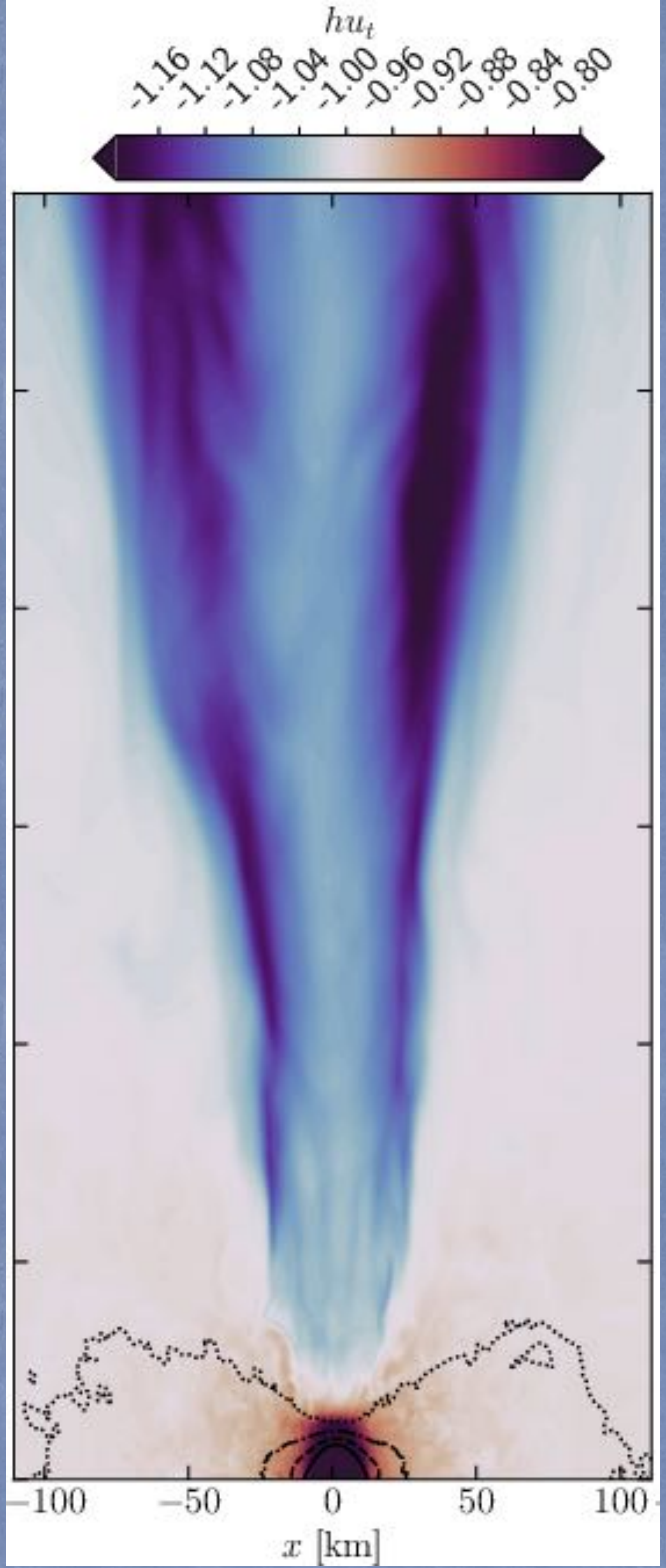

HMNS-powered jets?

Musolino, Most, LR (2025)

HMNS powering jets

The idea that an HMNS could power jets is old and appealing.

Pros

- HMNS naturally produced in BNS mergers and lifetime can be long: $\gtrsim 1\,\mathrm{s}$ (Gill+ 2019, Murguia-Bertier+2021 for GW170817).
- Plenty of (rotational) energy in the HMNS.
- Plenty of magnetic fields and emission easy to model.

Cons

- HMNS naturally produce baryon polluted environments.
- Short simulations showed no evidence of jets.
- Long simulations show evidence of outflows (!) but with a number of approximations (no neutrinos, no B-fields)

HMNS powering jets

We have carried out long-term, high-resolution, GRMHD simulations with neutrino transfer (M1).

this was typical timescale for evolutions: ~ 40 ms

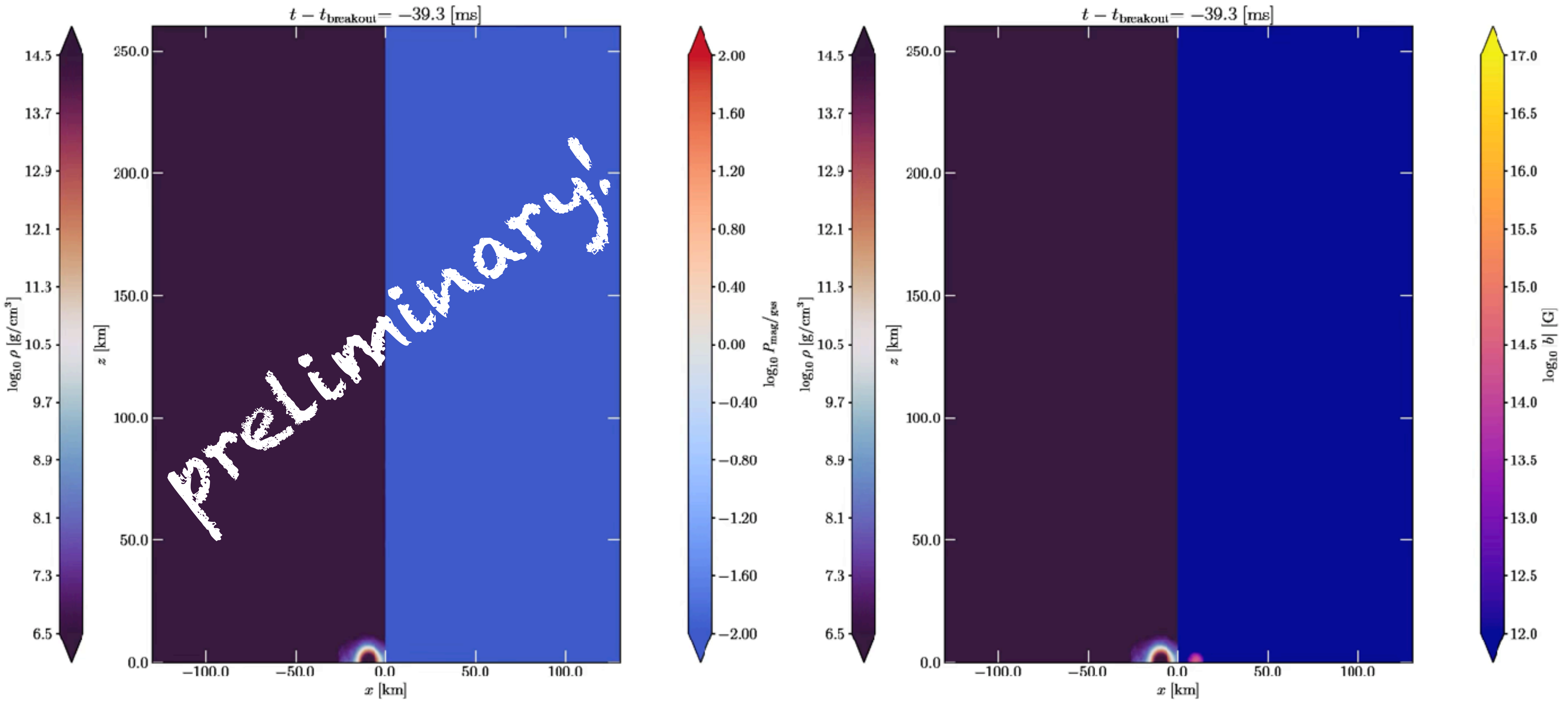

HMNS powering jets

We have carried out long-term, high-resolution, GRMHD simulations with neutrino transfer (M1).

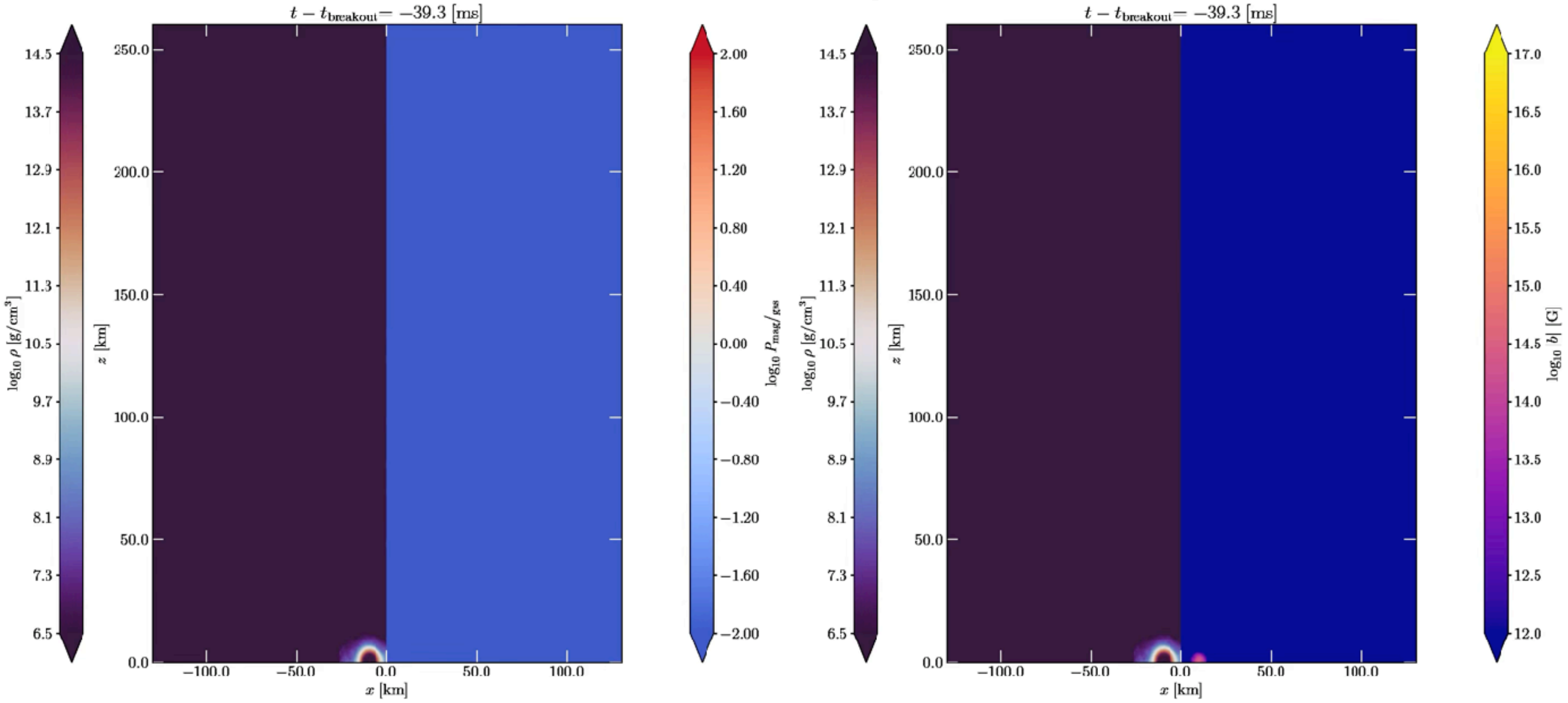

we have extended this by a factor of three

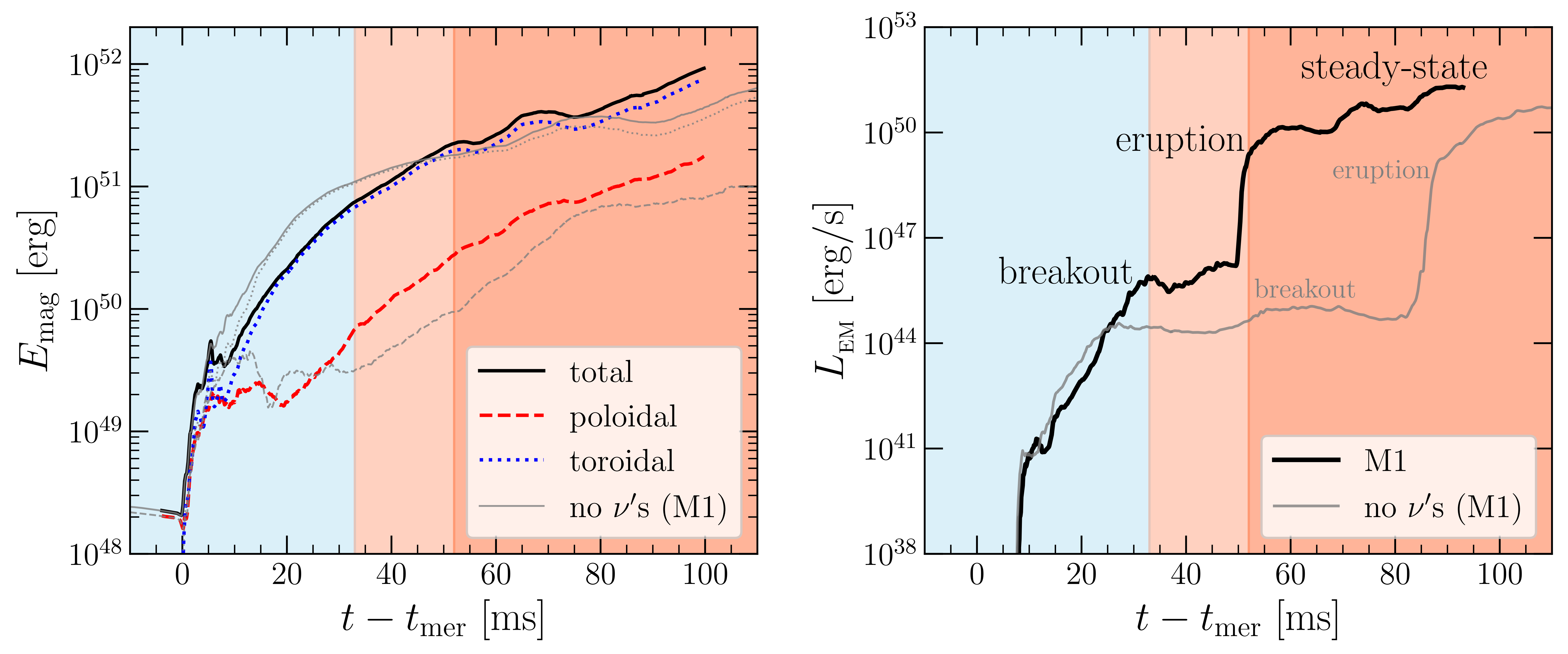

$E_{\rm mag}$ [erg]
10^{48}
10^{49}
10^{50}
10^{51}
10^{52}
0
20
40
60
80
100
$t - t_{\rm mer}$ [ms]
total
poloidal
toroidal
no ν's (M1)
$L_{\rm EM}$ [erg/s]
10^{38}
10^{41}
10^{44}
10^{47}
10^{50}
10^{53}
breakout
eruption
steady-state
breakout
eruption
M1
no ν's (M1)

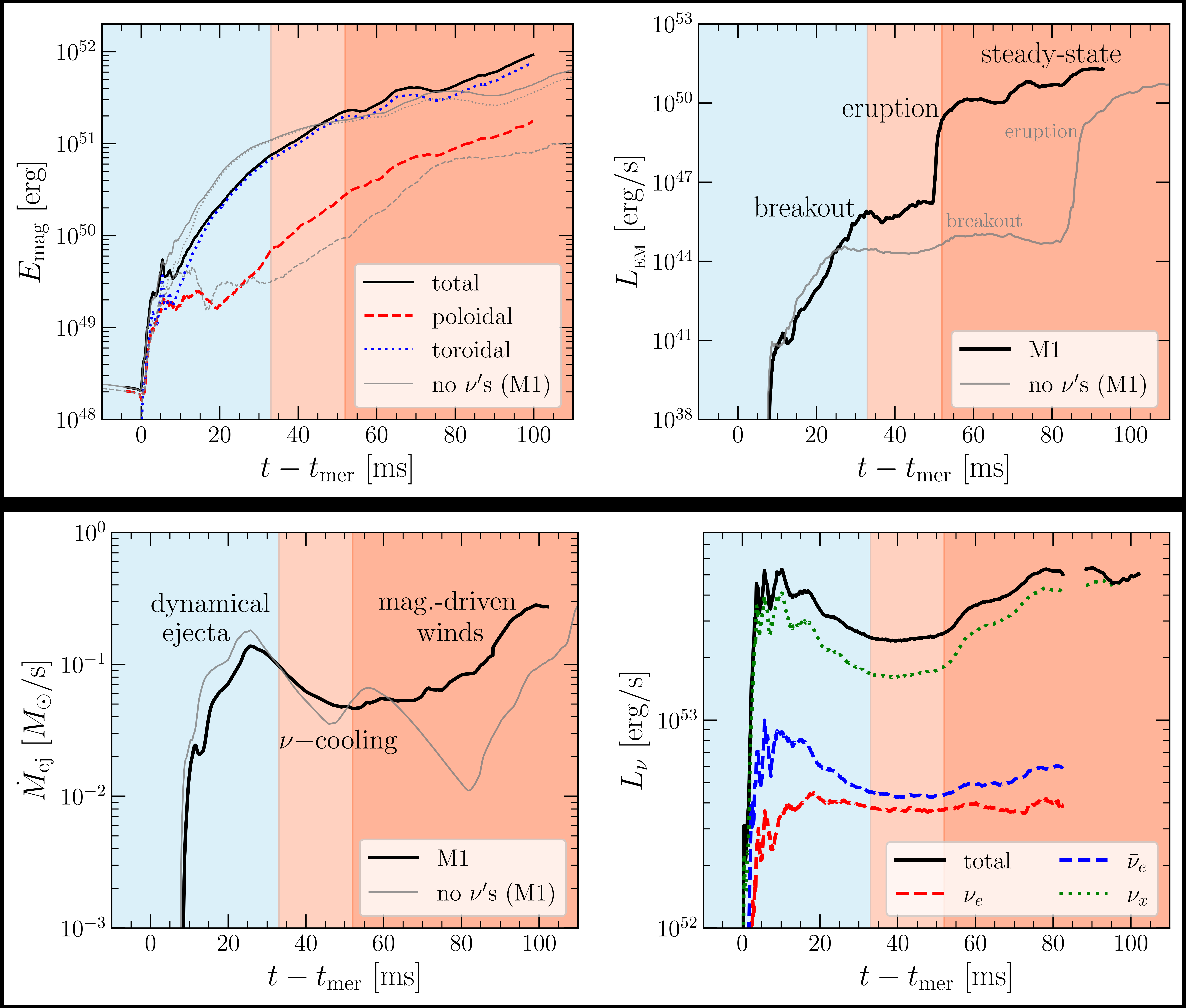

$E_{\rm mag}$ [erg]
10^{48}
10^{49}
10^{50}
10^{51}
10^{52}
total
poloidal
toroidal
no ν's (M1)
$t - t_{\rm mer}$ [ms]
0
20
40
60
80
100
$L_{\rm EM}$ [erg/s]
10^{38}
10^{41}
10^{44}
10^{47}
10^{50}
10^{53}
steady-state
eruption
breakout
eruption
breakout
M1
no ν's (M1)
$t - t_{\rm mer}$ [ms]
$\dot{M}_{\rm ej}$ [$M_\odot$/s]
10^{-3}
10^{-2}
10^{-1}
10^{0}
dynamical ejecta
$\nu-$cooling
mag.-driven winds
M1
no ν's (M1)
$t - t_{\rm mer}$ [ms]
L_ν [erg/s]
10^{52}
10^{53}
total
$\bar{\nu}_e$
ν_e
ν_x
$t - t_{\rm mer}$ [ms]

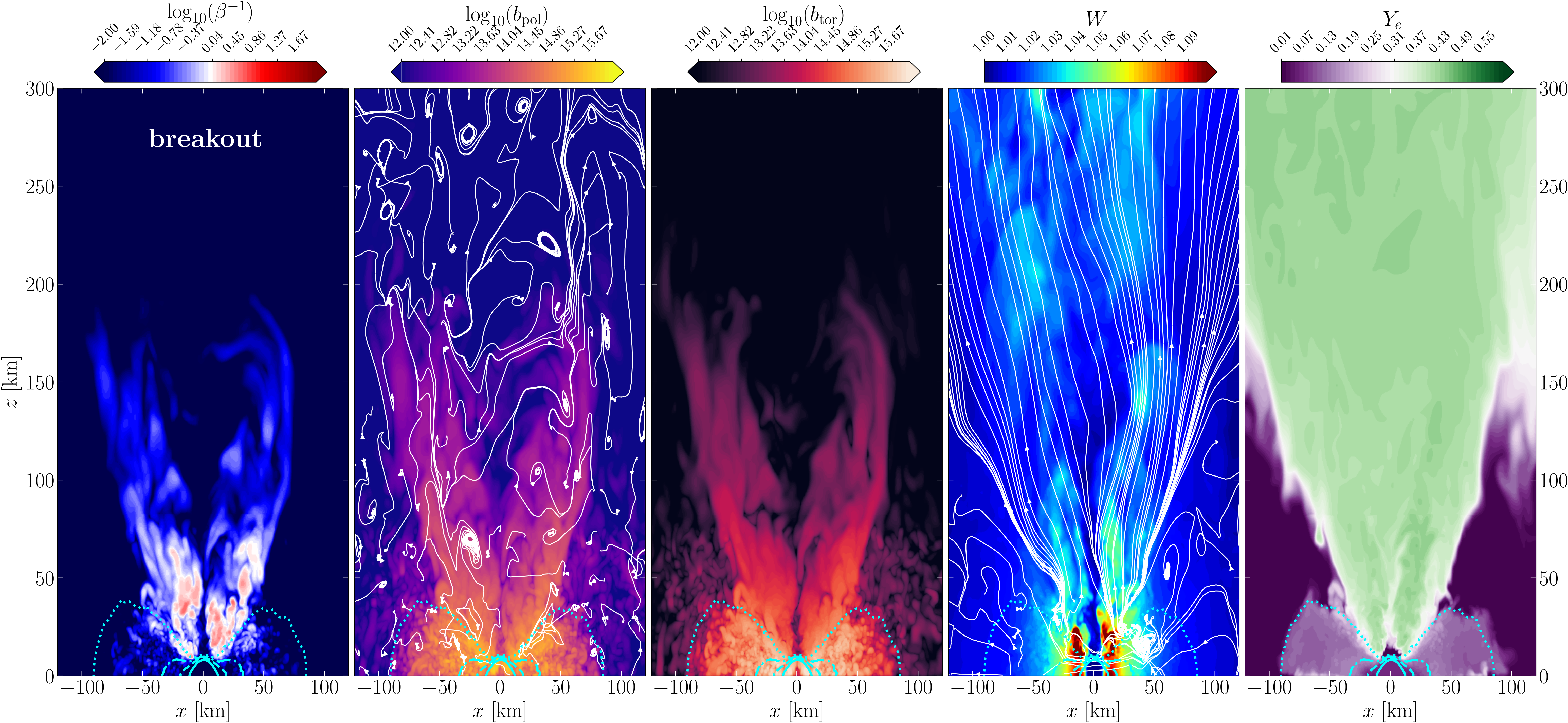

$\log_{10}(\beta^{-1})$
−2.00 −1.59 −1.18 −0.78 −0.37 0.04 0.45 0.86 1.27 1.67
$\log_{10}(b_{\rm pol})$
12.00 12.41 12.82 13.22 13.63 14.04 14.45 14.86 15.27 15.67
$\log_{10}(b_{\rm tor})$
12.00 12.41 12.82 13.22 13.63 14.04 14.45 14.86 15.27 15.67
W
1.00 1.01 1.02 1.03 1.04 1.05 1.06 1.07 1.08 1.09
Y_e
0.01 0.07 0.13 0.19 0.25 0.31 0.37 0.43 0.49 0.55
breakout
z [km]
0 50 100 150 200 250 300
−100 −50 0 50 100
x [km]

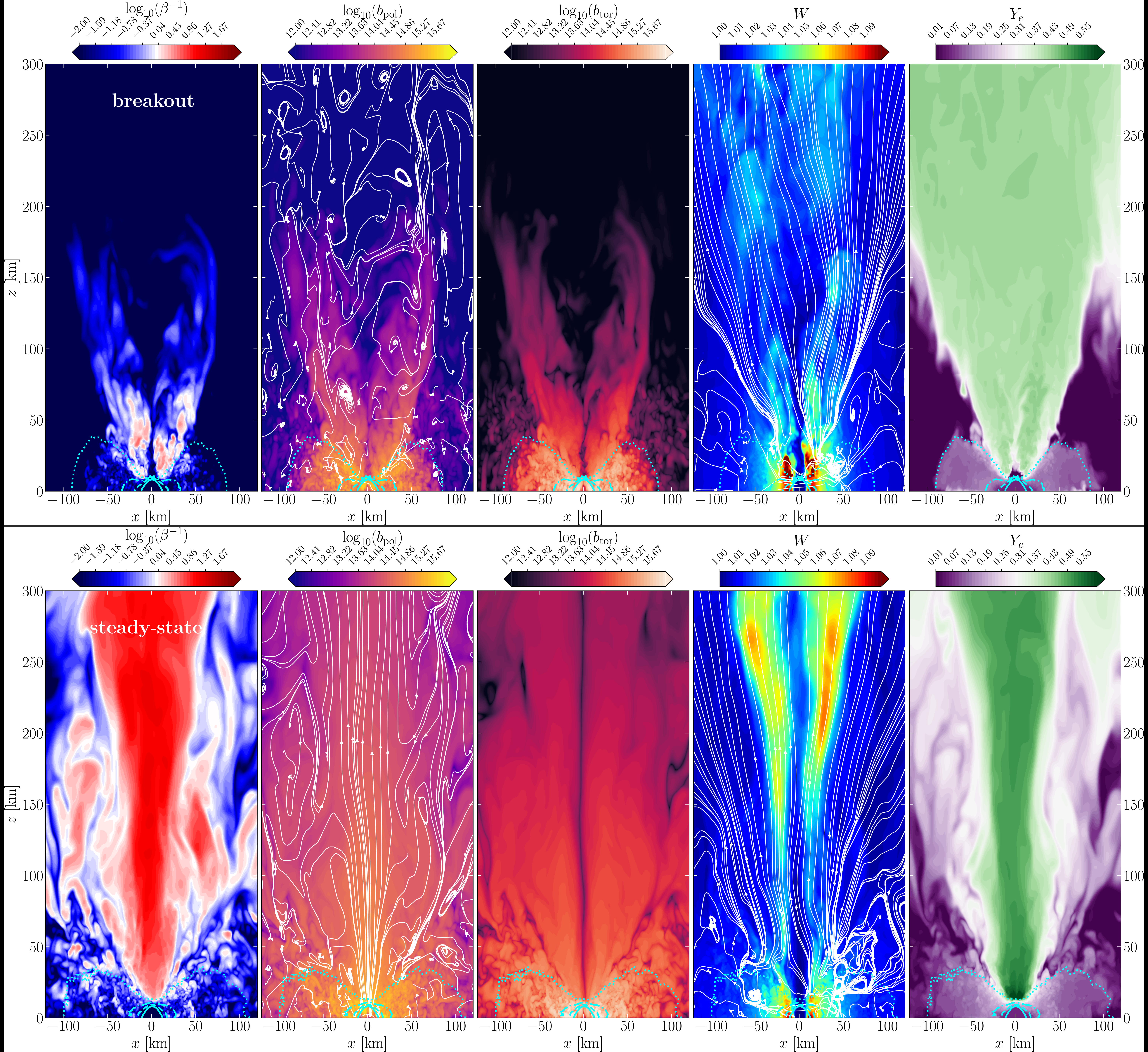
$\log_{10}(\beta^{-1})$
−2.00 −1.59 −1.18 −0.78 −0.37 0.04 0.45 0.86 1.27 1.67
$\log_{10}(b_{\rm pol})$
12.00 12.41 12.82 13.22 13.63 14.04 14.45 14.86 15.27 15.67
$\log_{10}(b_{\rm tor})$
12.00 12.41 12.82 13.22 13.63 14.04 14.45 14.86 15.27 15.67
W
1.00 1.01 1.02 1.03 1.04 1.05 1.06 1.07 1.08 1.09
Y_e
0.01 0.07 0.13 0.19 0.25 0.31 0.37 0.43 0.49 0.55
breakout
z [km]
0 50 100 150 200 250 300
x [km]
−100 −50 0 50 100
$\log_{10}(\beta^{-1})$
−2.00 −1.59 −1.18 −0.78 −0.37 0.04 0.45 0.86 1.27 1.67
$\log_{10}(b_{\rm pol})$
12.00 12.41 12.82 13.22 13.63 14.04 14.45 14.86 15.27 15.67
$\log_{10}(b_{\rm tor})$
12.00 12.41 12.82 13.22 13.63 14.04 14.45 14.86 15.27 15.67
W
1.00 1.01 1.02 1.03 1.04 1.05 1.06 1.07 1.08 1.09
Y_e
0.01 0.07 0.13 0.19 0.25 0.31 0.37 0.43 0.49 0.55
steady-state
z [km]
0 50 100 150 200 250 300
x [km]
−100 −50 0 50 100

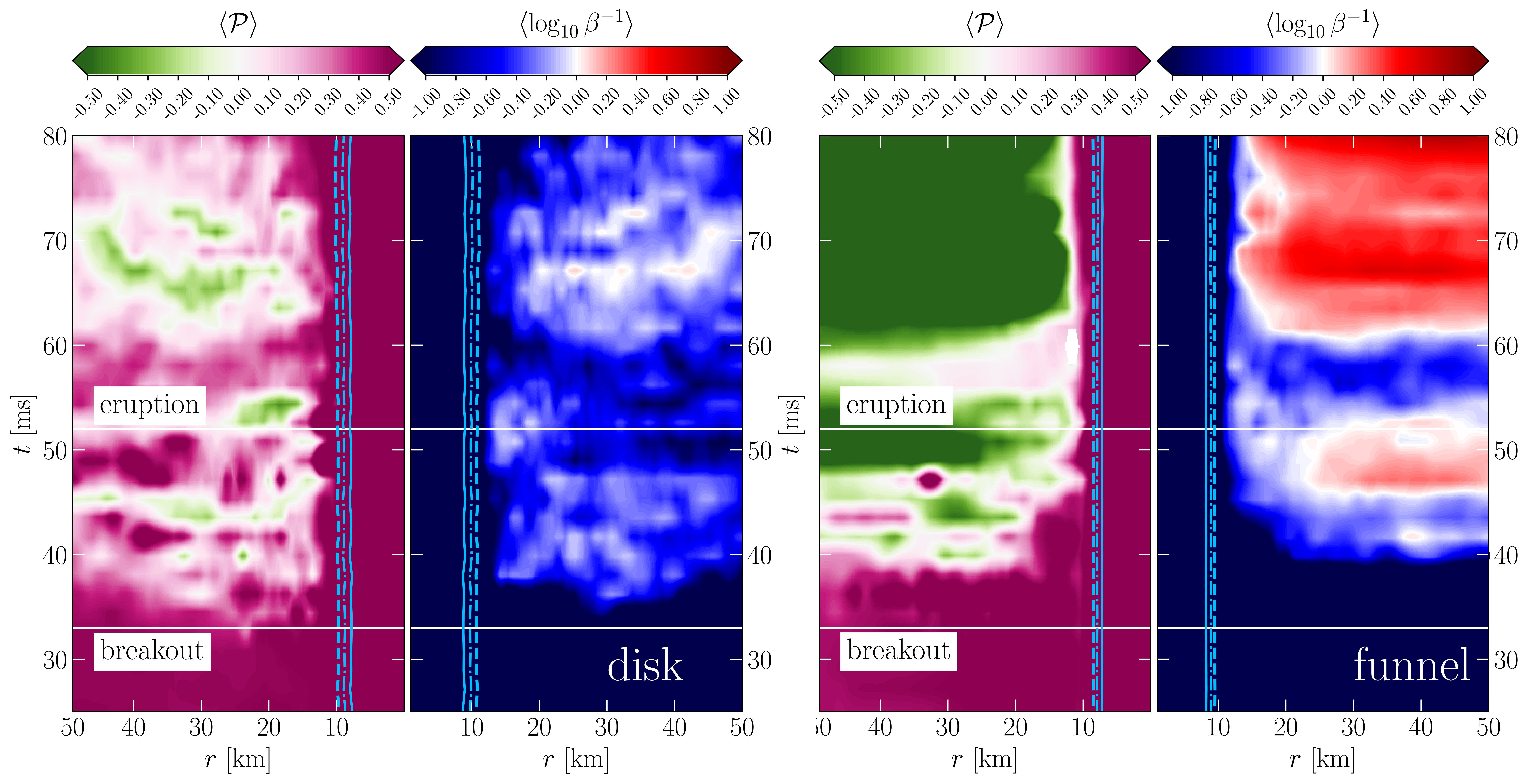
⟨$\mathcal{P}$⟩
⟨$\log_{10}\beta^{-1}$⟩
⟨$\mathcal{P}$⟩
⟨$\log_{10}\beta^{-1}$⟩
-0.50 -0.40 -0.30 -0.20 -0.10 0.00 0.10 0.20 0.30 0.40 0.50
-1.00 -0.80 -0.60 -0.40 -0.20 0.00 0.20 0.40 0.60 0.80 1.00
t [ms]
80 70 60 50 40 30
eruption
breakout
disk
funnel
r [km]
50 40 30 20 10
10 20 30 40 50

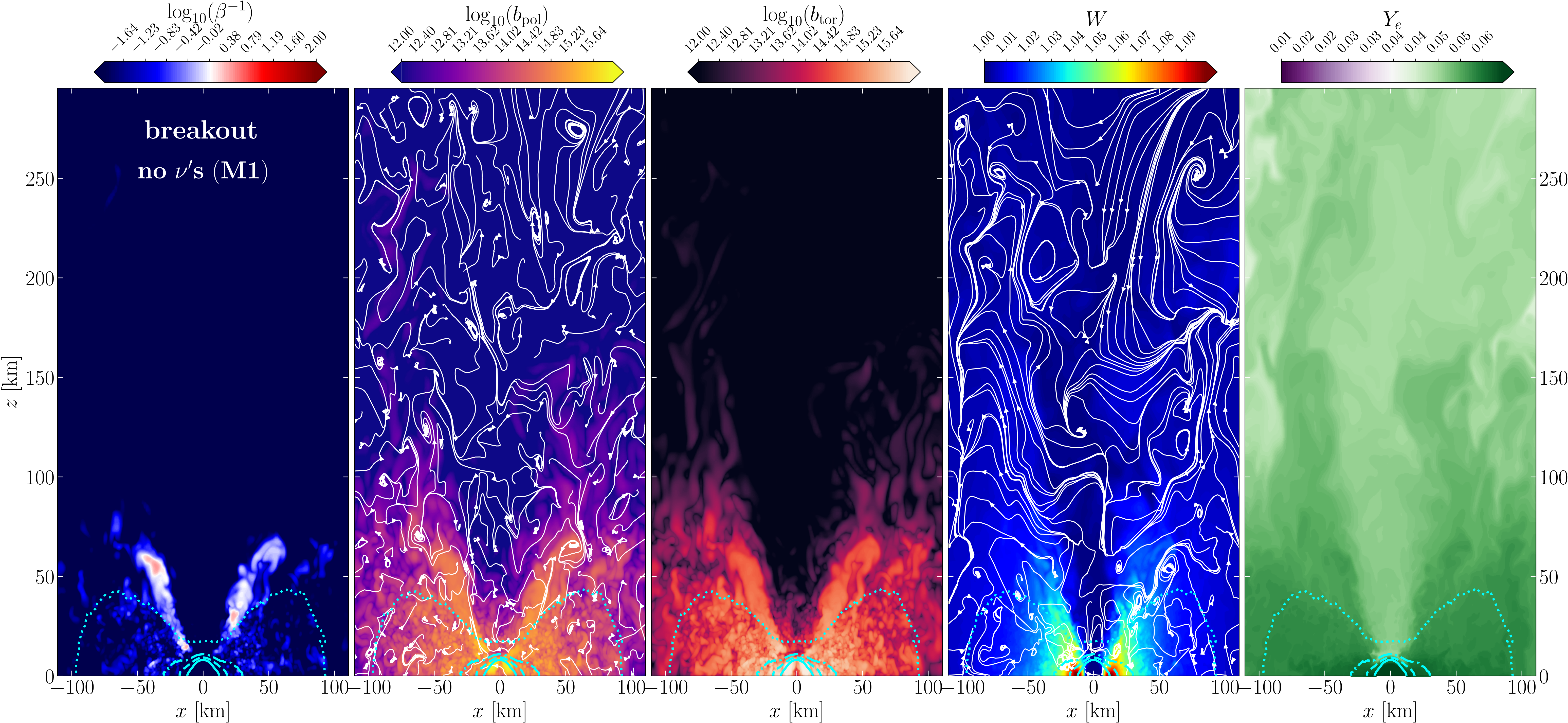
breakout
no ν's (M1)
$\log_{10}(\beta^{-1})$
−1.64 −1.23 −0.83 −0.42 −0.02 0.38 0.79 1.19 1.60 2.00
$\log_{10}(b_{\rm pol})$
12.00 12.40 12.81 13.21 13.62 14.02 14.42 14.83 15.23 15.64
$\log_{10}(b_{\rm tor})$
12.00 12.40 12.81 13.21 13.62 14.02 14.42 14.83 15.23 15.64
W
1.00 1.01 1.02 1.03 1.04 1.05 1.06 1.07 1.08 1.09
Y_e
0.01 0.02 0.02 0.03 0.03 0.04 0.04 0.05 0.05 0.06
z [km]
0 50 100 150 200 250
x [km]
−100 −50 0 50 100

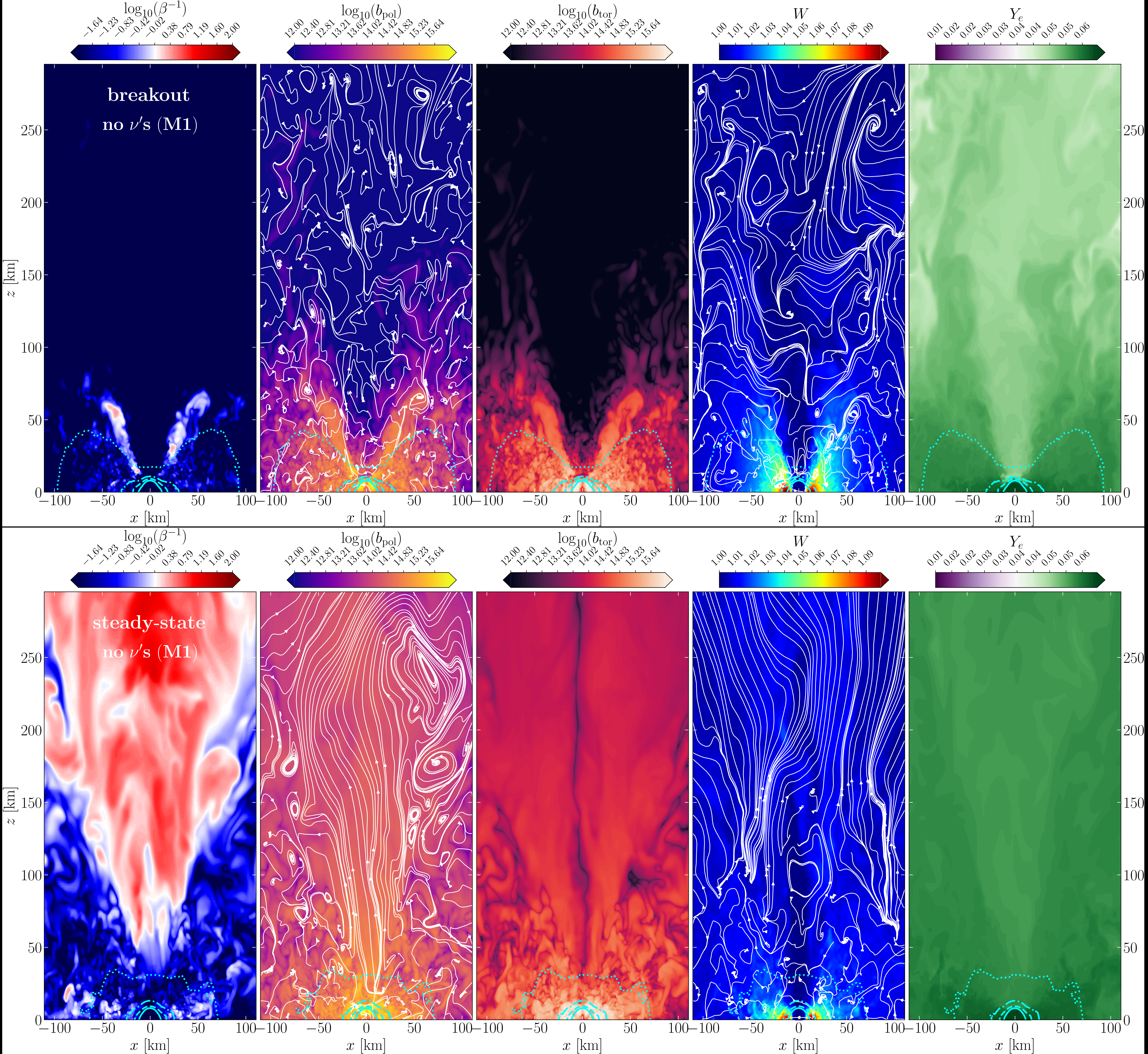
$\log_{10}(\beta^{-1})$
−1.64 −1.23 −0.83 −0.42 −0.02 0.38 0.79 1.19 1.60 2.00
$\log_{10}(b_{\rm pol})$
12.00 12.40 12.81 13.21 13.62 14.02 14.42 14.83 15.23 15.64
$\log_{10}(b_{\rm tor})$
12.00 12.40 12.81 13.21 13.62 14.02 14.42 14.83 15.23 15.64
W
1.00 1.01 1.02 1.03 1.04 1.05 1.06 1.07 1.08 1.09
Y_e
0.01 0.02 0.02 0.03 0.03 0.04 0.04 0.05 0.05 0.06
breakout
no ν's (M1)
steady-state
no ν's (M1)
z [km]
x [km]
−100 −50 0 50 100
0 50 100 150 200 250

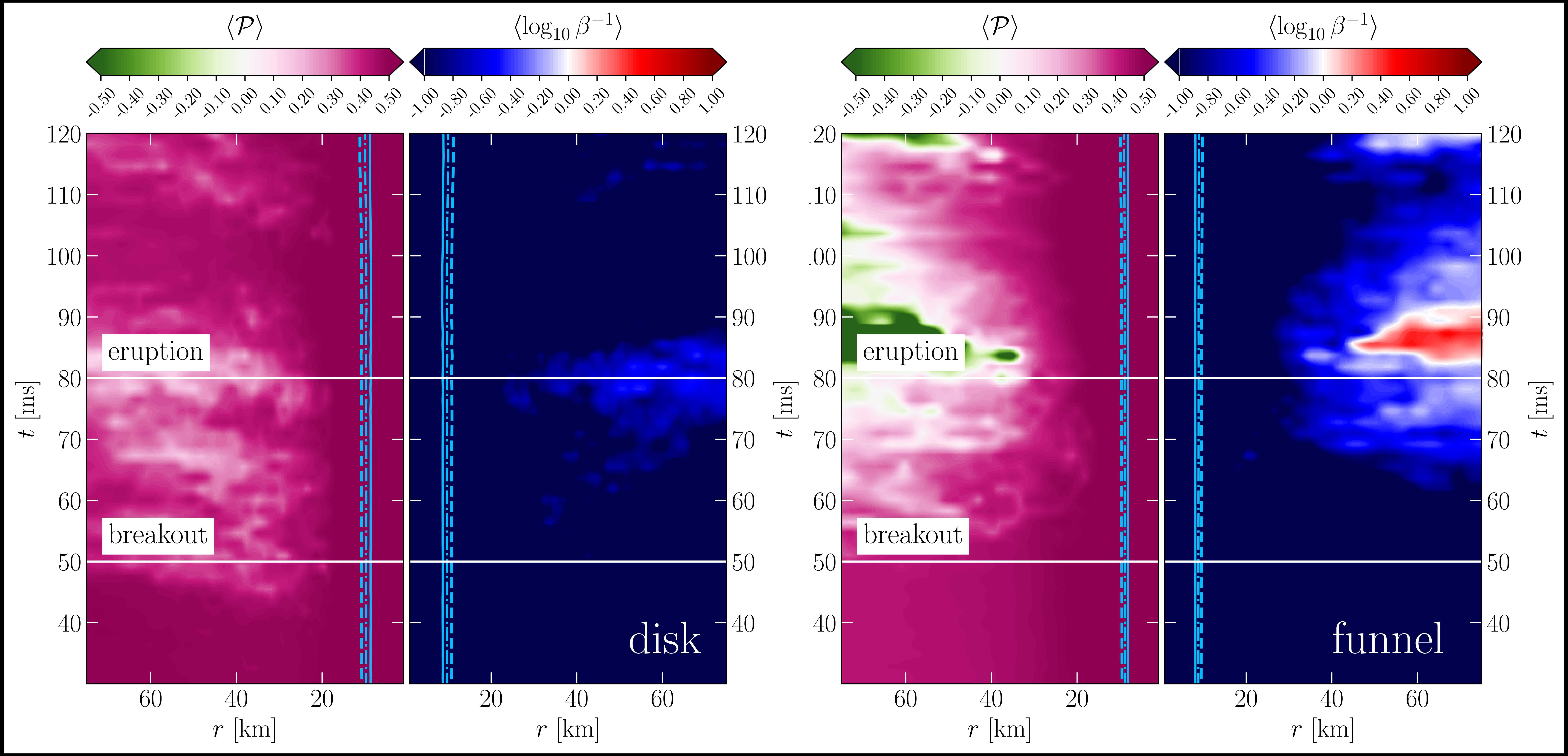

$\langle\mathcal{P}\rangle$
$\langle\log_{10}\beta^{-1}\rangle$
$\langle\mathcal{P}\rangle$
$\langle\log_{10}\beta^{-1}\rangle$
-0.50 -0.40 -0.30 -0.20 -0.10 0.00 0.10 0.20 0.30 0.40 0.50
-1.00 -0.80 -0.60 -0.40 -0.20 0.00 0.20 0.40 0.60 0.80 1.00
eruption
breakout
disk
funnel
t [ms]
120 110 100 90 80 70 60 50 40
r [km]
60 40 20
20 40 60

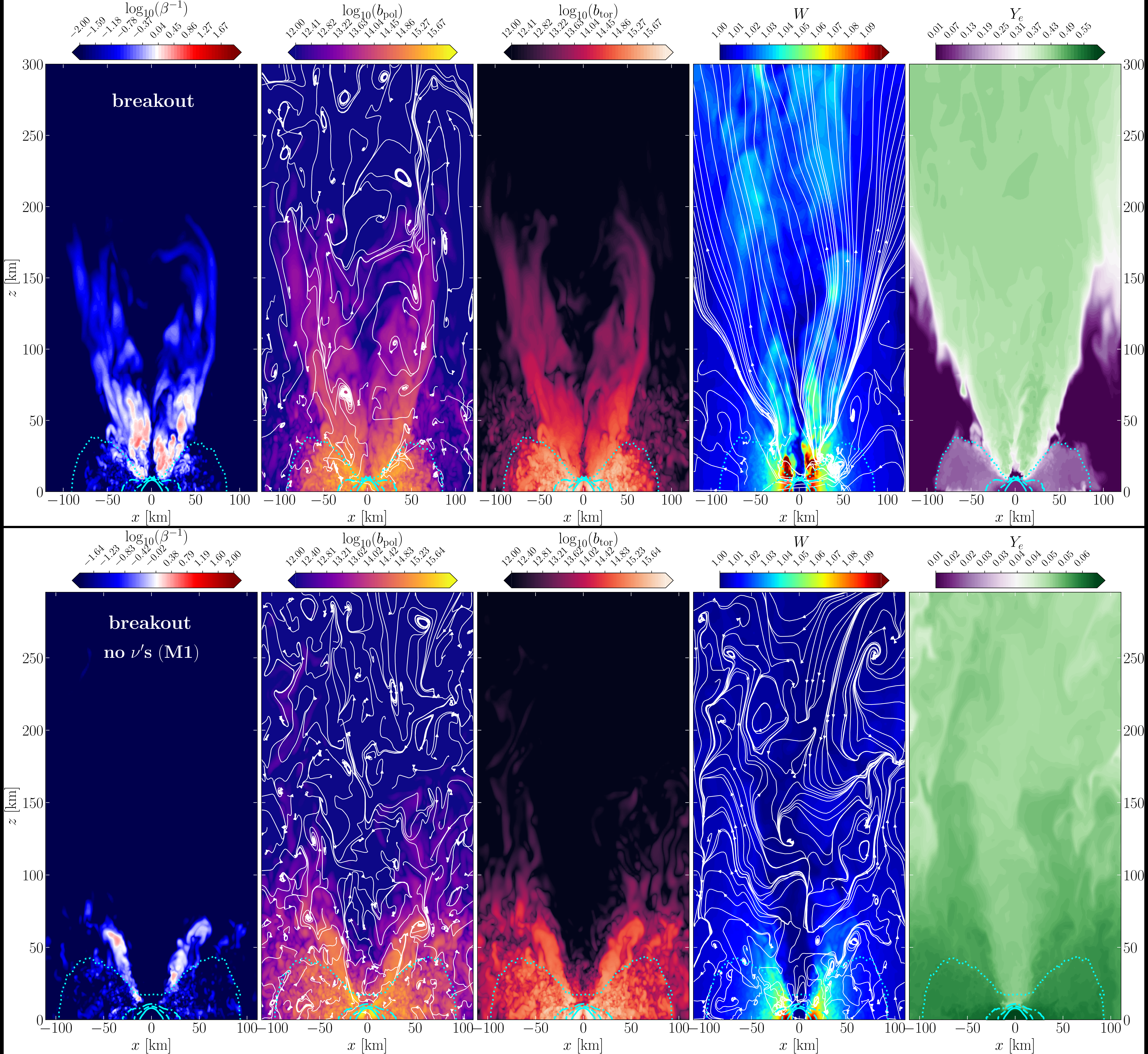
breakout
breakout
no ν's (M1)
$\log_{10}(\beta^{-1})$
−2.00 −1.59 −1.18 −0.78 −0.37 0.04 0.45 0.86 1.27 1.67
−1.64 −1.23 −0.83 −0.42 −0.02 0.38 0.79 1.19 1.60 2.00
$\log_{10}(b_{\rm pol})$
12.00 12.41 12.82 13.22 13.63 14.04 14.45 14.86 15.27 15.67
12.00 12.40 12.81 13.21 13.62 14.02 14.42 14.83 15.23 15.64
$\log_{10}(b_{\rm tor})$
12.00 12.41 12.82 13.22 13.63 14.04 14.45 14.86 15.27 15.67
12.00 12.40 12.81 13.21 13.62 14.02 14.42 14.83 15.23 15.64
W
1.00 1.01 1.02 1.03 1.04 1.05 1.06 1.07 1.08 1.09
Y_e
0.01 0.07 0.13 0.19 0.25 0.31 0.37 0.43 0.49 0.55
0.01 0.02 0.02 0.03 0.03 0.04 0.04 0.05 0.05 0.06
z [km]
0 50 100 150 200 250 300
x [km]
−100 −50 0 50 100

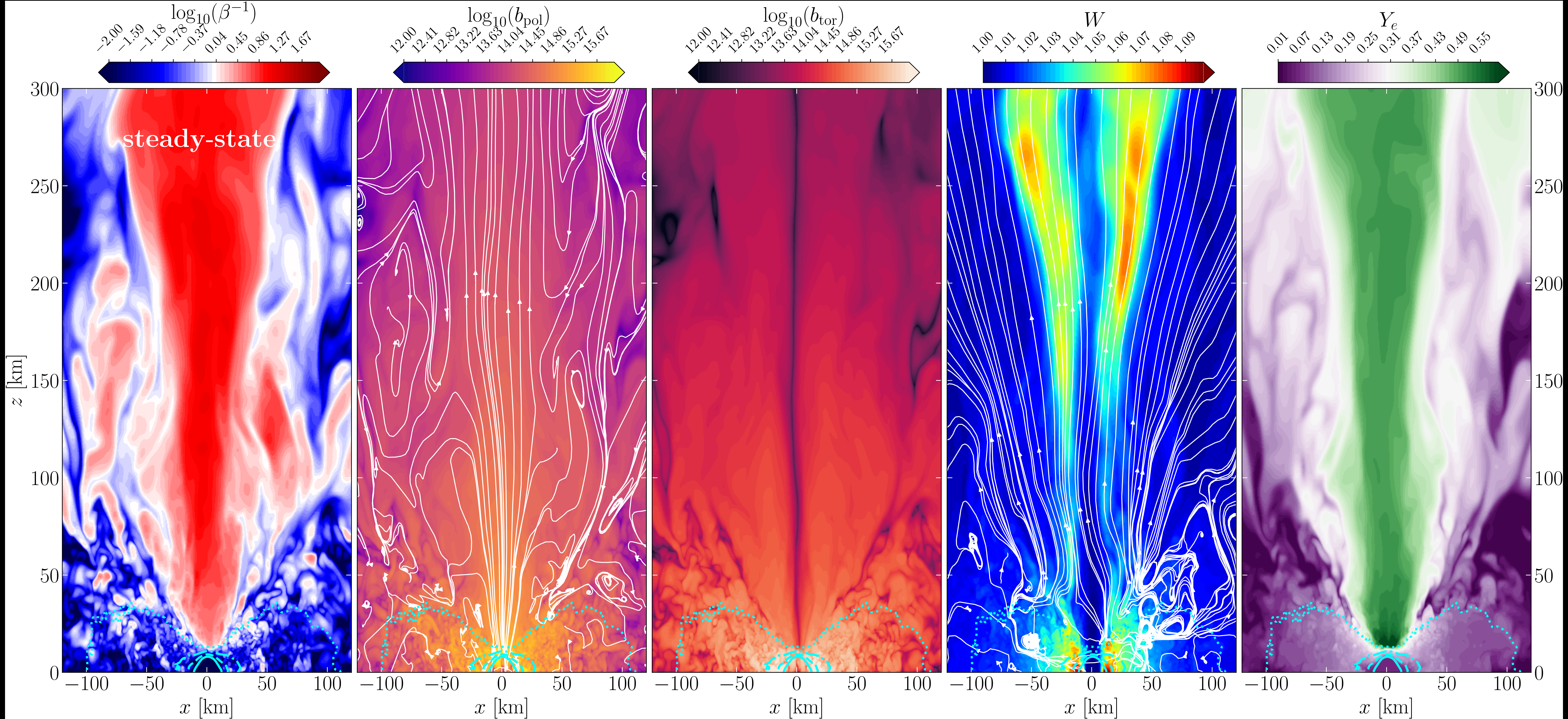
$\log_{10}(\beta^{-1})$
−2.00 −1.59 −1.18 −0.78 −0.37 0.04 0.45 0.86 1.27 1.67
$\log_{10}(b_{\rm pol})$
12.00 12.41 12.82 13.22 13.63 14.04 14.45 14.86 15.27 15.67
$\log_{10}(b_{\rm tor})$
12.00 12.41 12.82 13.22 13.63 14.04 14.45 14.86 15.27 15.67
W
1.00 1.01 1.02 1.03 1.04 1.05 1.06 1.07 1.08 1.09
Y_e
0.01 0.07 0.13 0.19 0.25 0.31 0.37 0.43 0.49 0.55
steady-state
z [km]
0 50 100 150 200 250 300
x [km]
−100 −50 0 50 100

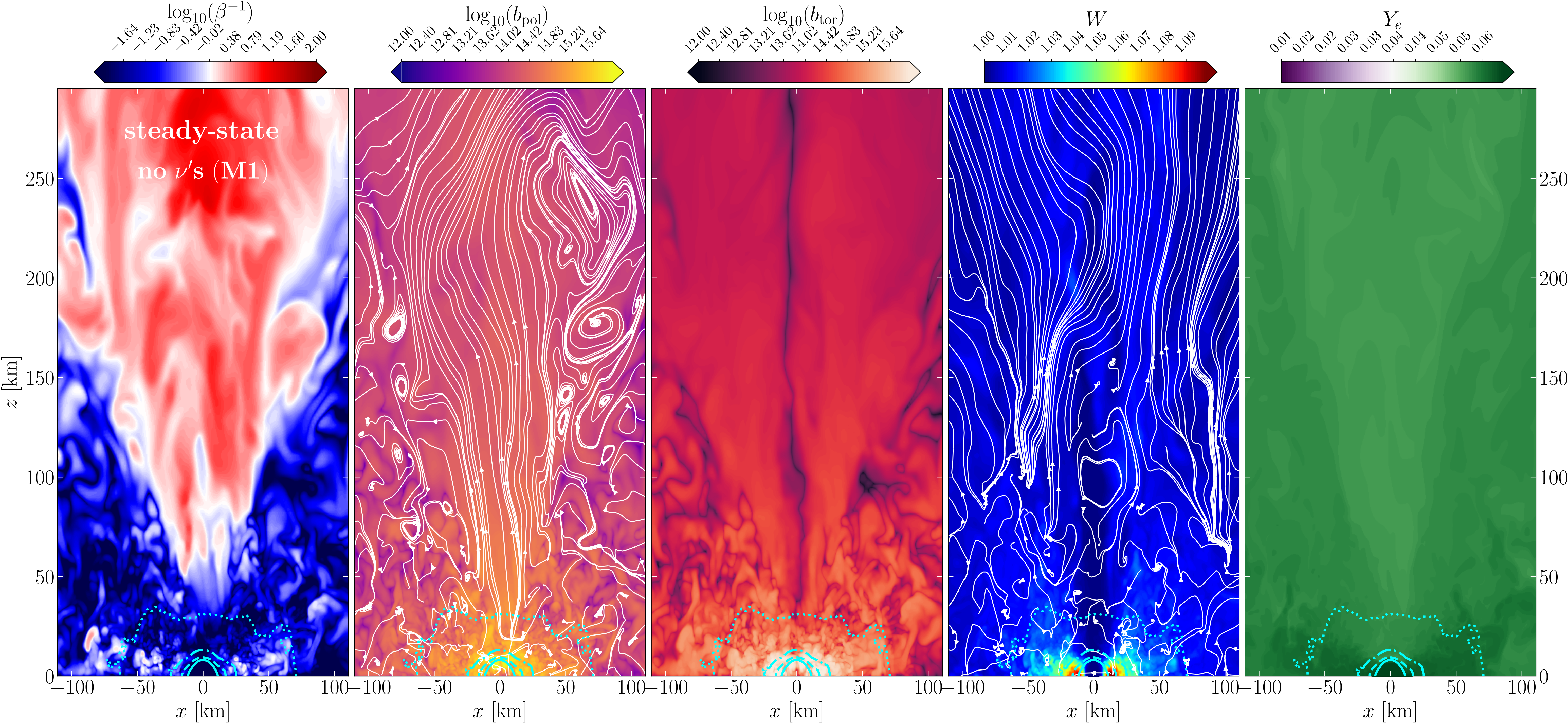
$\log_{10}(\beta^{-1})$
−1.64 −1.23 −0.83 −0.42 −0.02 0.38 0.79 1.19 1.60 2.00
$\log_{10}(b_{\rm pol})$
12.00 12.40 12.81 13.21 13.62 14.02 14.42 14.83 15.23 15.64
$\log_{10}(b_{\rm tor})$
12.00 12.40 12.81 13.21 13.62 14.02 14.42 14.83 15.23 15.64
W
1.00 1.01 1.02 1.03 1.04 1.05 1.06 1.07 1.08 1.09
Y_e
0.01 0.02 0.02 0.03 0.03 0.04 0.04 0.05 0.05 0.06
steady-state
no ν's (M1)
z [km]
0 50 100 150 200 250
x [km]
−100 −50 0 50 100

In essence:

- there is an outflow but not a relativistic jet ($\Gamma \lesssim 2$).
- Parker instability responsible for breakout at surface of torus and not core HMNS.
- Poynting flux jumps at breakout from 10^{43} to $10^{50}\,\mathrm{erg/s}$ and is ~ 2 orders of magnitude too small

Energy extraction from rotating BHs

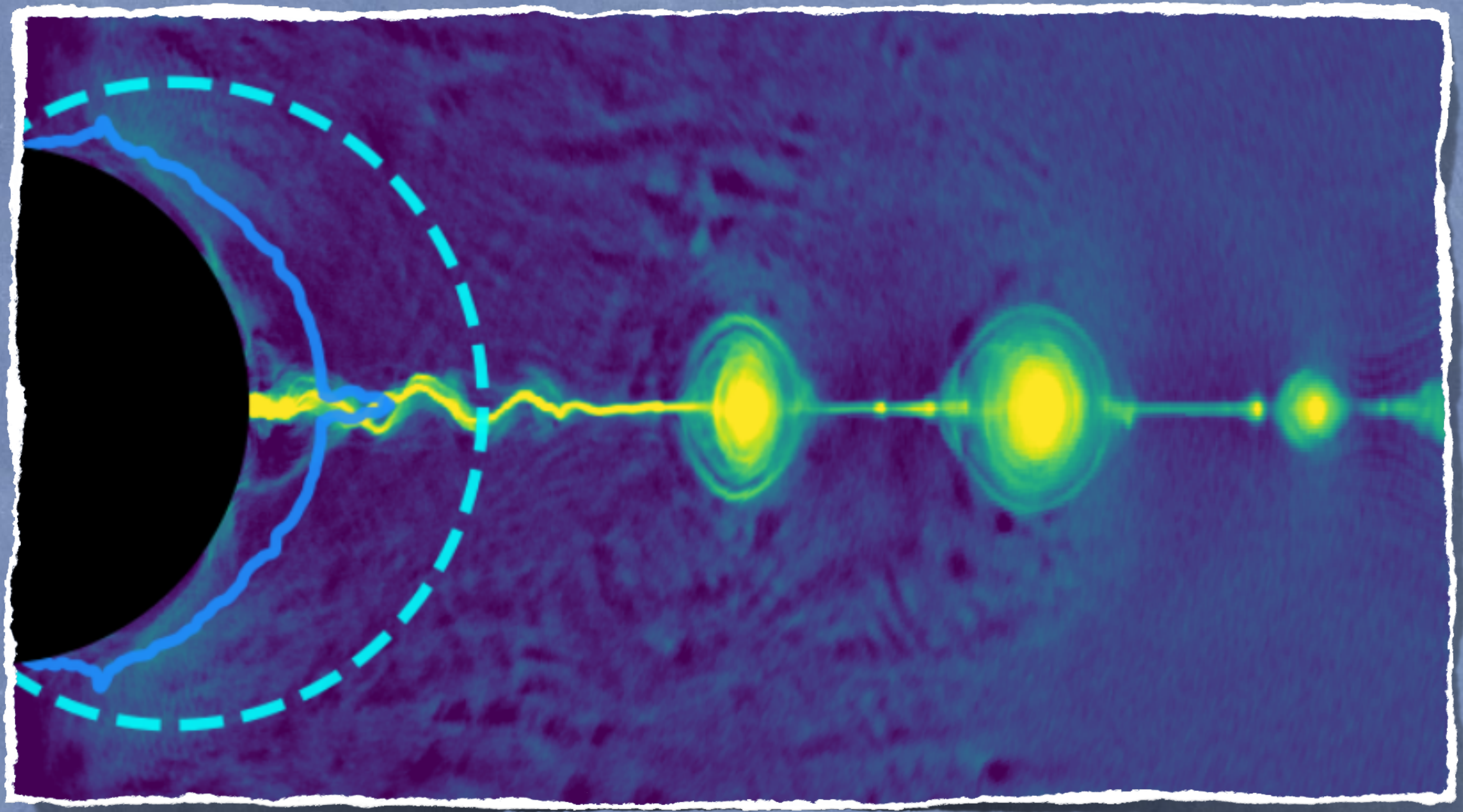

Meringolo+ 2507.08942 (2025)

A collisional description on BH scales: GRMHD simulations

- GRMHD simulations of accretion onto supermassive BHs have reached high level of sophistication and are able to reproduce morphology and energy spectrum of M87 jet
- The Blandford-Znajek (BZ) mechanism offers most natural route to extract the rotational energy from rotating BHs and power relativistic jets. However, it assumes a FF regime

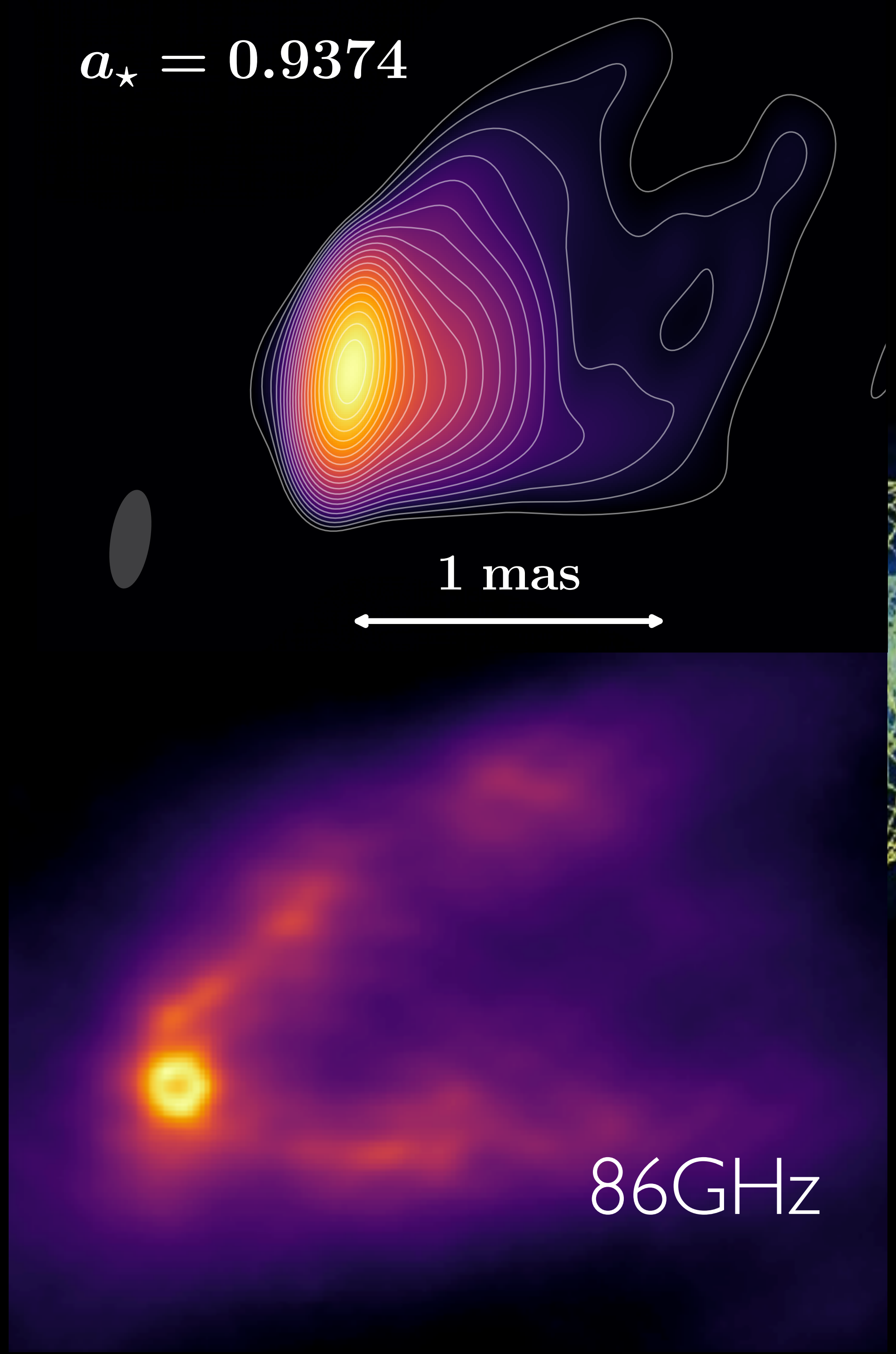

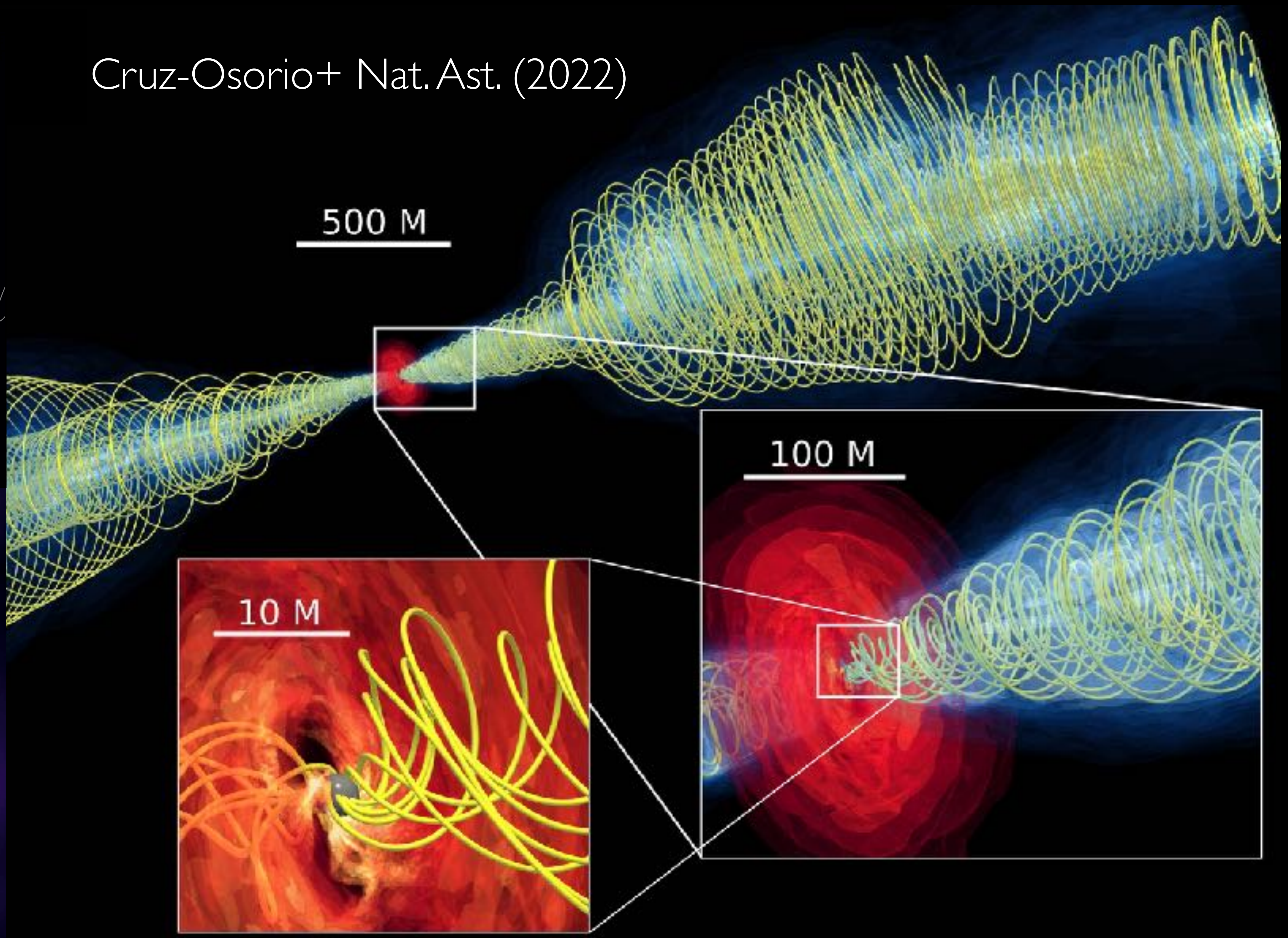

Cruz-Osorio+ Nat. Ast. (2022)

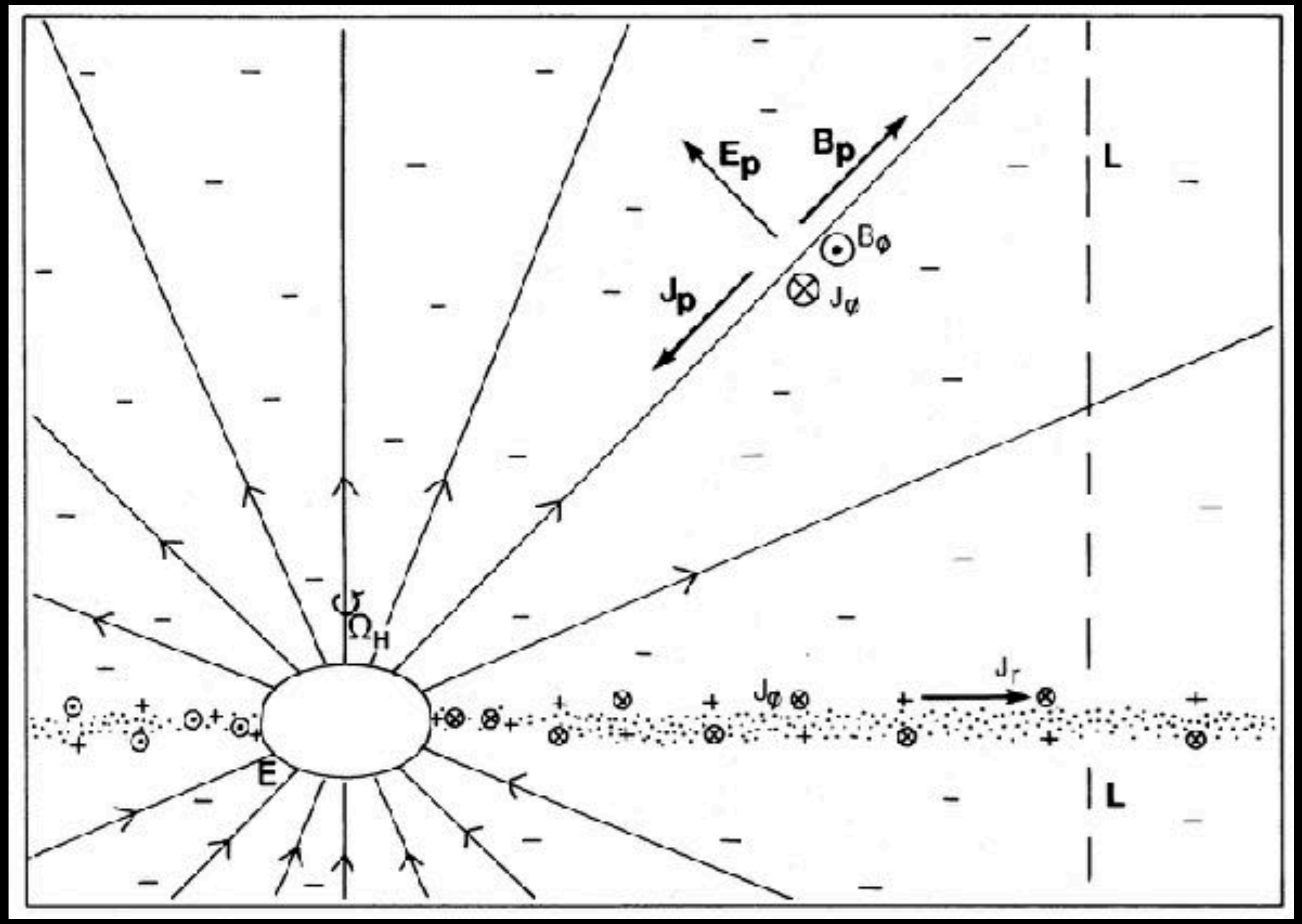

Blandford and Znajek MNRAS (1977)

A collisionless description on BH scales: PIC simulations

- Particle-in-cell simulations provide ab-initio description of FF conditions near BH
- Extension to GR not easy but provides first-principle dynamics near BHs
- Carried out extensive campaign of e_+/e_- pair plasma in 2D with new code **`FPIC`** and "classic" split-monopole of BZ solution

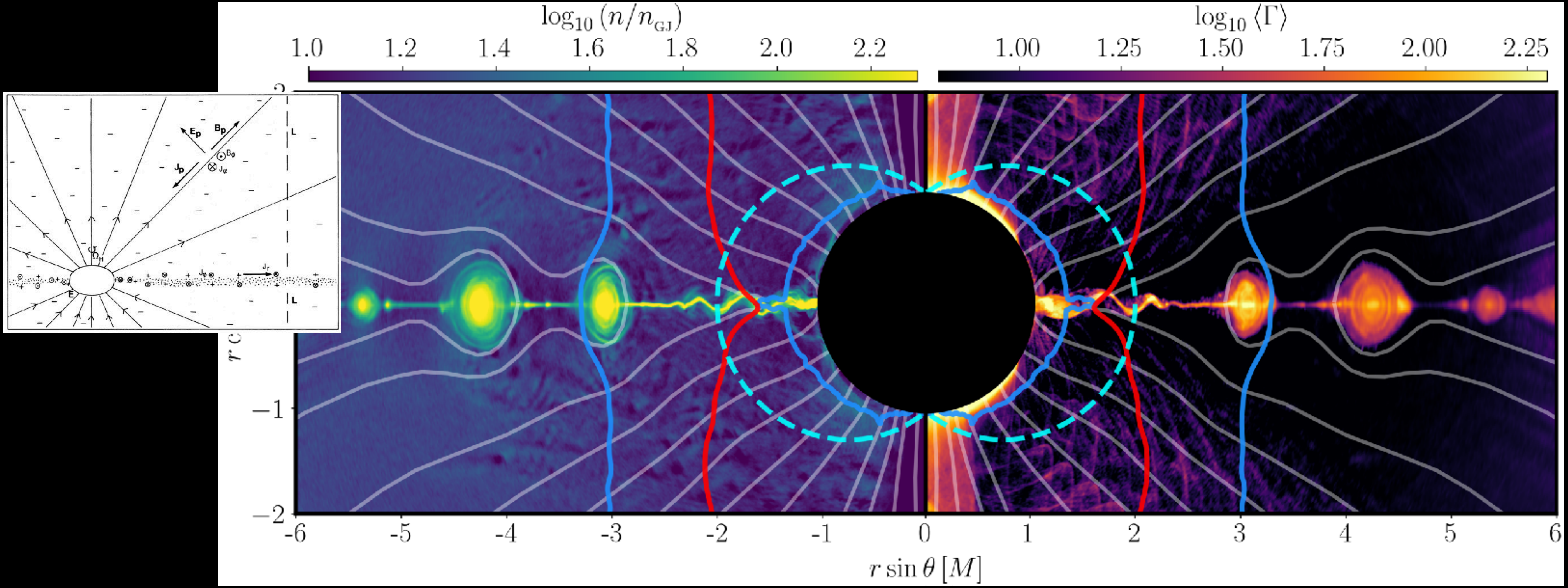

Microphysics on BH scales

- SR-PIC simulations provide important input for large-scale jet emission
- Extension to GR not easy but provides first-principle dynamics near BHs
- Carried out extensive campaign of e_+/e_- pair plasma in 2D with new code and "classic" split-monopole of Blandford-Znajek (BZ) solution

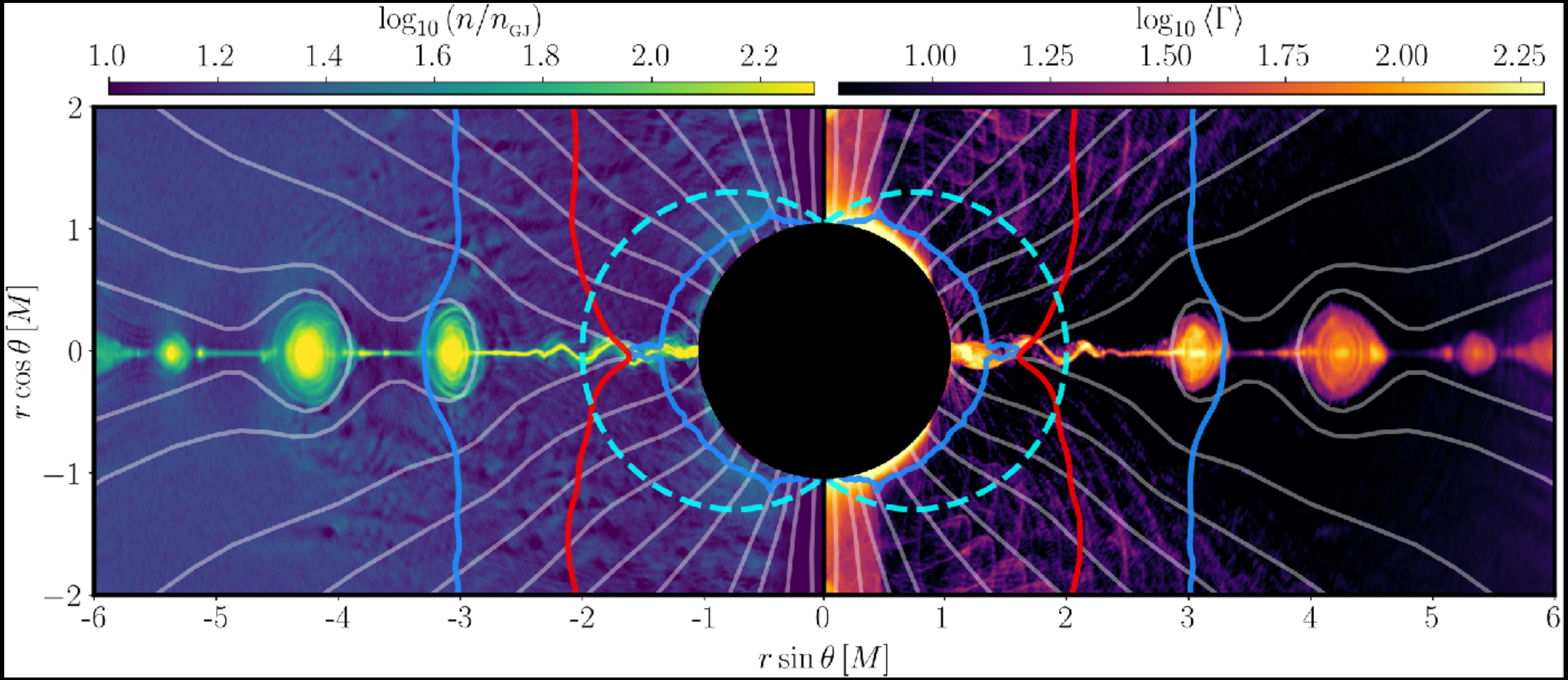

Among the new results…

- evidence plasmoids can collide and merge inside and outside ergosphere
- evidence plasmoids can also split inside ergosphere and reach infinity
- outgoing plasmoids have radial velocity $v \simeq 0.7$ independent of BH spin

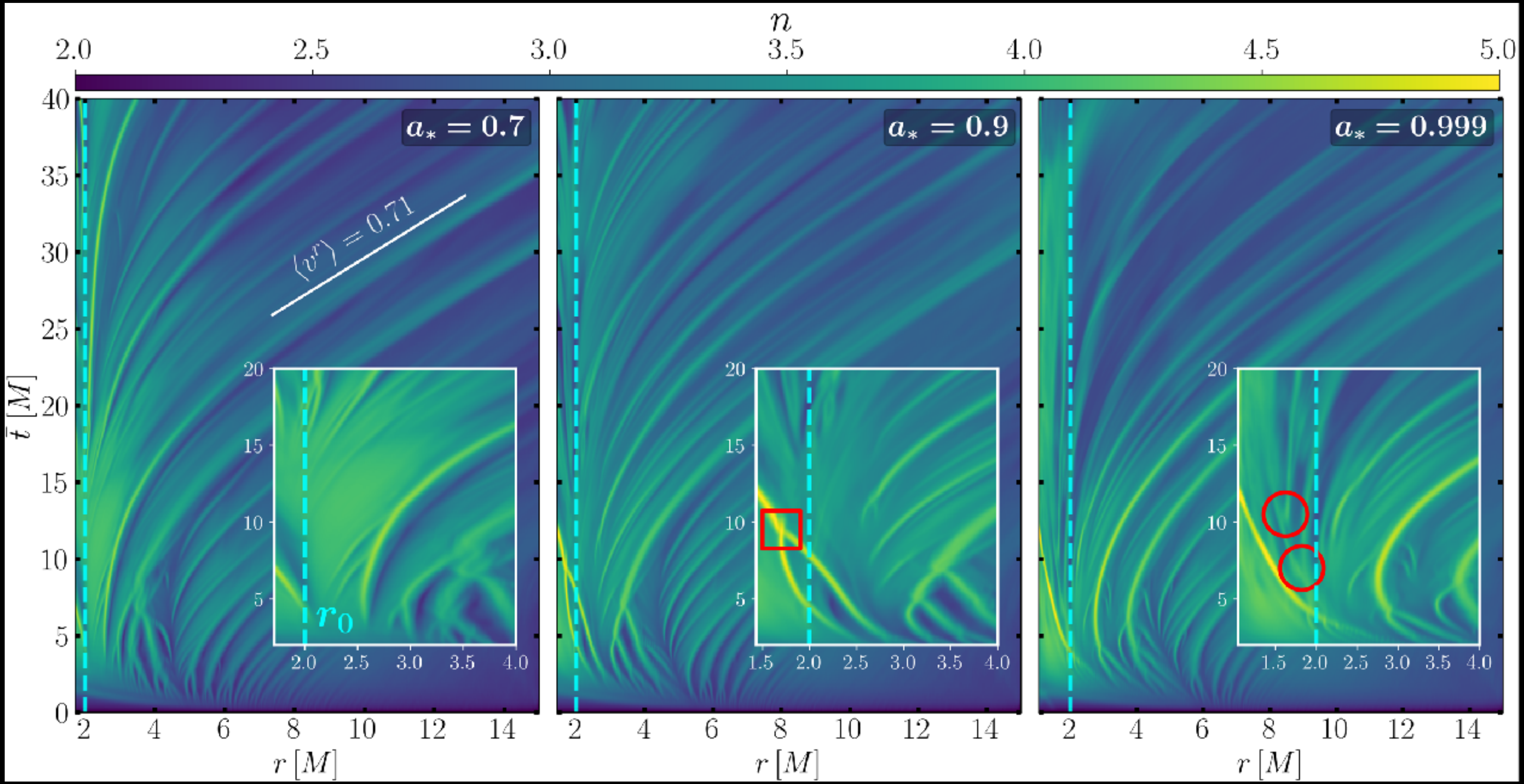

Reconnection rate

- reconnection rate $\mathscr{R}$ essential for all considerations of EM emission
- simulations allow to compute $\mathscr{R} = \mathscr{R}(r, a_*)$
- reconnection grows with BH spin and reaches maximum $\mathscr{R} \simeq 0.14$ inside ergosphere of maximally rotating BH

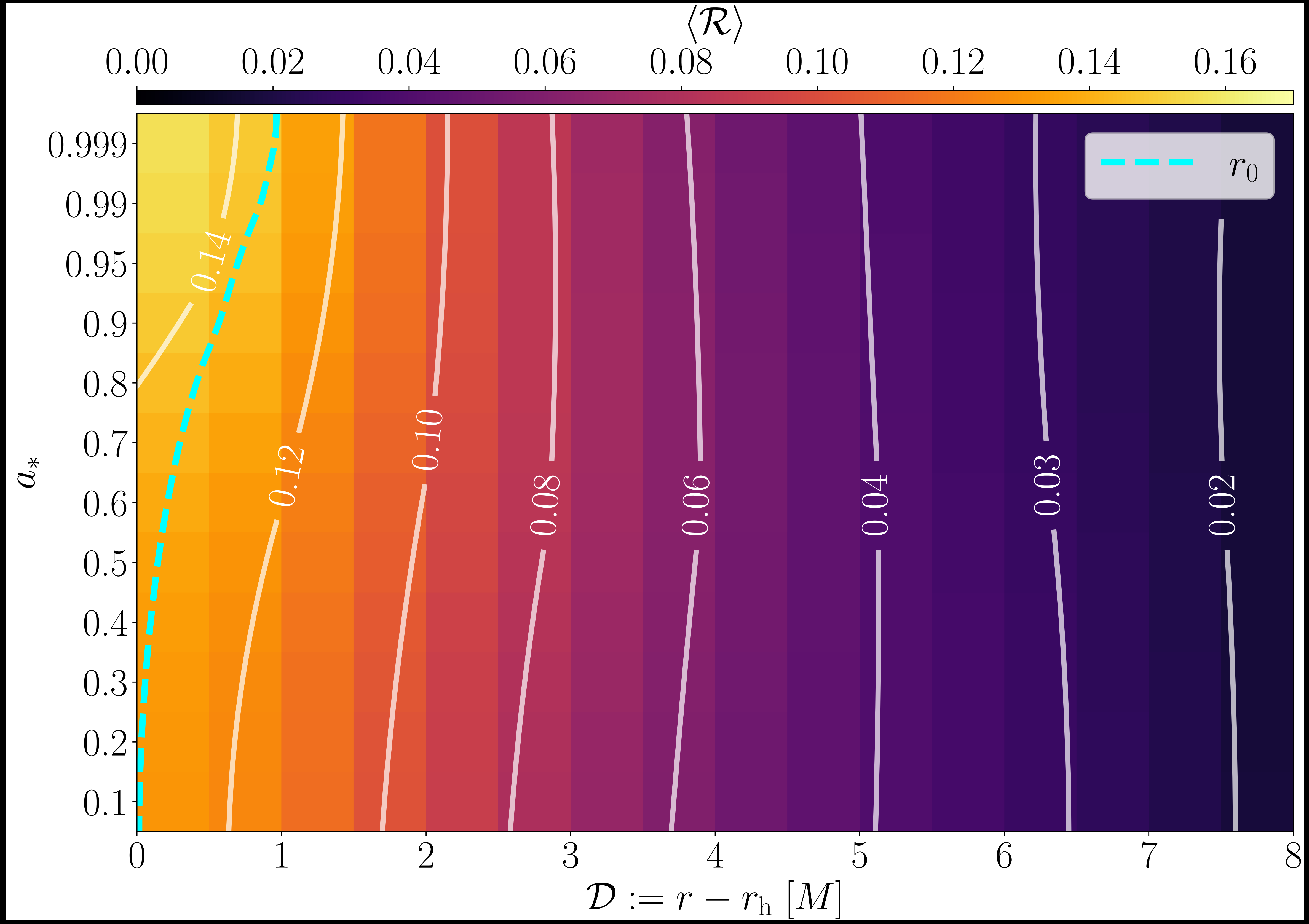

Blandford-Znajek luminosity

The BZ luminosity can be expressed very generically as

$$P_{\rm BZ} = \boxed{\frac{\kappa}{4\pi}}\boxed{\Phi_h^2}\boxed{F(\Omega_h)}$$

where (Camilloni+ JCAP 2022)

κ depends uniquely on the B-field topology ($\kappa_{sm} = 1/(6\pi)$ for split monopole)

Φ_h is the magnetic flux across the event horizon

$F_{\rm an}(\Omega_h)$ is a nonlinear function of the event-horizon velocity Ω_h:

$$F_{\rm an}(\Omega_h) = \Omega_h^2\left[1+\tilde{\alpha}(M\Omega_h)^2+\tilde{\beta}(M\Omega_h)^4+\tilde{\gamma}\,|M\Omega_h|^5+\left(\tilde{\delta}+\tilde{\epsilon}\log|M\Omega_h|\right)(M\Omega_h)^6\right]$$

Blandford-Znajek luminosity

The BZ can be measured from the simulations

$$P_{\mathrm{BZ}} = \frac{\kappa}{4\pi}\,\Phi_h^2\,F(\Omega_h)$$

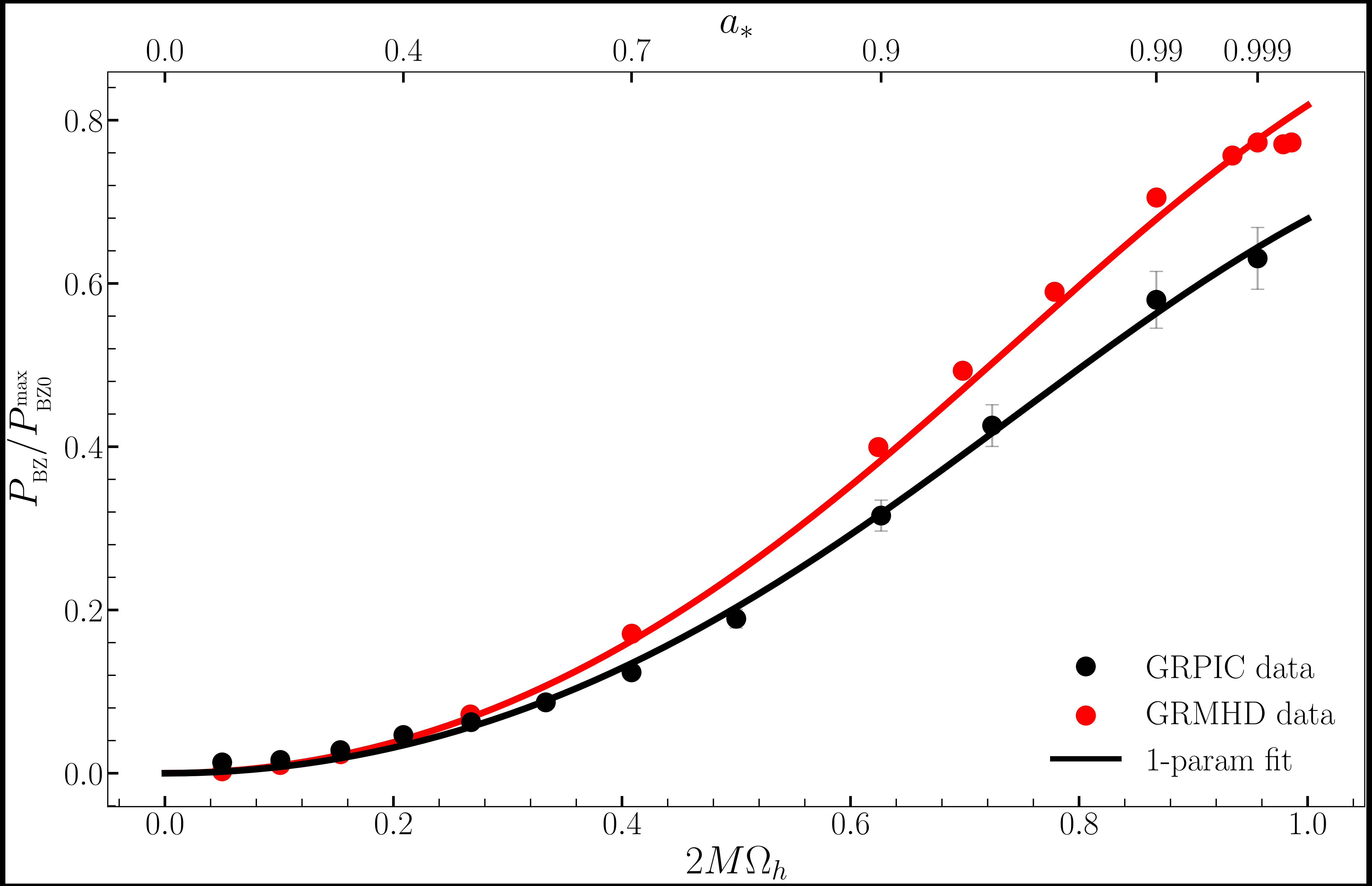

The measured BZ power matches very well analytic expression at $\mathcal{O}(\Omega_h^8)$

Good match is present also for GRMHD simulations; only difference is value of κ

Behaviour for extremal BHs can be captured with fit of quartic term

Evidence of Penrose process (PP)

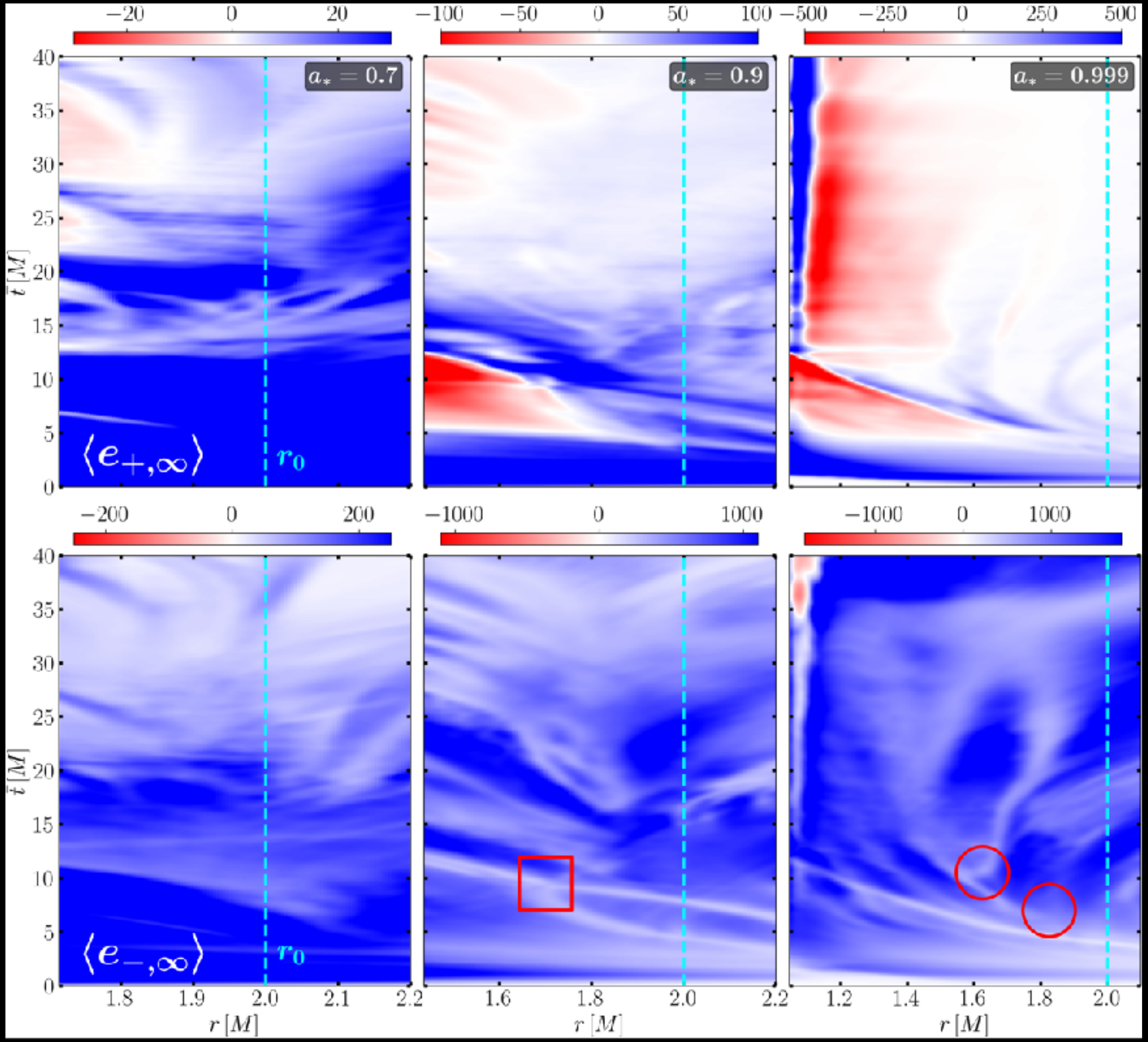

Evidence of negative-energy positrons inside ergosphere and accreting

Process is not steady and accretion rate increases with BH spin

Accretion of negative-energy particles also for electrons but with smaller rates

Results suggest that both BZ and PP are present in force-free magnetospheres of rotating BHs: extraction is combination of effects.

Probing neutron-star matter in the lab

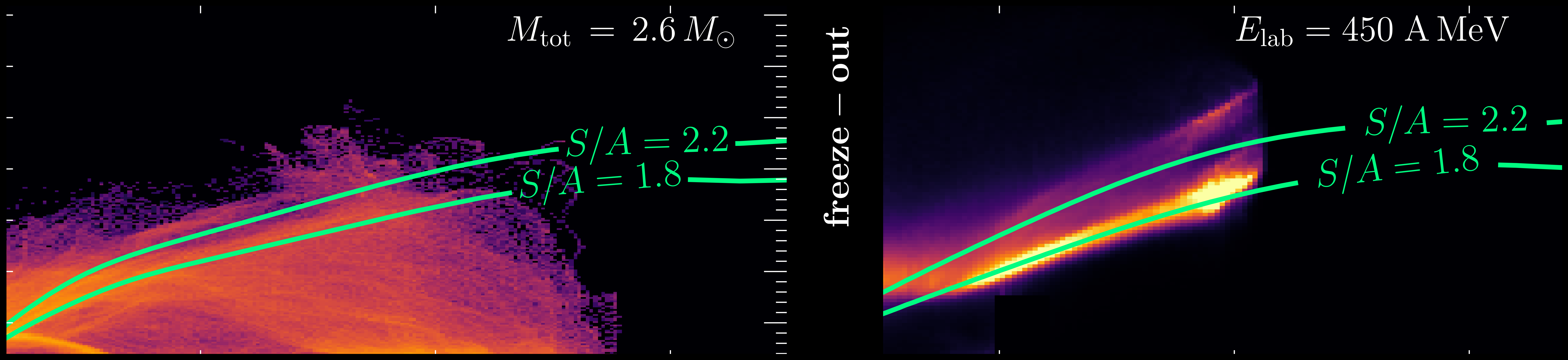

BNS mergers vs HICs

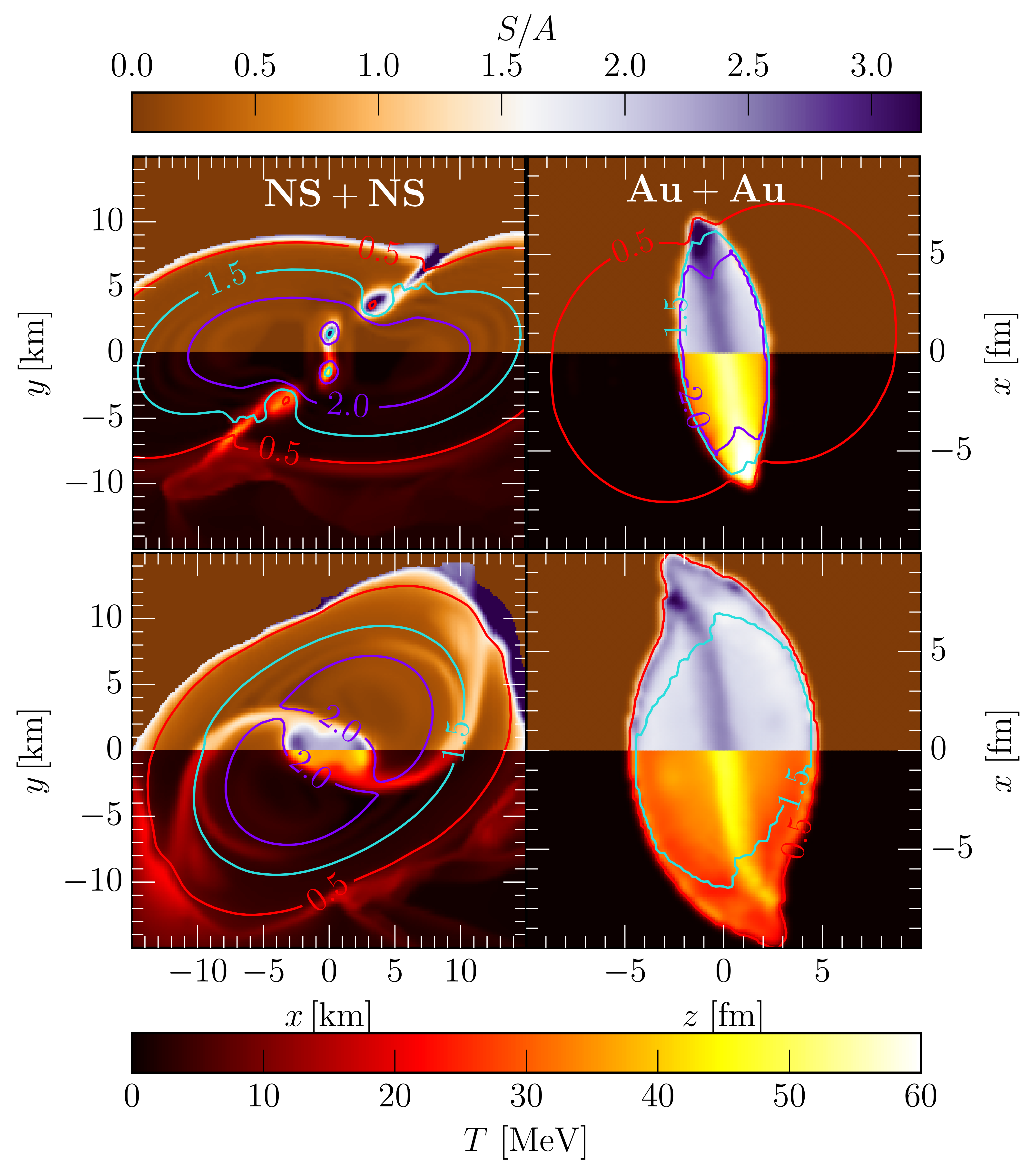

- We have explored the dynamics of BNS mergers and HIC using the same EOS.
- Chiral Mean Field model, based on the three-flavor chiral Lagrangian for hadronic matter.
- Crossover transition for deconfinement occurs at both, finite and zero temperature

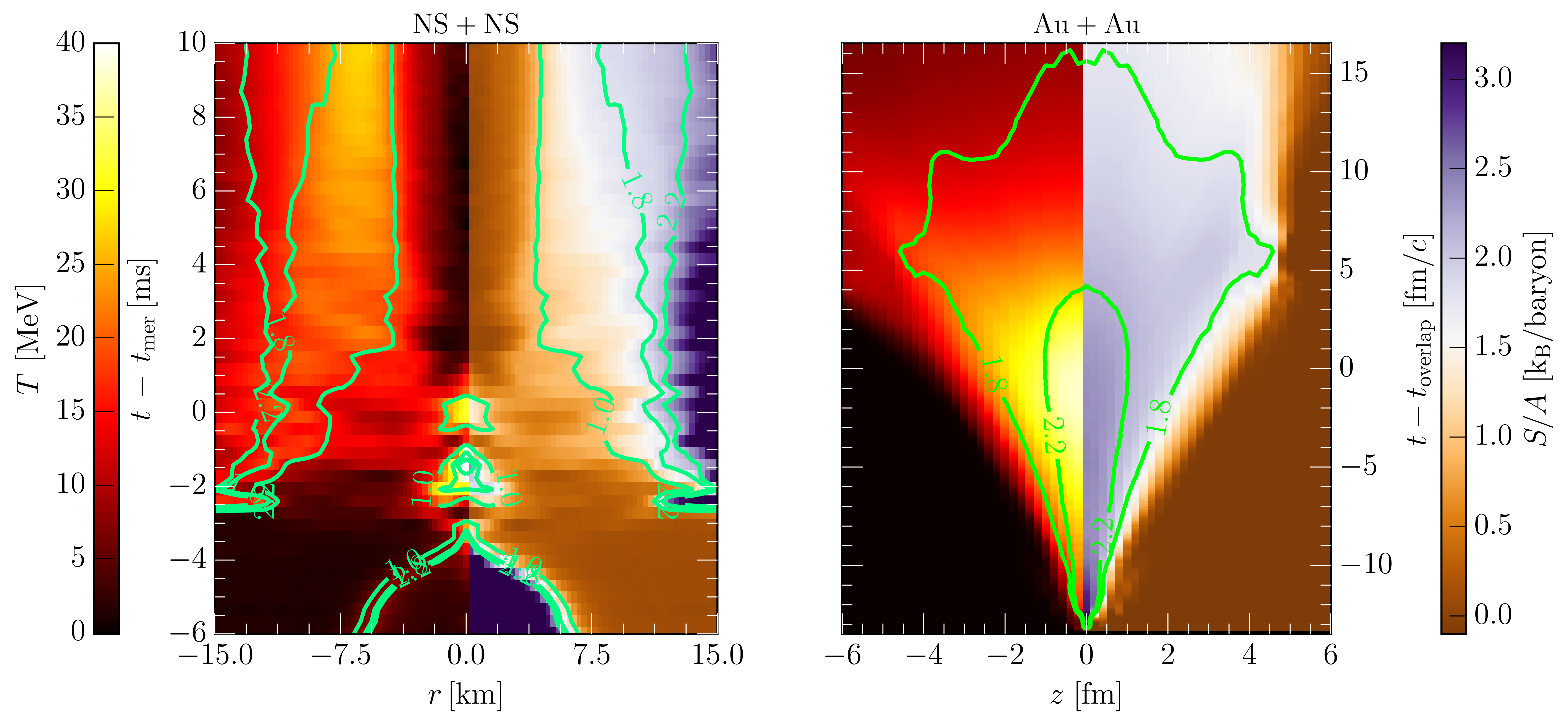

- **BNSs**: core is hot and with high entropy; hot and high entropy ring is formed. Remnant is gravitationally bound.
- **HICs**: collision product is hot and with high entropy but expands rapidly cooling isentropically.

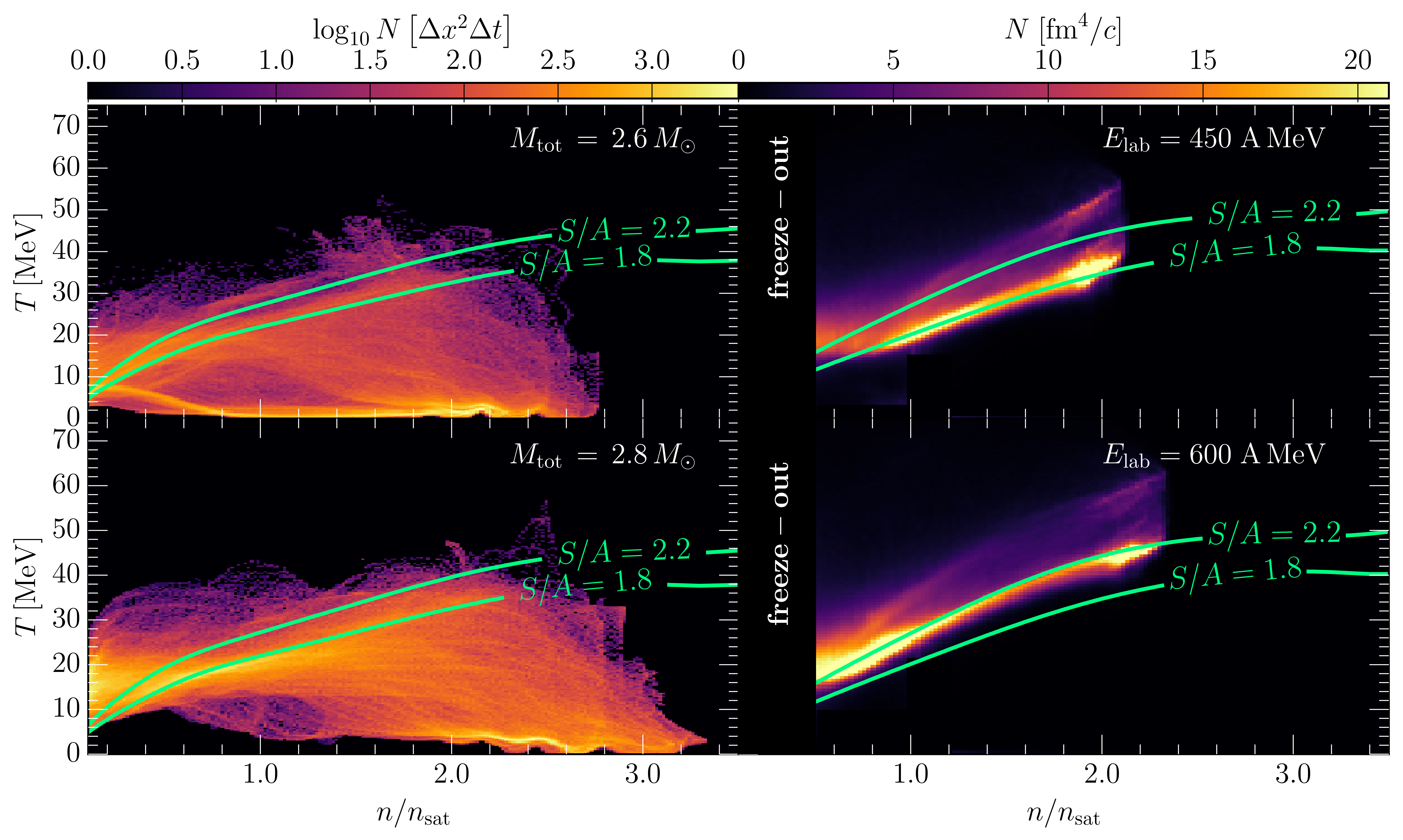

- **BNSs**: core is hot and with high entropy; hot and high entropy ring is formed. Remnant is gravitationally bound.
- **HICs**: collision product is hot and with high entropy but expands rapidly cooling isentropically.

Electromagnetic counterparts

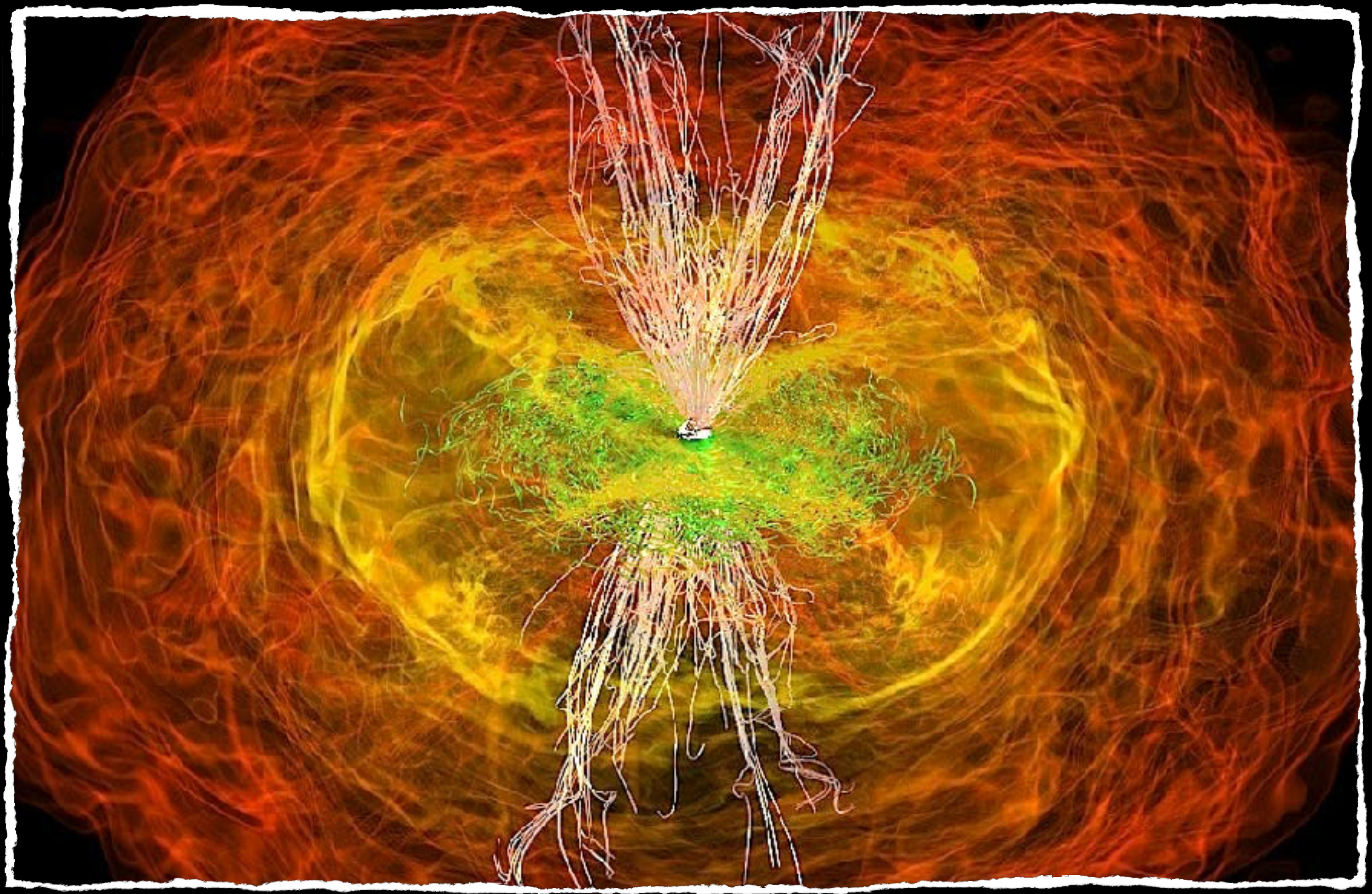

Electromagnetic counterparts

- Since 70's observed flashes of gamma rays observed with energies 10^{50-53} erg: **gamma-ray bursts (GRBs)**
- Two families of GRBs: "**long**" and "**short**"
- **Long:** last **tens-hundreds** of **seconds;** likely due to the collapse of very massive stars
- **Short:** last less than a second; due to NS mergers
- All GRBs show **jets** but how do you produce a jet from a binary merger?

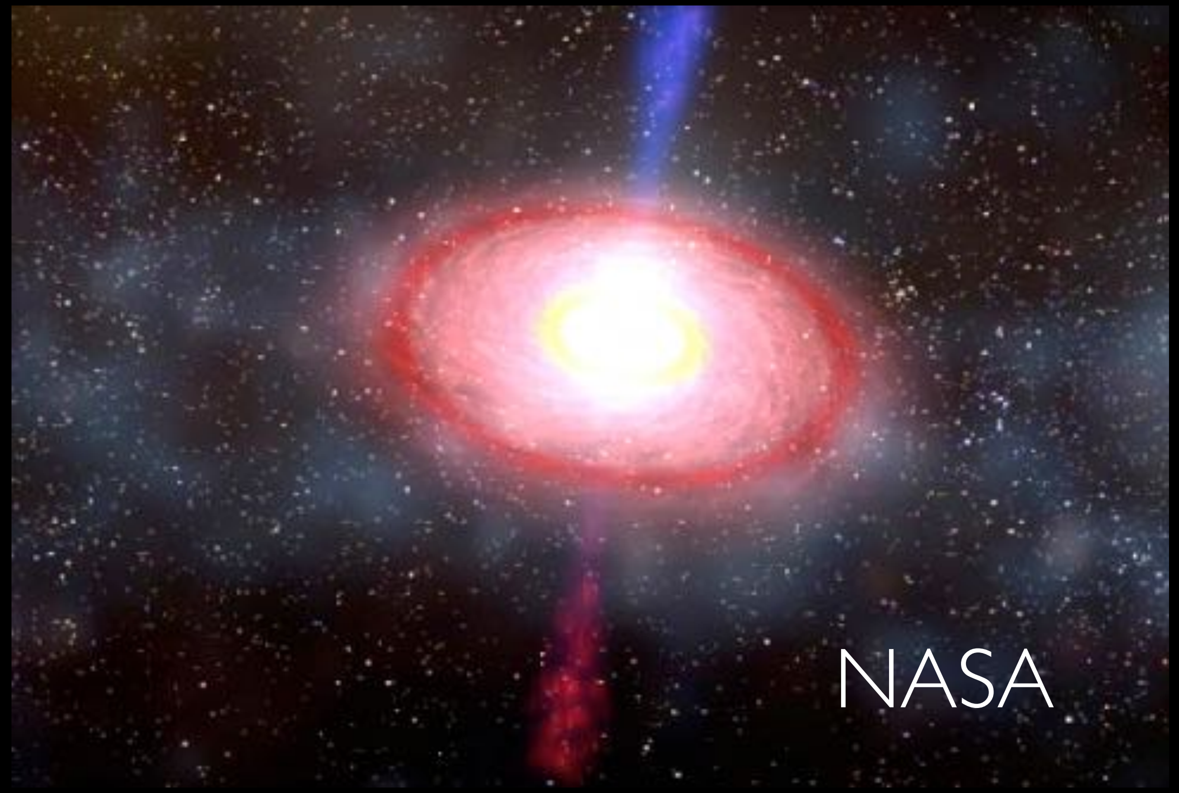
NASA

Electromagnetic counterparts

We have now evidence that gamma-ray bursts are associated with neutron star mergers

Presence of jets in gamma-ray bursts implies presence of large-scale magnetic fields

What happens when magnetised stars collide?

Need to solve equations of magnetohydrodynamics in addition to the Einstein equations

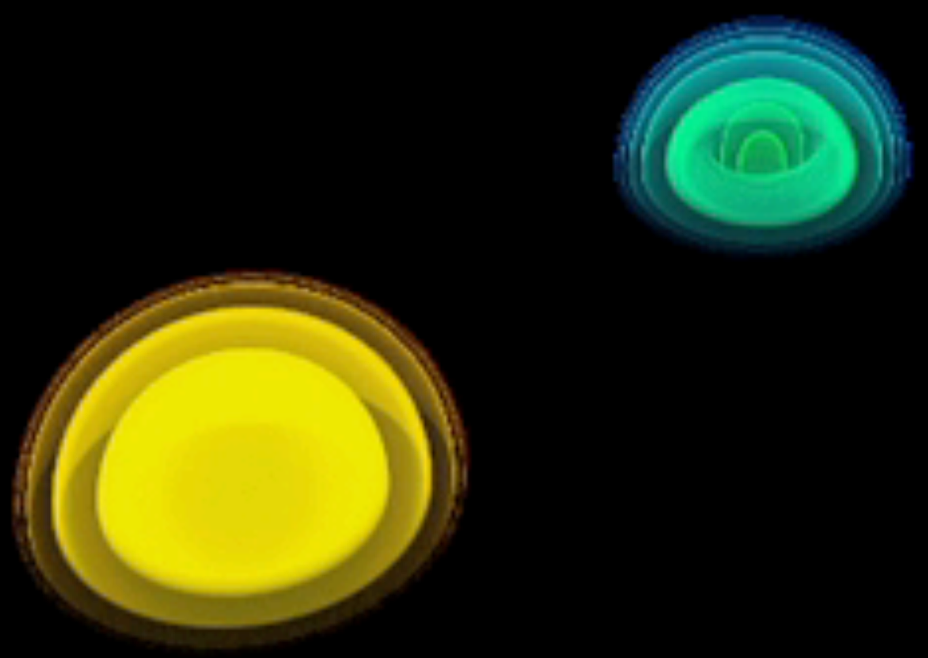

$$M = 1.5\,M_{\odot},\, B_0 = 10^{12}\,\mathrm{G}$$

Animations:, LR, Koppitz

What happens when magnetised stars collide?

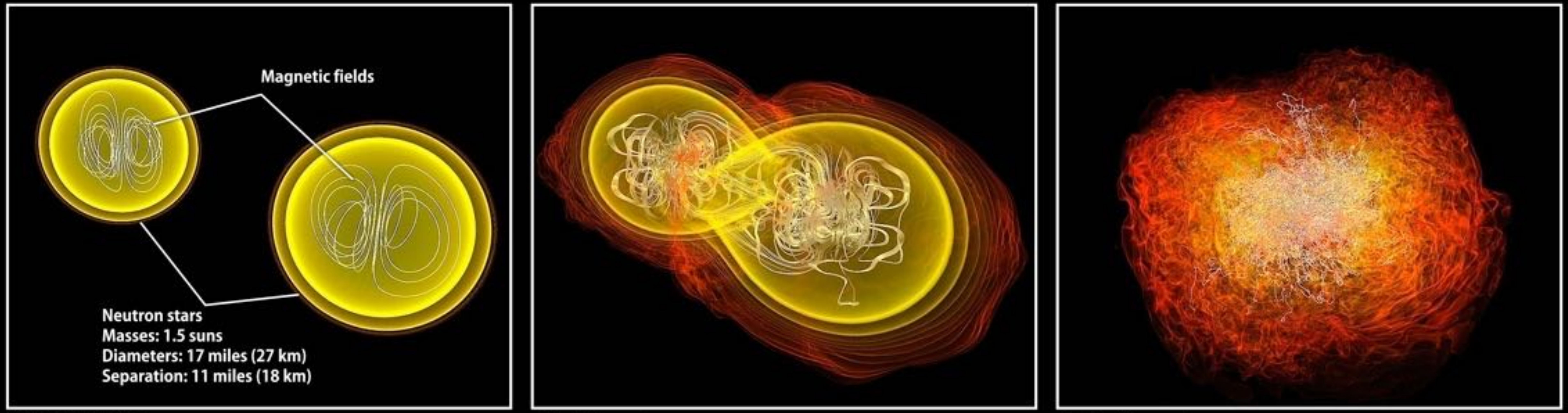

Simulation begins

7.4 milliseconds

13.8 milliseconds

Magnetic fields in the HMNS have complex topology: dipolar fields are destroyed.

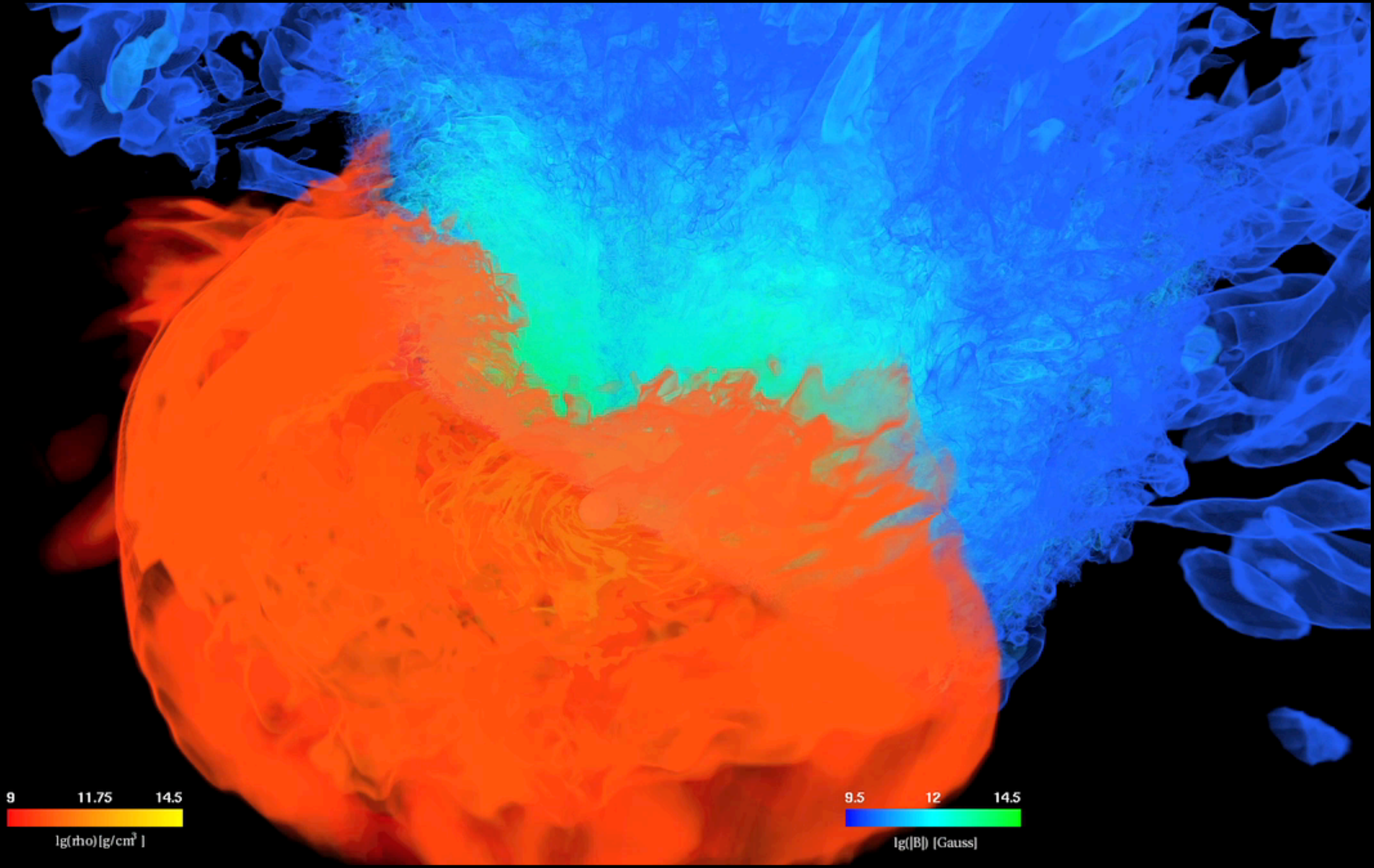
9
11.75
14.5
lg(rho) [g/cm³]
9.5
12
14.5
lg(|B|) [Gauss]

LR+ 2011

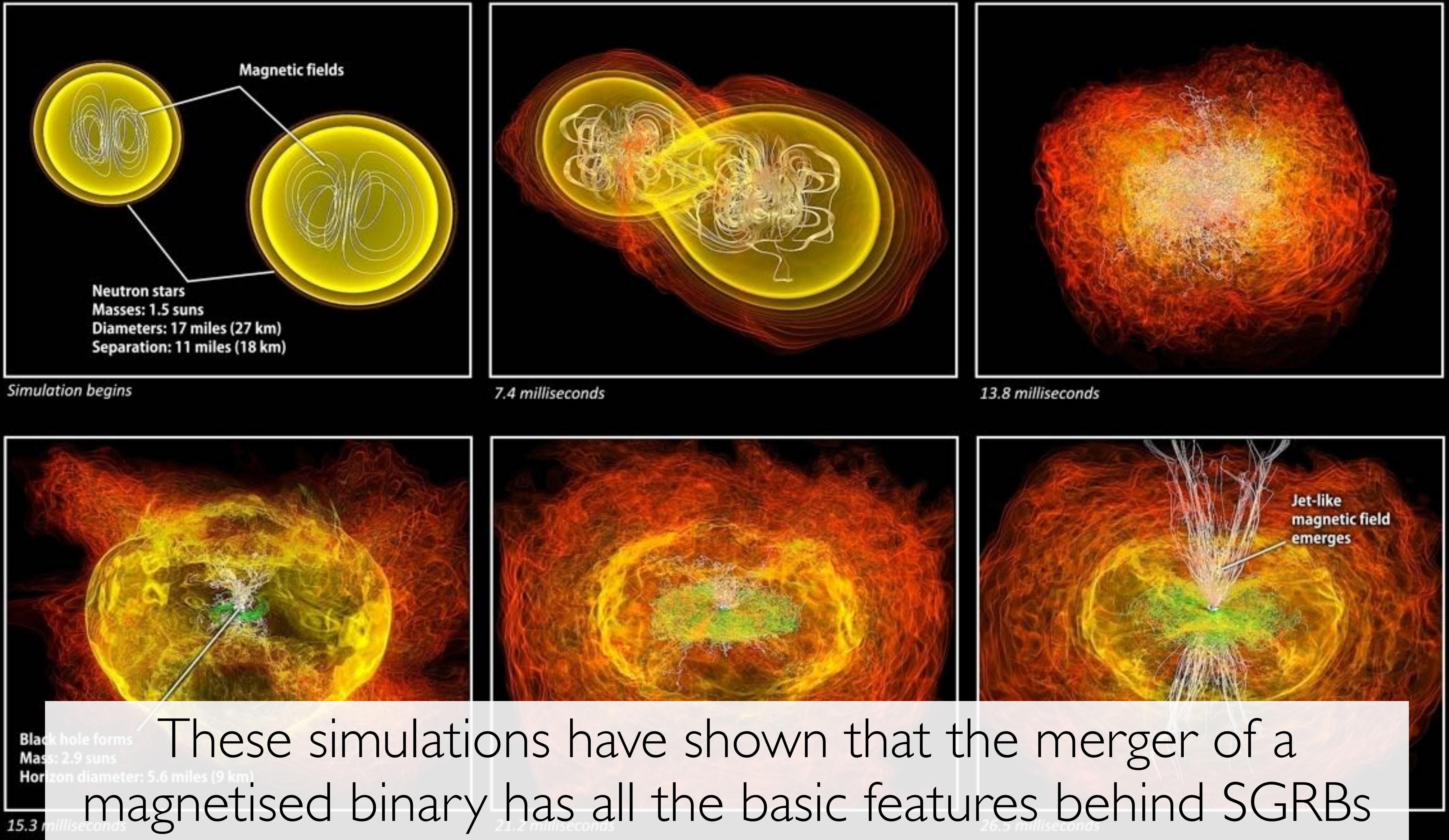

These simulations have shown that the merger of a magnetised binary has all the basic features behind SGRBs

Credit: NASA/AEI/ZIB/M. Koppitz and L. Rezzolla

$J/M^2 = 0.83$ $\mathrm{M_{tor}} = 0.063 M_\odot$ $\mathrm{t_{accr}} \simeq M_{\mathrm{tor}}/\dot{M} \simeq 0.3\ \mathrm{s}$

With due differences, other groups confirm this picture

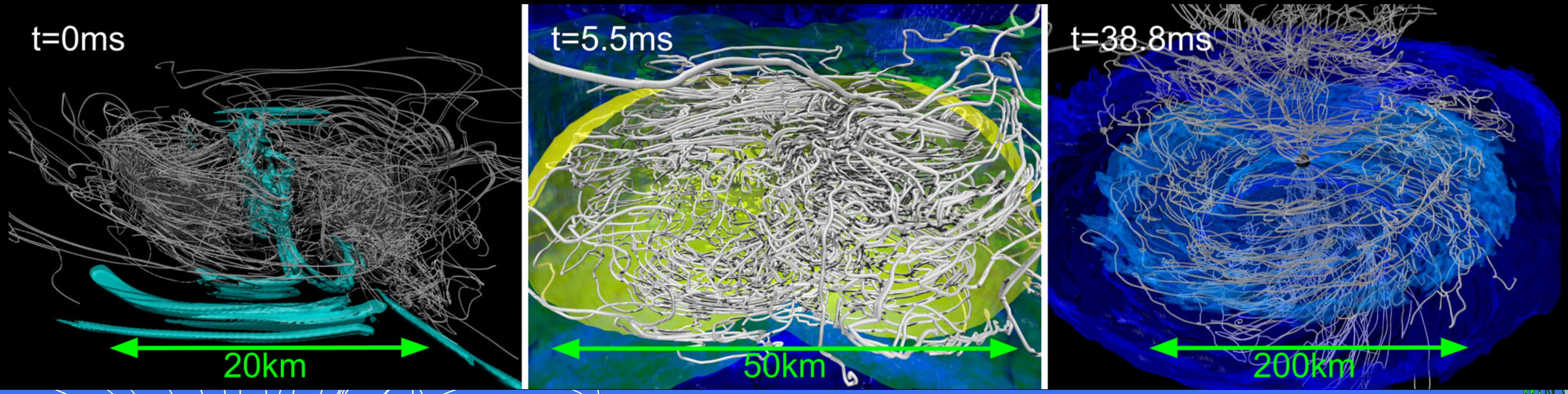

Kiuchi+ 2014

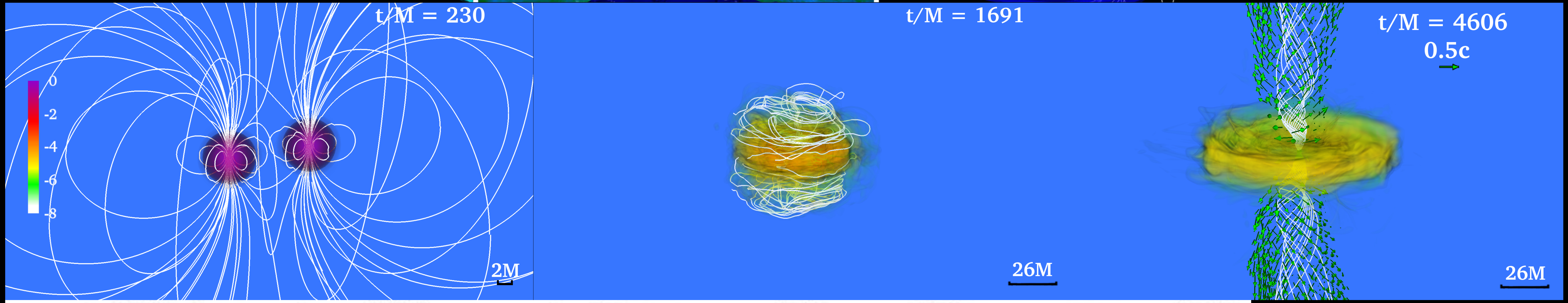

Ruiz+ 2016

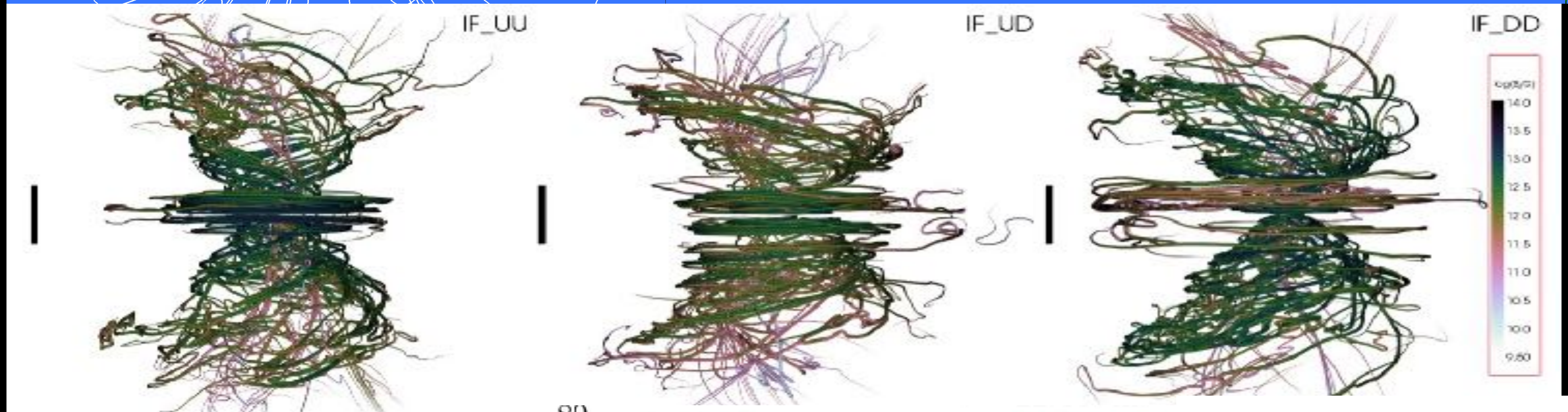

Kawamura+2016

Dionysopoulou+ 2015

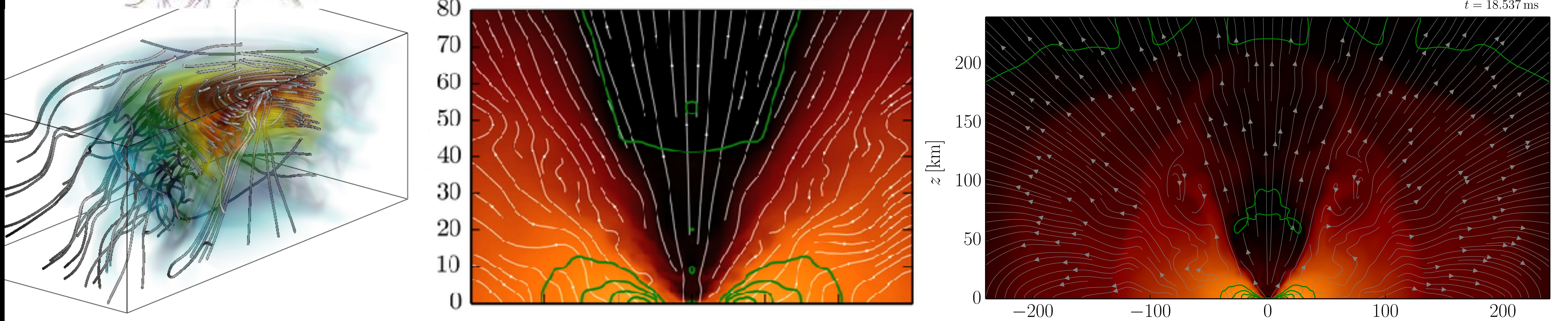

RMHD

Ejected matter and nucleosynthesis

Bovard+ (2017)

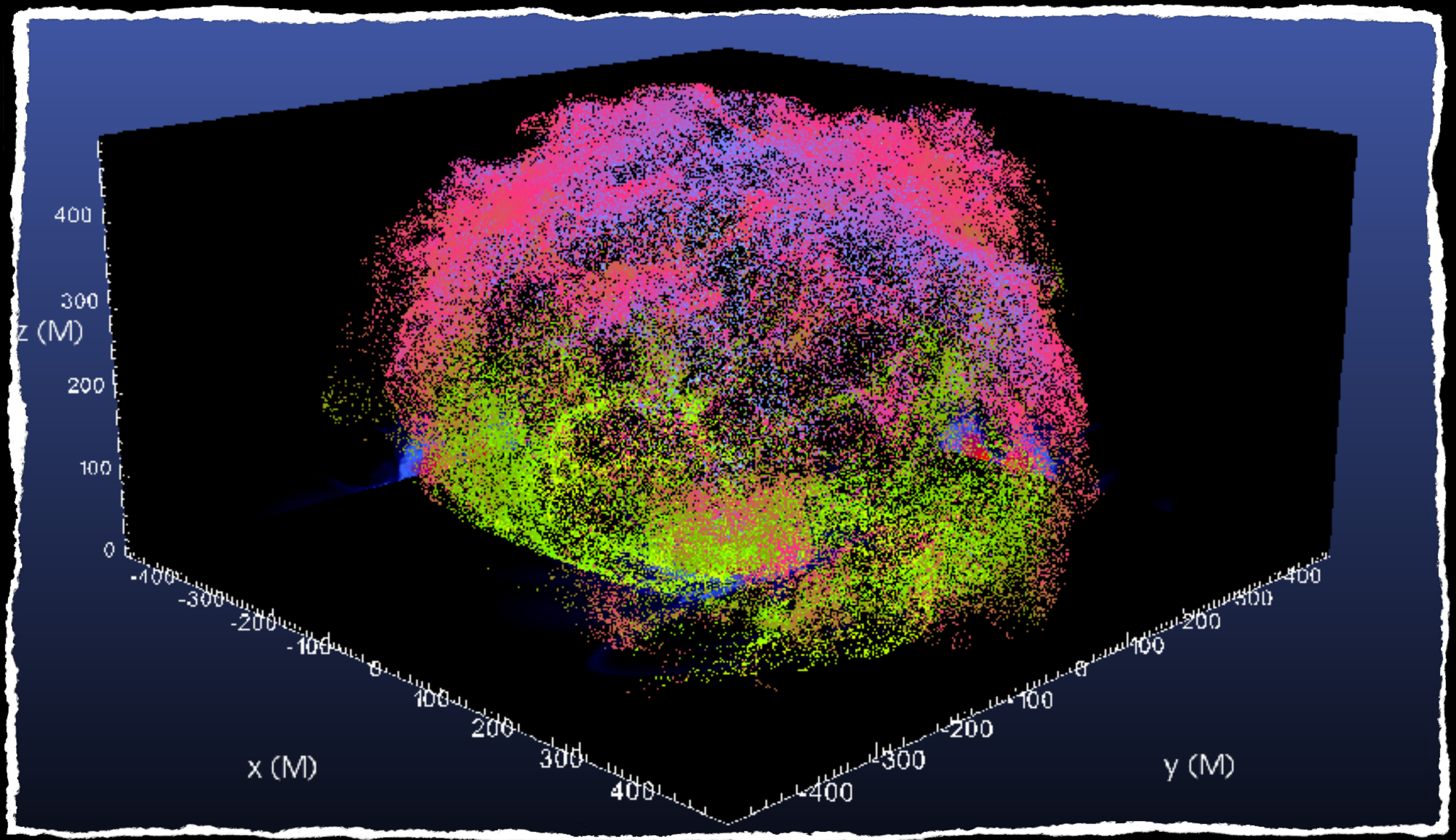

Nucleosynthesis

- Already in the 50’s, nuclear physicists had tracked the production of ele
stars via nuclear fusion.
- **Heavy elements** (*A>56*) cannot be produced in stellar interiors but ca
synthesised during a **supernova.**
- SN simulations have shown that temperatures/energies not enough to produce **“very heavy” elements** (*A>120*).
- To produce such elements very high temperatures and **“neutron-rich”** material is needed.
- **Neutron-star mergers** seem perfect candidates for this process!

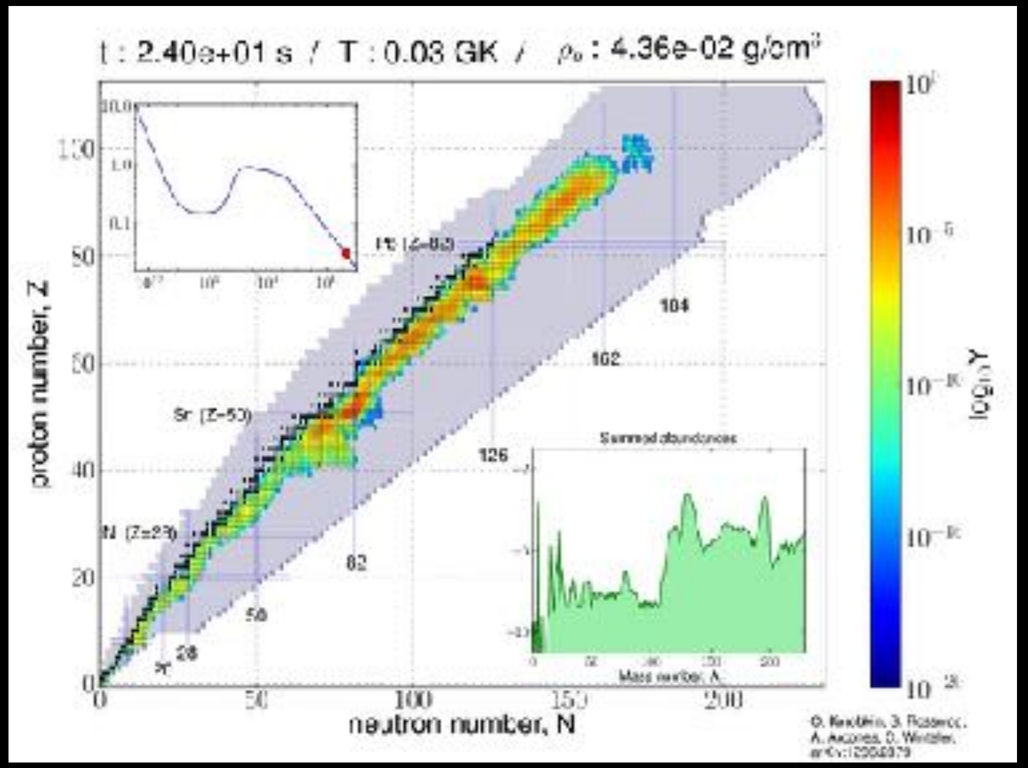

O. Korobkin, S. Rosswog, A. Arcones, C. Winteler, arXiv:1206.2379

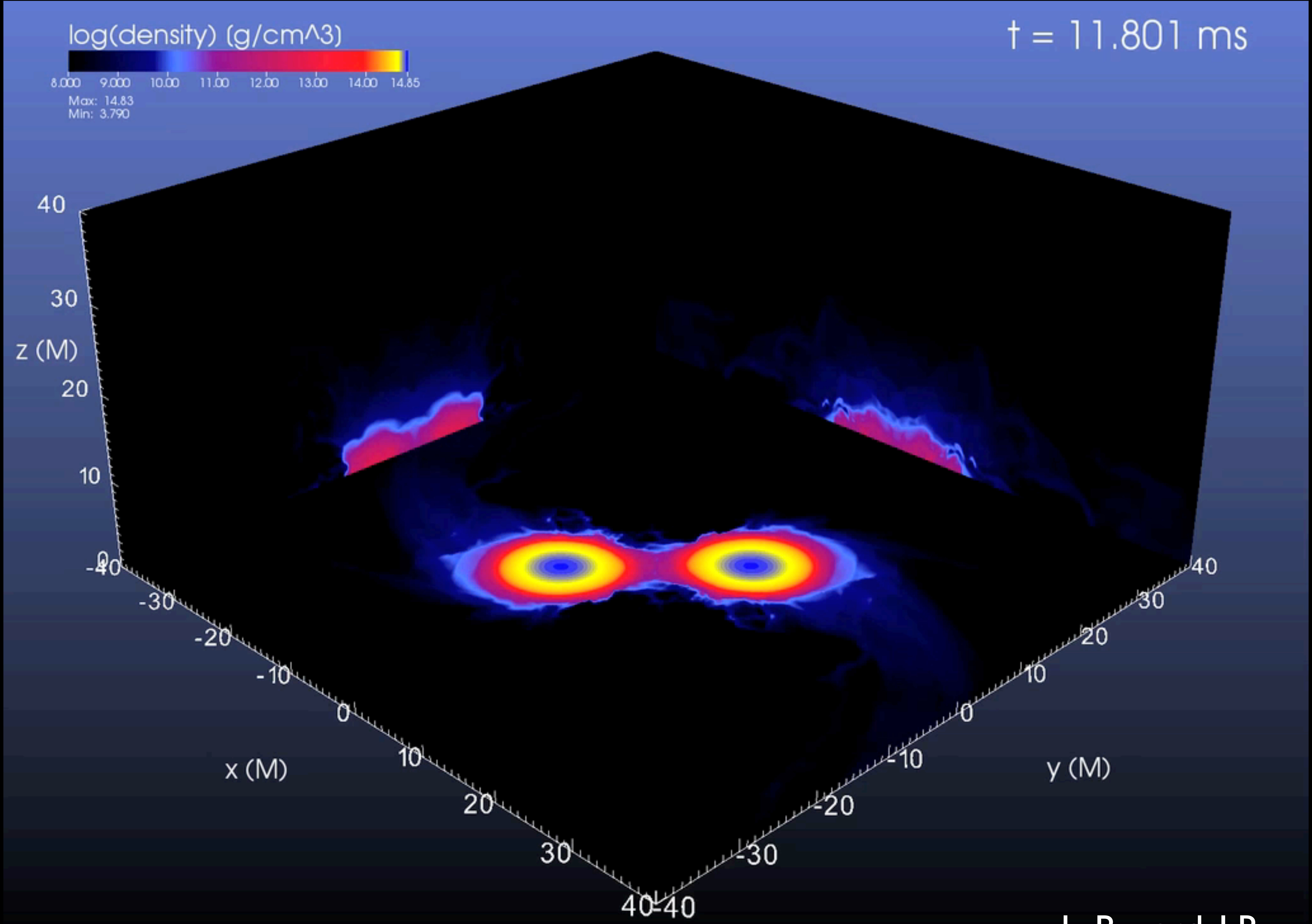
log(density) (g/cm^3)
8.000
9.000
10.00
11.00
12.00
13.00
14.00
14.85
Max: 14.83
Min: 3.790
t = 11.801 ms
z (M)
40
30
20
10
0
x (M)
-40
-30
-20
-10
0
10
20
30
40
y (M)
-40
-30
-20
-10
0
10
20
30
40

L. Bovard, LR

Ejection of mass

- After merger mass is lost in many different **channels** (shock heating, neutrino or magnetic-driven winds) and on very different **timescales** (**dynamical** and **secular**).

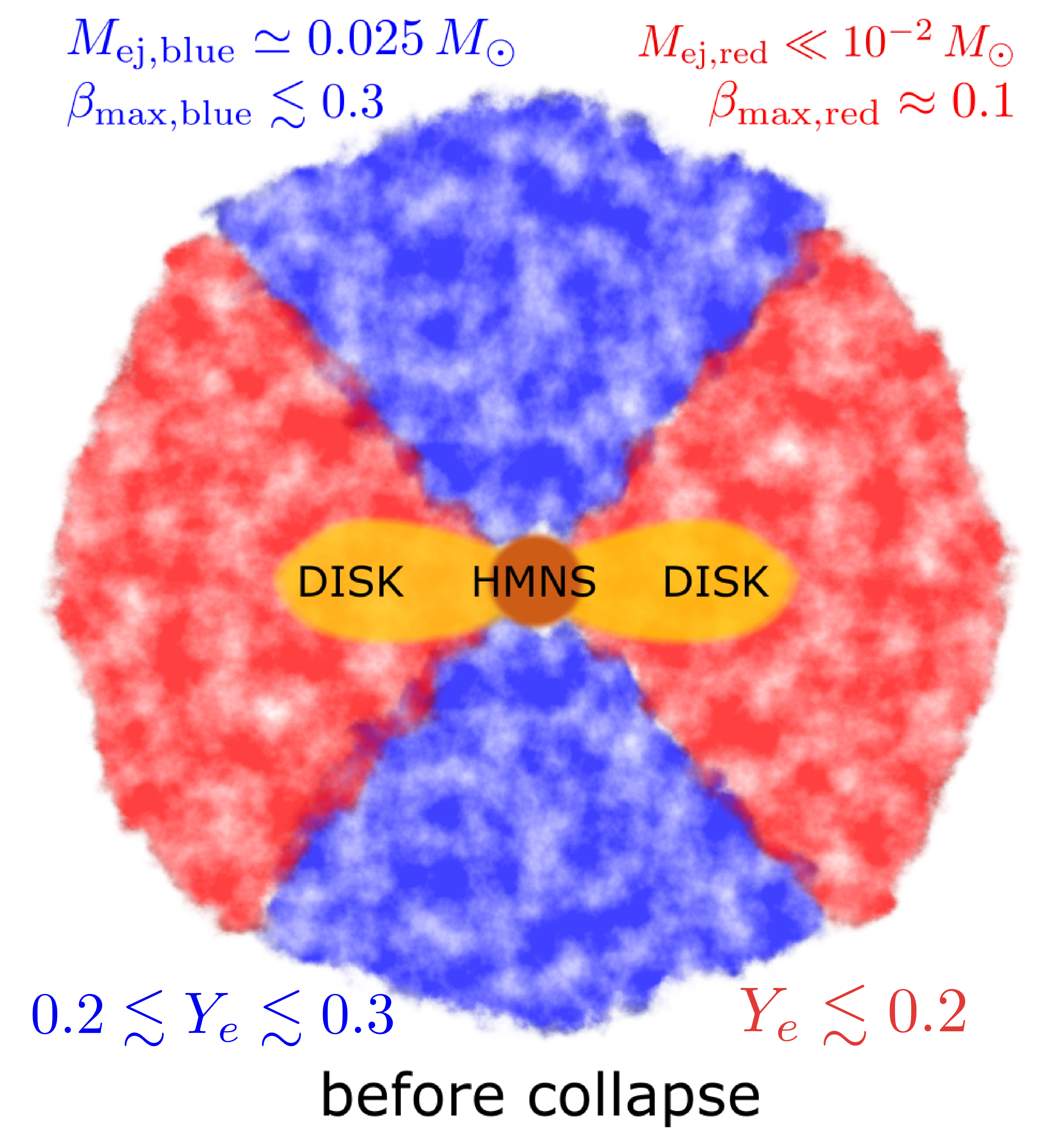

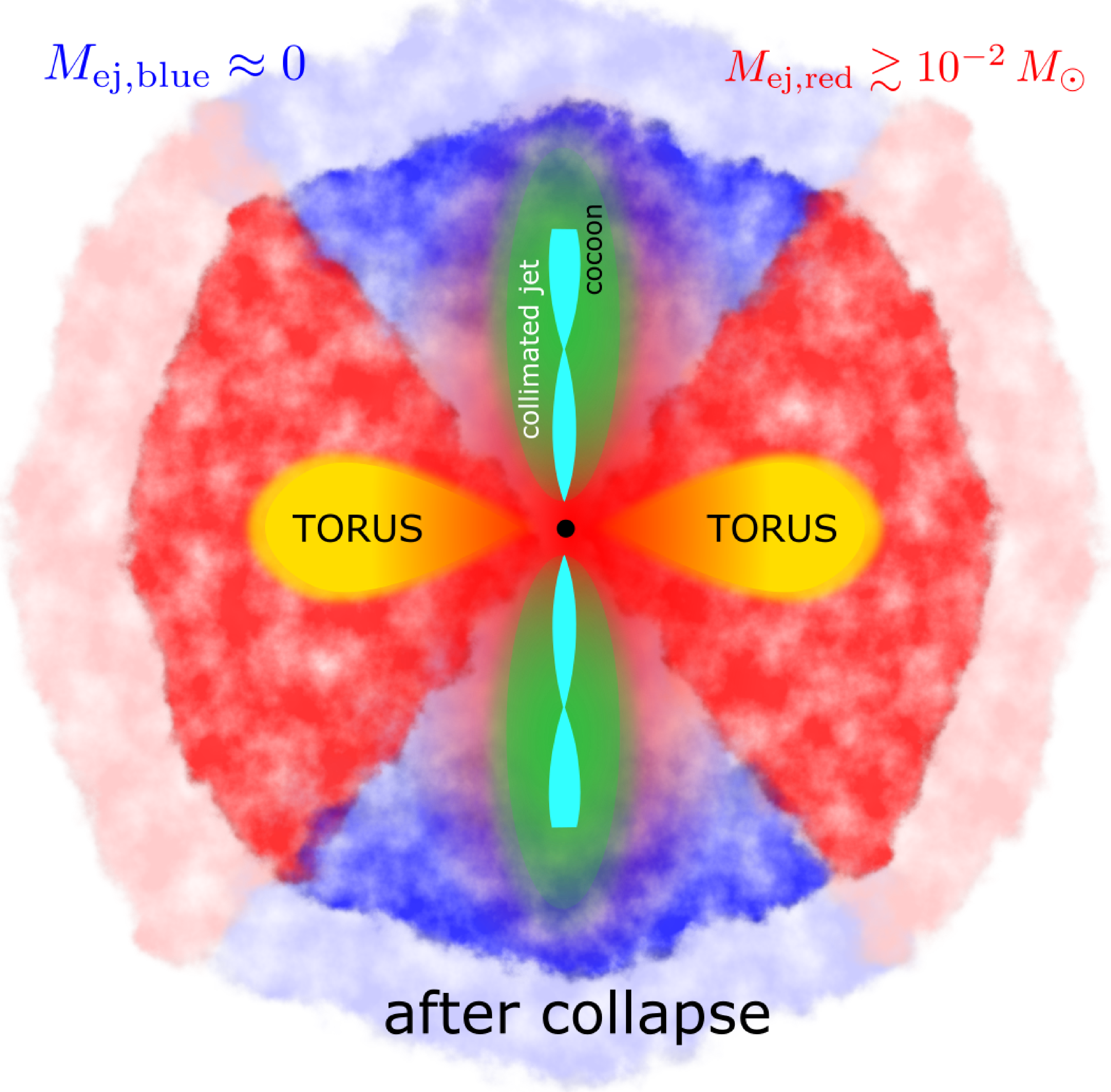

Relative abundances

- Mass ejection can either be **dynamical** (shocks; 100 ms) or **secular** (magnetic or neutrino-driven winds; 1-10 s).
- Even **tiny amounts** of ejected matter (*0.01 M*$_\odot$) sufficient to explain observed abundances.
- Abundances for *A>120* good agreement with solar. **robust** for different **EOSs, masses, nuclear reactions and merger type**

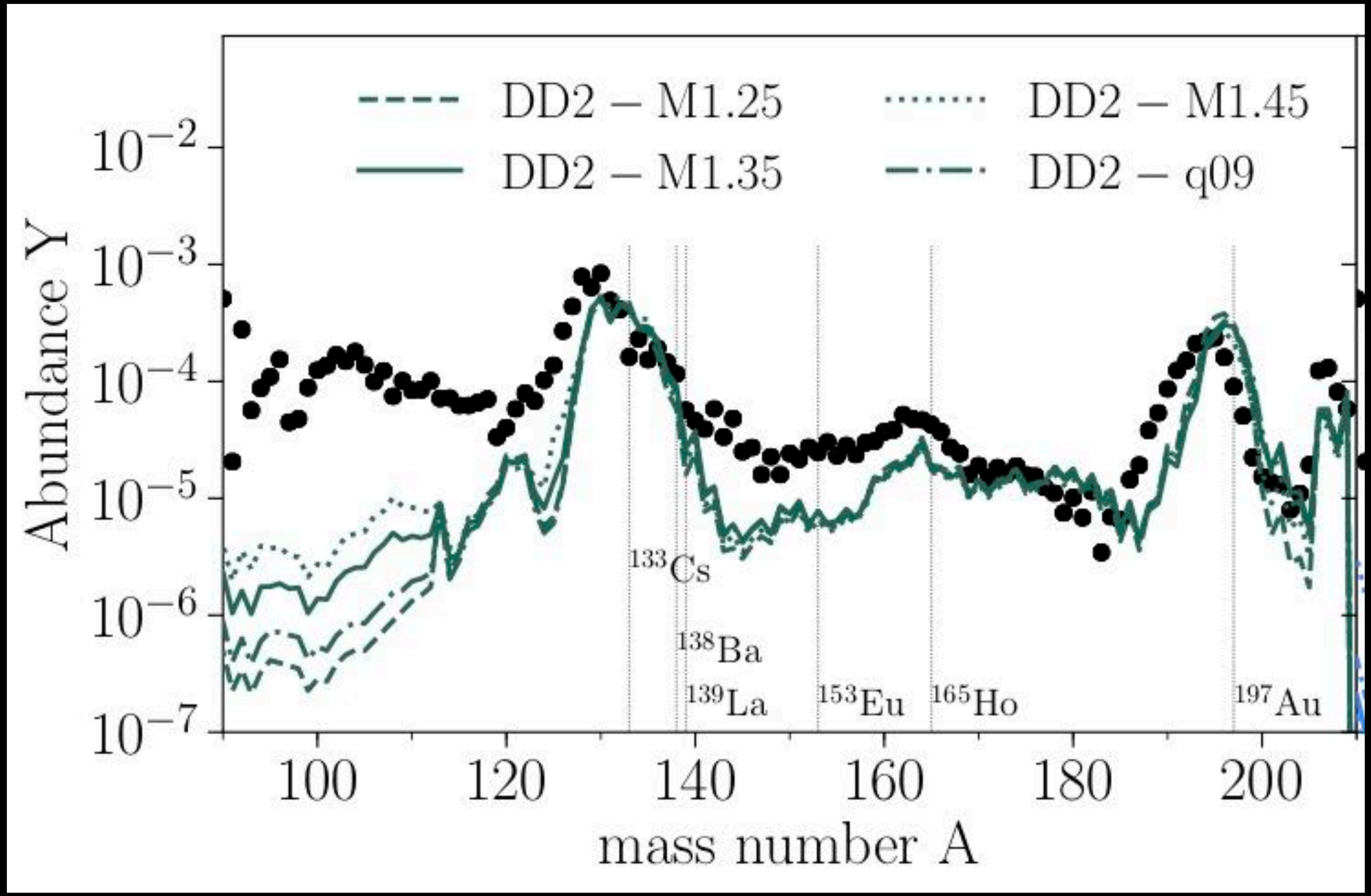

Relative abundances

- Mass ejection can either be **dynamical** (shocks; 100 ms) or **secular** (magnetic or neutrino-driven winds; 1-10 s).
- Even **tiny amounts** of ejected matter ($0.01\ M_\odot$) sufficient to explain observed abundances.
- Abundances for ***A>120*** good agreement with solar. **robust** for different **EOSs, masses, nuclear reactions and merger type**

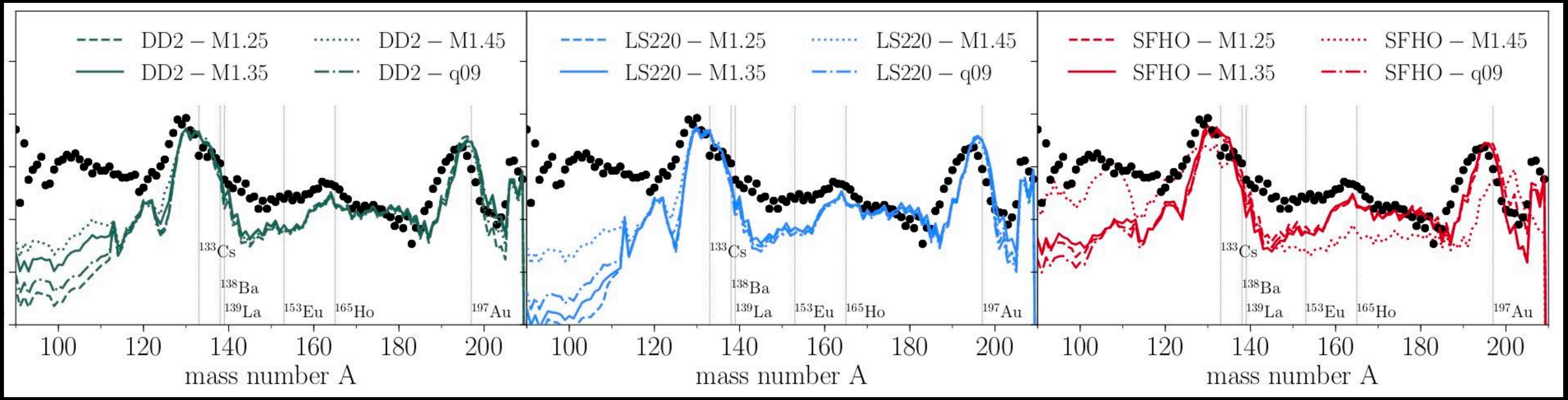

Relative abundances

- Mass ejection can either be **dynamical** (shocks; 100 ms) or **secular** (magnetic or neutrino-driven winds; 1-10 s).
- Even **tiny amounts** of ejected matter ($0.01\ M_\odot$) sufficient to explain observed abundances.
- Abundances for $A>120$ good agreement with solar. **robust** for different **EOSs, masses, nuclear reactions and merger type**

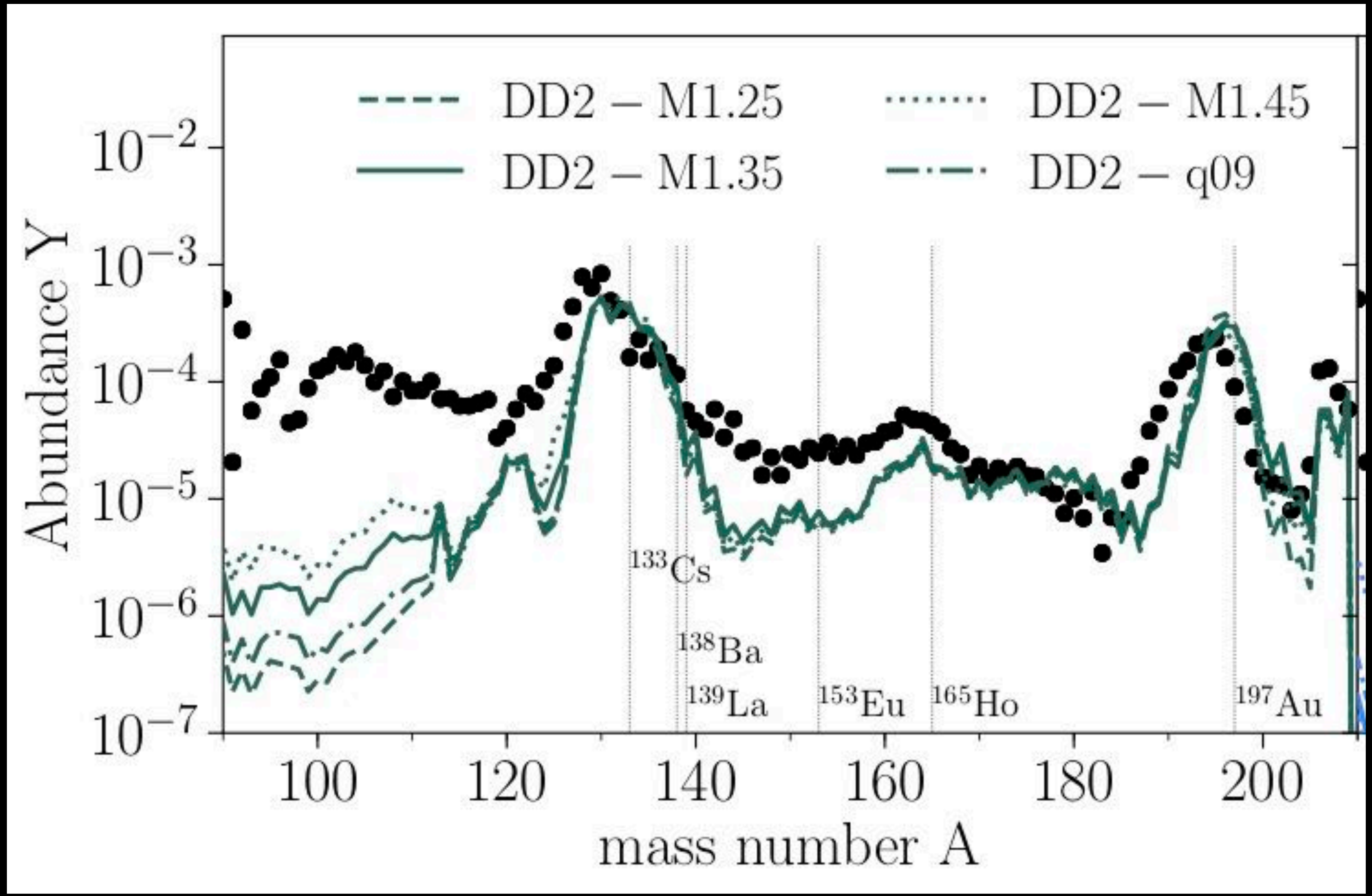

- GW170817 produced total of **16,000** times the mass of the Earth in heavy elements (**10** Earth masses in **gold/platinum**)
- We are not only **stellar dust** but also **neutron-star dust!**

Spatial distributions: M_{ej} Bovard+ 17

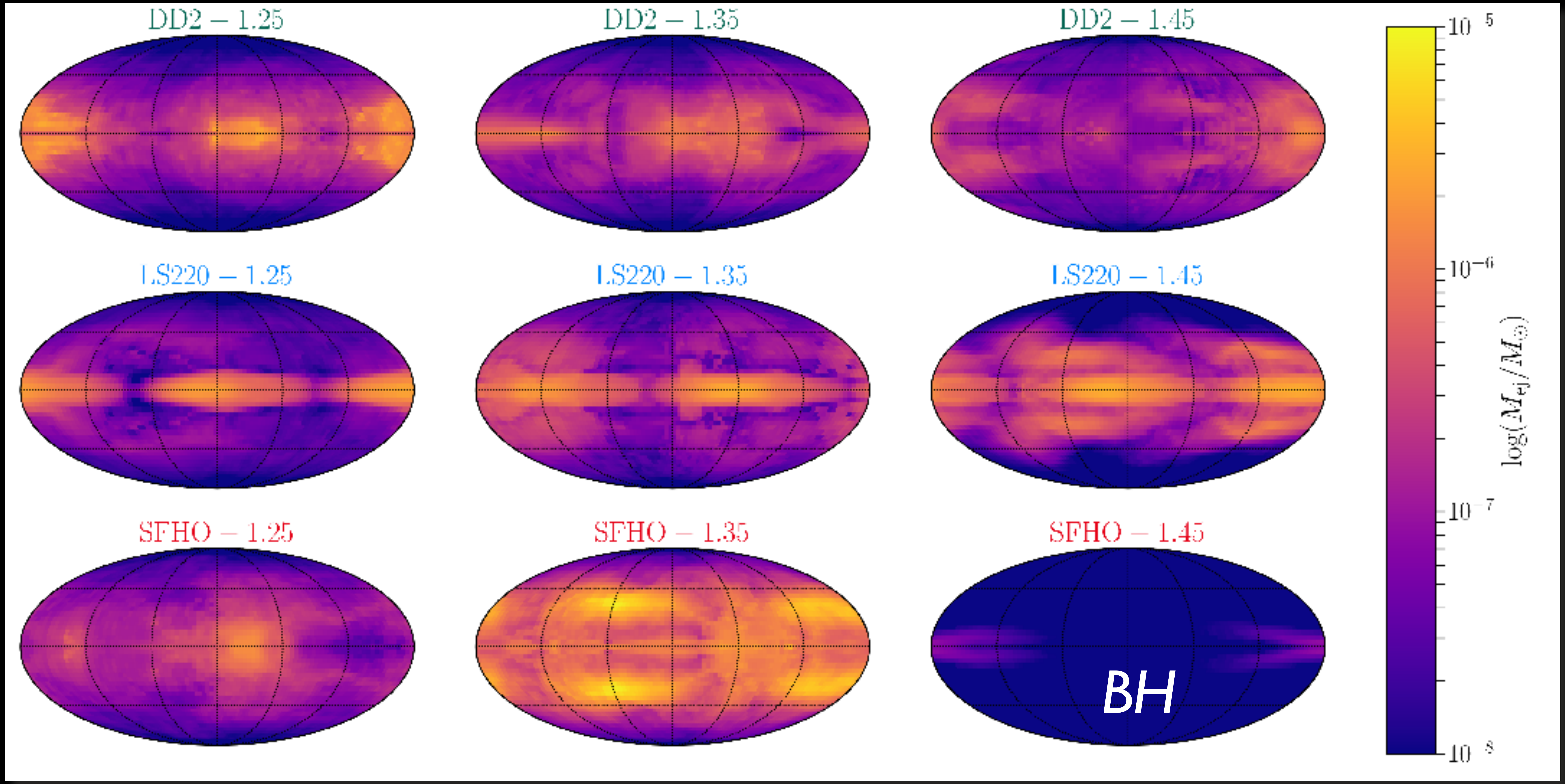

Spatial distribution of M_{ej} impacts detectability of EM counterpart:

- most of M_{ej} lost at low latitudes;
- depending on EOS/mass, contamination also in polar regions

Spatial distributions: Y_e

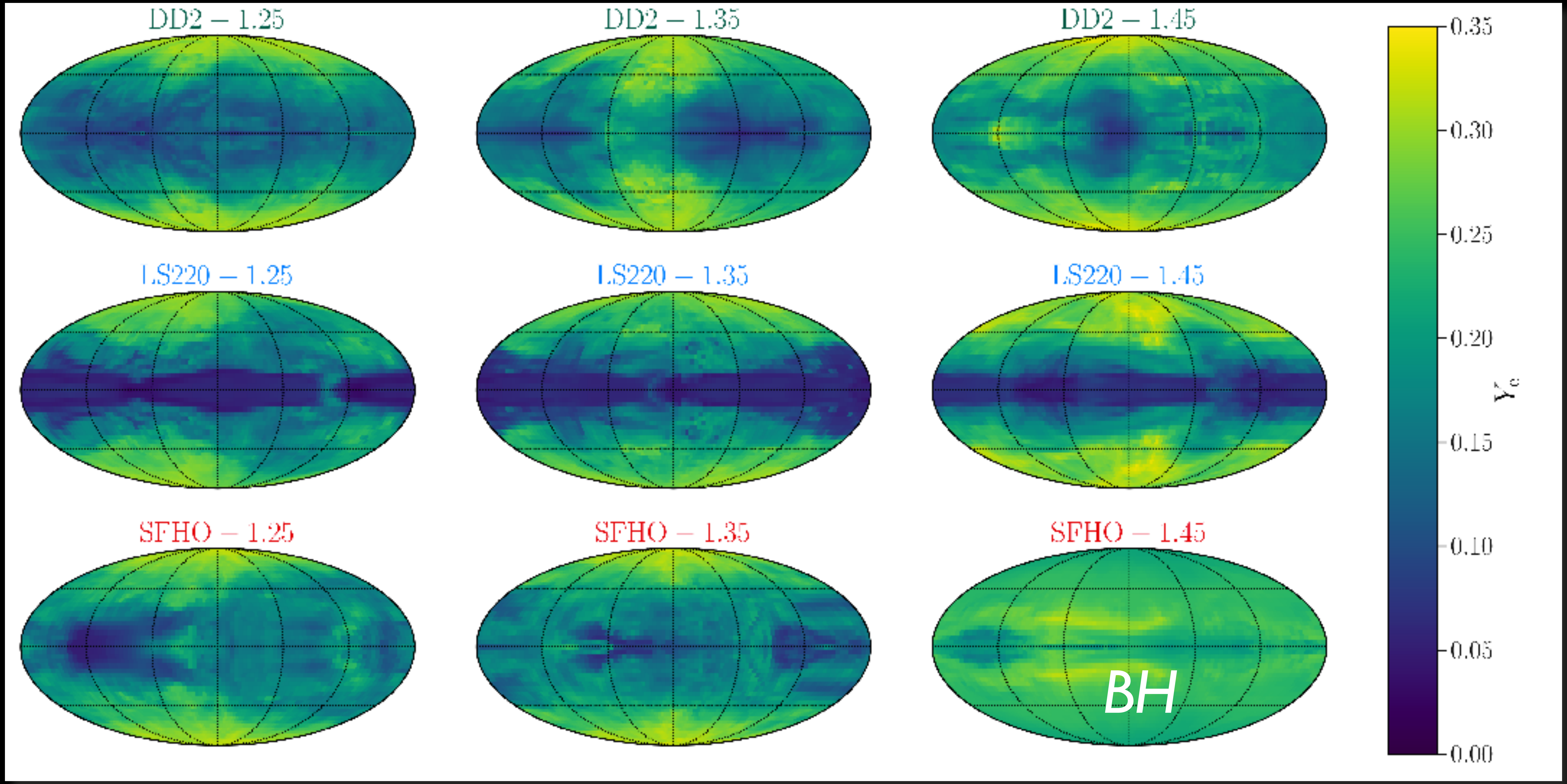

Spatial distribution of Y_e impacts detectability of EM counterpart:

- **high** Y_e in **polar** regions: **blue** (optical) macronova
- **low** Y_e in **equatorial** regions: **red** (FIR) macronova